
UNIVERSITY
*of*
GLASGOW

# SPATIAL AND TEMPORAL PATTERNS OF HYDROGEN ISOTOPE RATIOS DESCERNED FROM N-ALKANOIC ACIDS IN PLANT LEAF WAXES

Luke Harwood BSc

Masters by Research Thesis

Supervised by Professor Jaime L. Toney

APRIL 27, 2021

UNIVERSITY OF GLASGOW
SCHOOL OF GEOGRAPHICAL AND EARTH SCIENCES

# Abstract

Hydrogen isotope ratios in *n*-alkanoic acids derived from plant leaf waxes from 49 lakes across the Canadian Prairies were measured and correlated with a range of environmental variables. δD values are found to produce correlations with temperature, precipitation amount, precipitation δD, elevation, SPEI, latitude and longitude, after spatial separation based on geographic location. This has allowed a series of calibrations to be produced which can now be used downcore to estimate past environmental change. In addition, correlations produced between δD and the δD of precipitation have allowed conclusions to be drawn about the recharge mechanisms for lakes across the Canadian Prairies which may provide useful information about ENSO events. This study shows that environmental variables can be used to separate a large number of lakes in a methodical way which produces strong calibrations across a region. While many previous studies have utilised transects, this study selects lakes with no particular bias in order to analyse spatial patterns of hydrogen isotopes indiscriminately. A lack of research to date has resulted in some ambiguity around the success of using *n*-alkanoic acids as a moisture proxy, this study confirms that *n*-alkanoic acids are a viable moisture proxy and should be used in future studies.

# Acknowledgements

I would like to thank Jaime for the opportunity to complete this research, despite being a challenging time it has been thoroughly enjoyable. I would like to thank the BECS group for continuous support, ideas and discussions that made this piece of work possible. Our weekly meetings left me feeling so enthused with a buzz that I will miss moving on. I would like to thank Mike for being patient and voluntarily lending his time to show me useful software such as Climate WNA, this was such an important leg up that probably ended up saving me months. I would also like to thank Bianca for her help and discussions when solving problems with the data. Finally, I would like family for all their help and Millie who supports me every day.

# Declaration

"I declare that, except where explicit reference is made to the contriubution of others, that this dissertation is the result of my own work and has not been submitted for any other degree at the University of Glasgow or any other institution"

# Table of Contents

# List of Figures

# Chapter 1 Plant leaf waxes and the hydrological cycle

Presently, the frequency and severity of extreme flooding and drought events is universally on the rise (Levy et al., 2016) and anticipated to worsen due to climate change (He et al., 2020). If modern society is to function efficiently, adequate and reliable water supplies are vital, which is dependent on a concrete understanding of the palaeo-hydrological cycle. Not only is a tangible understanding of the hydrological cycle important on a regional scale, detailed regional information in certain areas may allow for assumptions about larger atmospheric phenomena, such as El Niño-Southern Oscillation (ENSO) (Pham et al., 2009), which exerts a strong influence on global climate and is predicted to change as climate change warms the Pacific Ocean (Wara et al., 2005).

A lack of high resolution, universally applicable moisture proxies spanning adequate timescales makes past hydrologic reconstructions challenging. Until recently, methods attempting to constrain hydrologic change have often adopted multi-proxy approaches and have reconstructed hydrologic and climatic change qualitatively rather than quantitatively. A more novel approach involves the analysis of stable isotope ratios. Hydrogen and oxygen isotope ratios in precipitation vary throughout the water cycle (Gat, 1996) and exhibit certain patterns spatially in response to climatic changes, therefore analysis of stable hydrogen and oxygen isotope ratios may be the most effective and quantitative proxy available for past climate variability (Hou et al., 2008). Consequently, stable isotope analysis of palaeoarchives such as ice cores, speleothems or microfossils in sediment cores can provide valuable information about the hydrologic cycle (Sachse et al., 2012; Hou et al., 2008). However, ice core drilling is constrained to high latitude and high-altitude regions of Earth, while microfossils and speleothems are often constrained spatially due to preservation or by conditions that are not conducive to their existence (Hou et al., 2008; Sachse et al., 2012). While the presence of stable isotopes in lake sediments has the potential to yield results which allow hydrologic reconstructions, previous attempts using bulk sedimentary organic matter have been complicated due to the wide variety of organisms with different photosynthetic pathways contributing to the signal (Sachse et al., 2012).

Recent developments in compound specific stable isotope analysis of organic matter is not limited by these constraints and is effective at quantifying past climate variability (Hou et al., 2007). *n*-Alkyl lipids, such as *n*-alkanoic acids, *n*-alkanes, *n*-alkanols and triterpenoid compounds are found in abundance within the epicuticular waxes of vascular higher plant leaves (Chikaraishi and Naraoka, 2007; Eglinton and Hamilton, 1967). Plant leaf waxes are resistant to biodegradation, found ubiquitously in soils and marine and lacustrine sediments and are easier to analyse than other terrestrial biomarkers such as isoprenoid compounds (Chikaraishi and Naraoka, 2007).

This study focusses on hydrogen isotopes and *n*-alkanoic acids, for which the covalent bonds between lipid hydrogen with carbon atoms tend to inhibit the exchange of hydrogen with ambient water below temperatures of 150˚C (Sessions et al., 2004). Thus, hydrogen isotopes preserved in leaf waxes of aquatic and terrestrial plants, which can be extracted from marine and lacustrine sediments, have hydrogen isotope ratios (δD – expressed in per-mil (‰)) offset, but highly correlated with environmental water (Feakins et al., 2016; Freimuth et al., 2017; Hou et al., 2008; Huang et al., 2002). Published literature using *n*-alkanoic acids in conjunction with hydrogen isotopes is scarce in comparison to that of *n*-alkanes (Freimuth et al., 2017), however, existing literature has shown *n*-alkanoic acids are correlated with the hydrogen isotopic signal of environmental water (Feakins et al., 2016; Freimuth et al., 2017; Hou et al., 2008).

### 1.1.1 Objectives

The aim of this thesis is to present a spatial calibration using hydrogen isotopes in *n*-alkanoic acids from plant leaf waxes for a large area within the Canadian prairies, that can subsequently be used down-core to discern past climatic change. These results may in turn be used in future climate models. In addition to this, the relationship between hydrologic change in the Canadian Prairies and ENSO (El Niño Southern Oscillation) events (Bonsal and Lawford, 1999; Pham et al., 2009) means results may be significant on a larger scale with respect to climate change, flooding and drought.

Furthermore, significant correlations observed between stable hydrogen isotopes in *n*-alkanoic acids and environmental variables will confirm *n*-acids as a viable

moisture proxy applicable to a wide range of environments spanning suitable timescales.

### 1.1.2 Hydrogen Isotopes and *n*-alkyl Compounds

Fundamentally, the resultant hydrogen isotopic signal (δD) of plant leaf waxes is derived from that of the source water (Sachse et a., 2012). Source water δD values are a function of climatic variables and precipitation-evaporation relationships (Craig and Gordon, 1965; Dansgaard, 1964; Bowen and Revenaugh, 2003). However, additional fractionation may occur once xylem water flows into the plant leaves via transpiration, the magnitude of which depends on leaf structure and climate (Kahmen et al., 2008). A correct interpretation of the isotopic ratio requires an understanding of the factors affecting local precipitation δD value, which is arguably the most important control on plant leaf wax δD (Berke et al.,2015; Hou et al., 2008). The δD of local precipitation is a function of factors such as temperature, altitude, the direction of seasonal air masses which provide moisture to a region, distance from the coast and humidity (Berke et al., 2015). Thus, plant leaf waxes found in sediments have the potential to track hydrological changes, which can be deduced using the hydrogen isotopic signature discerned from n-alkyl compounds. Sachse et al. (2012) provide a complete framework for the interpretation of hydrogen-isotopic ratios of lipid biomarkers. *n*-Alkyl compounds (*n*-alkanoic acids, *n*-alkanes and *n*-alkanols) are biosynthetically related straight-chain molecules with the common precursor acetyl-CoA, the structure of each is illustrated in figure 1 (Chikaraishi and Naraoka, 2007).

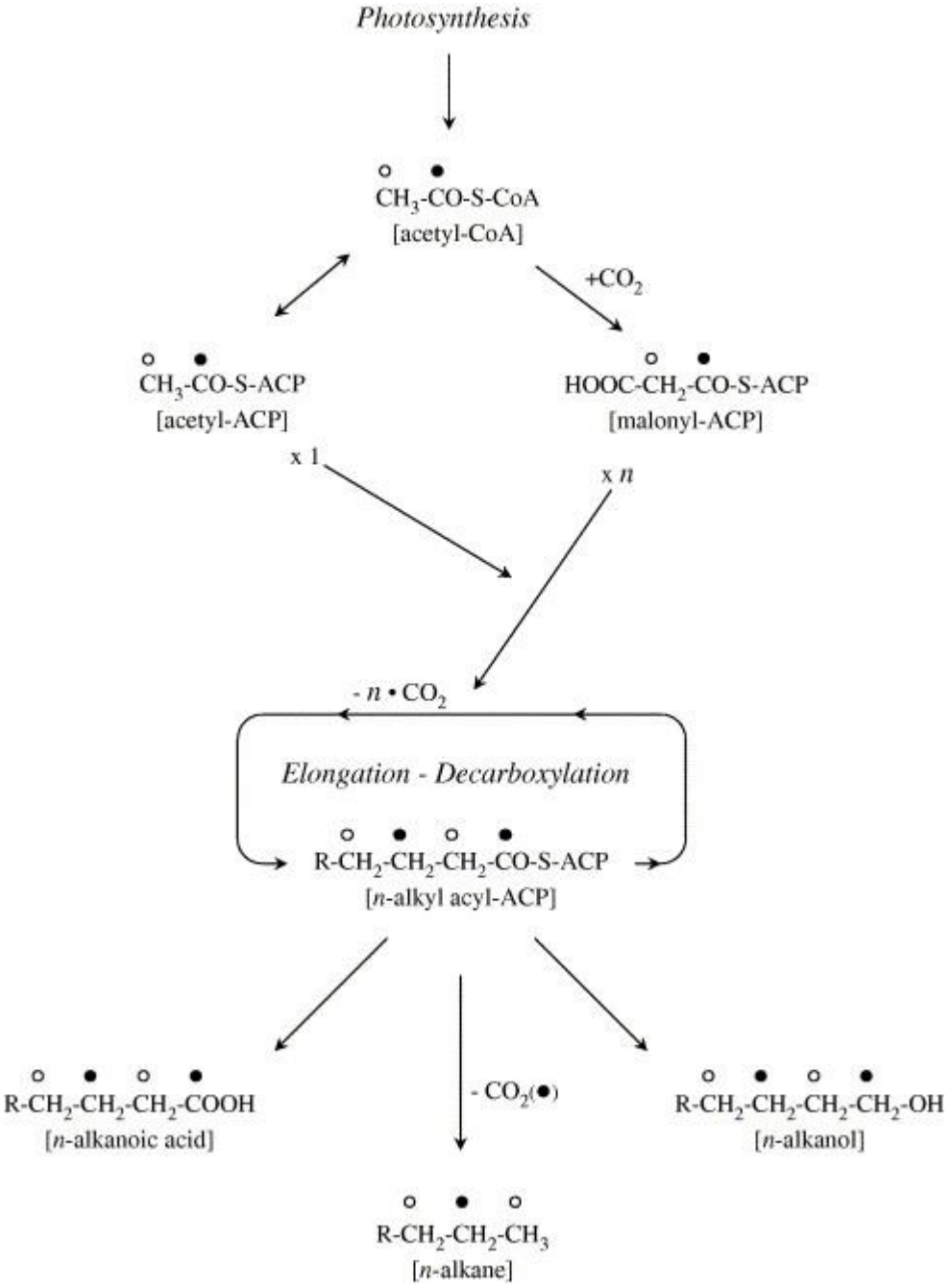


**Figure 1:** An illustration of the biosynthetic network of n-alkyl compounds in higher plants. Taken from Chikaraishi and Naraoka (2007) (after Kolattukudy, 1976; Cheesbrough and Kolattukudy, 1984; Avato et al., 1985; Post-Beittenmiller, 1996). Open circles represent Carbon positions derived from methyl carbon of acetyl-CoA, closed circles represent carbon positions derived from the carboxyl group.

### 1.1.3 Methylation

As discussed in section 1.1.2, the methylation processes occurring during sample preparation modifies the hydrogen isotopic signal from that of the original *n*-alkanoic acid (Makou et al., 2007). This can be corrected using a simple mass balance equation (eqn. 3).

$$\delta D = \frac{(2n + 2) \times \delta D_{measured} - 3 \times \delta D_{MeOH}}{2n - 1}$$

equation 3: Mass balance equation used to correct for methylation processes (Tierney et al., 2011).

However, it can be assumed the modification to the isotopic signal will be constant for all samples, therefore the methylation process should not affect correlations with environmental parameters. For this reason, the mass balance equation has not been applied to δD $C_{24}$ values obtained. Furthermore, the calibration presented is still applicable to downcore studies for the same reason.

### 1.1.4 $C_3$ and $C_4$ Grasses

Following plant water uptake, the hydrogen isotopic signal is modified further by transpiration, where protium preferentially evaporates and diffuses in air faster than deuterium (Sachse et al., 2012), however this is also a function of climate (Smith and Freeman, 2006). Different photosynthetic pathways affect plant leaf wax δD due to differences in the way hydrogen isotopes are fractionated within the pathway, however, leaf anatomy and growth form are the primary controls influencing deuterium enrichment subsequent to plant water uptake (Smith and Freeman, 2006). Since transpiration rates vary between $C_3$ and $C_4$ species (Ehleringer and Pearcy, 1983), it is important to acknowledge these potential differences when interpreting the hydrogen isotopic signal of long chain *n*-alkyl compounds from terrestrial plants (Smith and Freeman, 2006). A greenhouse study examining the effect physiology has on the δD of leaf wax in *n*-alkanes found that high molecular weight ($C_{27}$ – $C_{33}$) chain lengths in $C_4$ grasses were enriched in deuterium by ca. 20‰ relative to their $C_3$ counterpart (Smith and Freeman, 2006). A second study examining the $C_{29}$ and $C_{31}$ in $C_3$ and $C_4$ grasses also describes the

deuterium enrichment of $C_4$ relative to $C_3$ species in *n*-alkanes (Gamarra et al., 2016). However, both of these studies investigate high molecular weight *n*-alkanes, therefore, there is uncertainty surrounding how other chain lengths and other *n*-alkyl compounds may behave with respect to hydrogen isotopes in $C_3$ and $C_4$ species, which may be clarified with similar studies investigating shorter chain lengths. Regardless, vegetation type could potentially affect downcore interpretations of δD values following calibration.

In addition to the hydrogen isotopi$_c$ signal of *n*-alkanoic acids being altered by the factors discussed above, the addition of a methyl group during the methylation process, occurring during the preparation of samples, modifies the signal further (Makou et al., 2007; Huang et al., 2002). Thus, the sample analysed differs slightly in structure, and therefore hydrogen isotopic composition, from the original *n*-alkyl compound (Makou et al., 2007). The methylation process and its effect on the analysis of hydrogen isotopes in *n*-alkanoic acids is discussed in section 4.7.

### 1.1.5 Variables Affecting the Hydrogen Isotopic Signal

Rayleigh type processes, occurring during evaporation and condensation, are particularly important when comparing the spatio-temporal variation of hydrogen isotopes. Protium ($H_2O$), the lighter of the two isotopes, has a higher evaporation rate relative to deuterium (HDO), therefore when water evaporates, the corresponding vapor is depleted in deuterium (Sachse et al., 2012). Likewise, 'the continental effect' outlines that the heavy isotope, deuterium, is preferentially incorporated into precipitation. Therefore, as air masses move over a landmass, the hydrogen isotopic signal becomes progressively lighter as deuterium is preferentially rained out (Sachse et al., 2012). Figure 2 is a basic schematic diagram of the processes occurring causing isotopic fractionation.

The 'temperature effect' occurs in regions characterised by strong temperature variability. In this case, the rainout process is highly correlated with temperature such that at warmer temperatures liquid water is enriched in deuterium, relative to its vapor source, to a greater degree than at colder temperatures. Therefore,

colder temperatures produce precipitation with a more negative δD signal and vice versa (Sachse et al., 2012).

The 'amount effect' occurs in regions with limited temperature variability but by strong seasonality in rainfall. In this case, the isotopic composition of precipitation is related to the amount of precipitation with stronger depletion in deuterium at higher precipitation rates (Sachse et al., 2012).

While the processes described by Sachse et al. (2012) may be considered the dominant influences on the hydrogen isotope signal, there may be exceptions where the application of rules becomes complex. For example, a study by Munksgaard et al. (2012) documents isotopic variations of to 86‰ within a 4 hour window in a tropical region of Australia. Isotopic variations of this magnitude over such a short timescale question the applicability of fractionation rules in certain extreme regions. contemporary studies document the influence of microbes and methane (e.g. Chen et al., 2021 and Xia and Gao, 2019). Microbial influences on δD may be an important factor to account for when considering δD values of high latitude and desolate lakes (Chen et al., 2021). In addition, the presence of methane should be monitored with respect to clumped isotopes ($^{13}CH_3D$ and $^{12}CH_2D_2$), since the variability in δD methyl groups may be expressed positively or negatively depending on the stage of methane generation (Xia and Gao, 2019).

The SPEI (standardised precipitation evapotranspiration index) is a climatic drought index based on temperature and precipitation data. The SPEI was calculated for the purpose of this study as evaporation exceeds precipitation in the Canadian Prairies (Pham et al., 2008). Following precipitation, evaporation is likely to have a strong effect on environmental water and therefore the water used by terrestrial plants. The SPEI is easy to interpret; higher numbers indicate more humid conditions whilst lower numbers indicate aridity. The study area ranges in aridity from SPEI values of around 0.6 to 1.3. It is hypothesised in areas characterised by more arid conditions that δD values will be more positive, as aridity in the Canadian Prairies is characterised by high temperatures and less precipitation, which is conducive to loss of protium from environmental water.

Local precipitation δD value is imperative when considering plant leaf wax δD values (Berke et al.,2015; Hou et al., 2008), furthermore it is particularly helpful

when considering regional weather patterns. The δD value of leaf wax lipids is known to track the δD of precipitation (Hou et al., 2008; Freimuth et al., 2017), therefore the δD of precipitation has a direct control on δD. Consequently, seasonal δD values, along with δD values for the growing season were calculated in order to develop the most appropriate calibration, in addition, this will provide an understanding of the source water used by photosynthesising organisms in the Canadian Prairies.

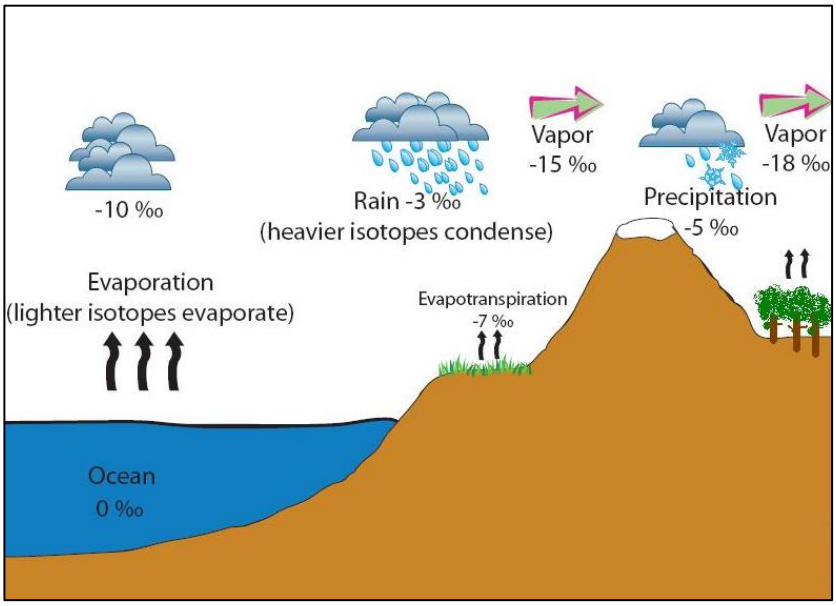


**Figure 2**: Basic schematic of isotopic fractionation processes (Stable Isotope Primer and Some Hydrological Applications, 2022).

## 1.2 Study Area

The Canada Committee on Ecological Land Classification (1989) divided Canada into areas called ecozones (Ironside, 1989) (figure 2). An ecozone can be defined as an area of land distinct to those adjacent based on adjusting biotic and abiotic factors such as climate, geology, vegetation, soil, geomorphological features and human activity. Ecozones are subdivided further into smaller areas delineated into discrete systems based on the same factors (Ecological Stratification Working Group Canada, 1996). Together, Canada's ecozones and ecoregions form a diverse ecological mosaic. The Canadian Prairies, the southernmost ecozone (figure 2), are particularly susceptible to droughts due their positioning in southern Saskatchewan, far from substantial moisture sources and in the lee of the Western Cordillera (Bonsal et al., 2013). Relative to other ecozones, the Canadian Prairies

are particularly arid, characterised by hot summers, cold winters and more evaporation than precipitation. Canada relies on water for agriculture, human health, industry, recreation, forestry and the sustenance of aquatic ecosystems (Gan, 1998; Bonsal et al., 2013). Hence, prolonged droughts are one of Canada's most costly natural disasters (Bonsal et al., 2013). An annual deficit of precipitation (300 – 500mm) with respect to evaporation (600 – 1000mm) means the Canadian Prairies are highly sensitive to hydrologic change (van der Kamp et al., 2003). In addition to this, the convergence of the Arctic, Pacific and tropical air masses make the region particularly climatically sensitive (Brown et al., 2005). The three Prairie Provinces, Alberta, Saskatchewan and Manitoba are of particular interest as they are heavily dependent on surface water supplies (Gan, 1998).


**Figure 3:** A map showing Canada's ecozones. Adapted from Wiken et al. (1996).

### 1.2.1 Climate

Mean annual temperature in the Canadian Prairies has risen significantly since 1901 and currently varies between 1.5˚C and 3.5˚C (Cui et al., 2017). Mean summer and winter temperatures are 16˚C and -10 ˚C respectively, although this will vary between ecoregions (Shorthouse, 2010). There are a number of factors and dynamics to consider when thinking about precipitation and what source of water is retained in the soil as moisture for plants to utilise. In winter, soil may freeze to depths up to 1m or more, while accumulating seasonal winter snowfall can equate to 10 – 150mm of water equivalent (van der Kamp et al., 2003).

Isotopic analysis of lakes has suggested winter precipitation and groundwater may be the most influential source of water for lakes, despite only ~30% of annual precipitation falling in winter (Pham et al., 2009). Other studies report spring snowmelt and summer precipitation as equally important sources of water for Prairie lakes (Su et al., 2000). Additionally, atmospheric moisture is recycled as rain which is estimated to account for approximately 24 to 35% of total summer rainfall (Raddatz, 2000).

Regardless, seasonal variability and evaporation during summer months are important variables to consider (Pham et al., 2009). The majority of precipitation falls during the summer months, typically between mid-June and early July (Bonsal et al., 1999; Quiring and Papakyriakou, 2005). This trend varies from the south to north, with the Southern Prairies experiencing the highest levels of precipitation during June and the Northern Prairies experiencing the highest levels of precipitation during July (Chakravarti, 1972).

Air masses carrying water from the Pacific Ocean and Gulf of Mexico are the most important sources of atmospheric water for the Canadian Prairies (Raddatz, 2000; Quiring and Papakyriakou, 2005). The Pacific air mass flows from west to east and exerts a stronger influence than that of the south to north flow of the tropical air mass (Gullet and Skinner, 1992; Quiring and Papakyriakou, 2005). However, the high elevation of the Rocky Mountains in the west, together with cooler temperatures in the Pacific Ocean relative to the Gulf of Mexico, means the Pacific air masses are dry (Quiring and Papakyriakou, 2005). Consequently, the Prairies are semi-arid (Gullet and Skinner, 1992). The topography of the Rocky Mountains also impedes the flow of the Pacific air masses, this leaves the Prairies susceptible to incursions of cold polar air from the Arctic and warm tropical air from the Gulf of Mexico, explaining the temperature extremes seen in areas like Regina (Gullett and Skinner, 1992). Convergence of these three air masses can cause storms, while relative shifts between air masses can rapidly change meteorological conditions (Covich et al., 1997). Figure 3 illustrates the different isotopic signatures of precipitation from the three converging air masses.

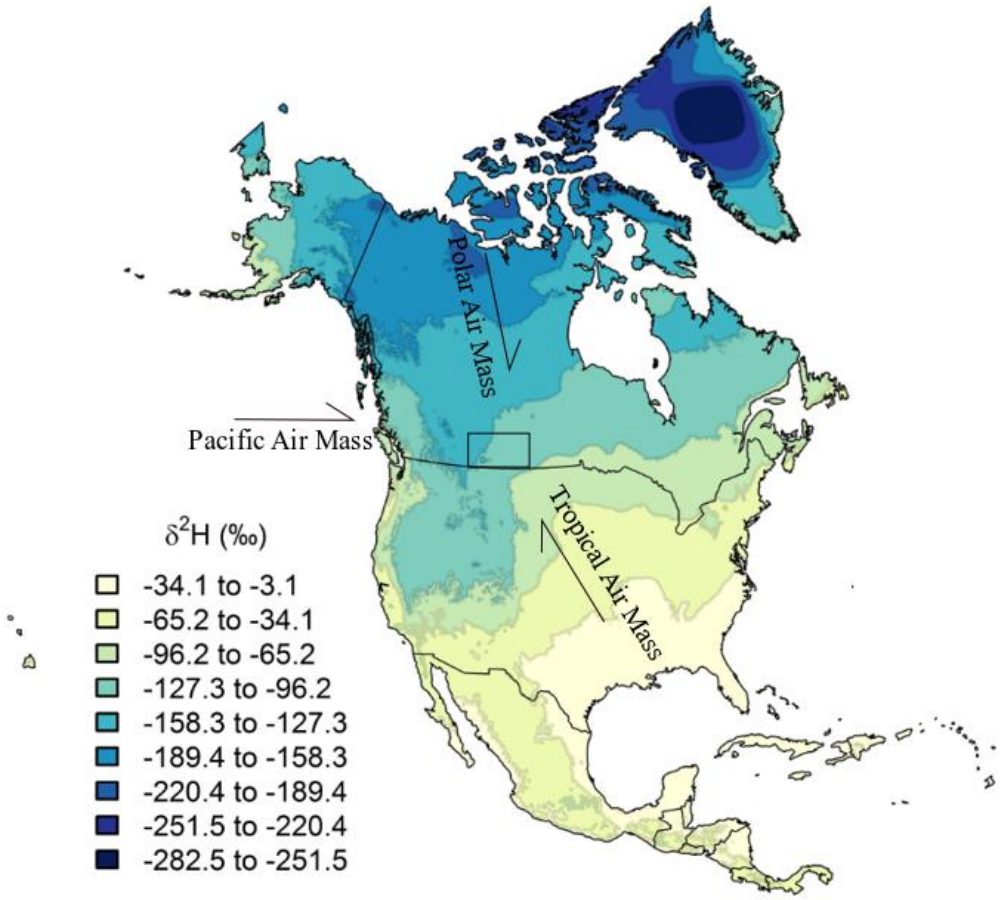


**Figure 4:** Air masses converging over the Study area (black box) are annotated. Hydrogen Isotope ratios of precipitation ($\delta D/\delta^2H$) are coded by colour (Modified after Bowen, G. J. (2017) The Online Isotopes in Precipitation Calculator, version 3.1.)

#### 1.2.1.1 El Niño Southern Oscillation

Larger atmospheric phenomena, important to climate science research, influence these air masses and therefore regional climate and hydrology. For example, El Niño events can split the Pacific air masses causing the jet stream to diverge north and south of the Canadian Prairies resulting in warm and dry winter conditions, little snow-pack and low spring run-off (Shabbar and Skinner, 1997; Pham et al., 2009). This is supported by a significantly higher number of extended summer dry spells occurring during El Niño events, than extended dry spells occurring in non-El Niño years (Bonsal and Lawford, 1999). Conversely, La Niña events can cause the winter jet stream to diverge south of the Canadian Prairies causing cold, wet winters (Pham et al., 2009). In addition to this, teleconnections between La Niña

and El Niño, North Pacific sea surface temperature anomalies and extended summer (June, July and August) dry spells, which can lead to droughts, have been suggested (Bonsal and Lawford, 1999). These events can vary in intensity depending on climatic variations associated with the Pacific decadal oscillation (PDO) (McCabe et al., 2004; Pham et al., 2009).

### 1.2.2 Geology, Geomorphology and Hydrology

The repeated advance and retreat of Pleistocene glaciers have shaped the geomorphology of the Canadian Prairies to produce a hummocky topography called the Prairie Pothole Region (Conly and Van der Kamp, 2001). The Prairies are relatively flat, with no major relief topographies; however, the land gradually slopes to lower elevations from west to east (Gullet and Skinner, 1992) (figure 4). The wetlands formed in the Pothole Region are moulded from thick clay-rich glacial till, with lesser silt, sand and gravel deposits, which range from tens to hundreds of meters thick (Conly and van der Kamp, 2001), and usually overlay Cretaceous shale (Cummings et al., 2012). The glacial till has generally low permeability, except surficial deposits containing macropores or that are heavily jointed. Prairie wetland hydrology is influenced by snowmelt run-off, precipitation and evaporation, groundwater exchange and to a lesser degree, occasional surficial connections (van der Kamp and Hayashi, 2009). Consequently, aquifers comprised of sand and gravel, located at depths below glacial till, receive very slow recharge (Pennock et al., 2014; van der Kamp and Hayashi, 2009). Figure 5 summarises the geology, hydrogeology and surficial sediment cover in the Canadian Prairies using ArcMap software with lake co-ordinates overlayed. Despite limited groundwater flow in the deep impermeable till, transpiration in the wetland margin encourages the lateral flow of shallow groundwater which exerts a strong influence on wetland water balance (van der Kamp and Hayashi, 2009).

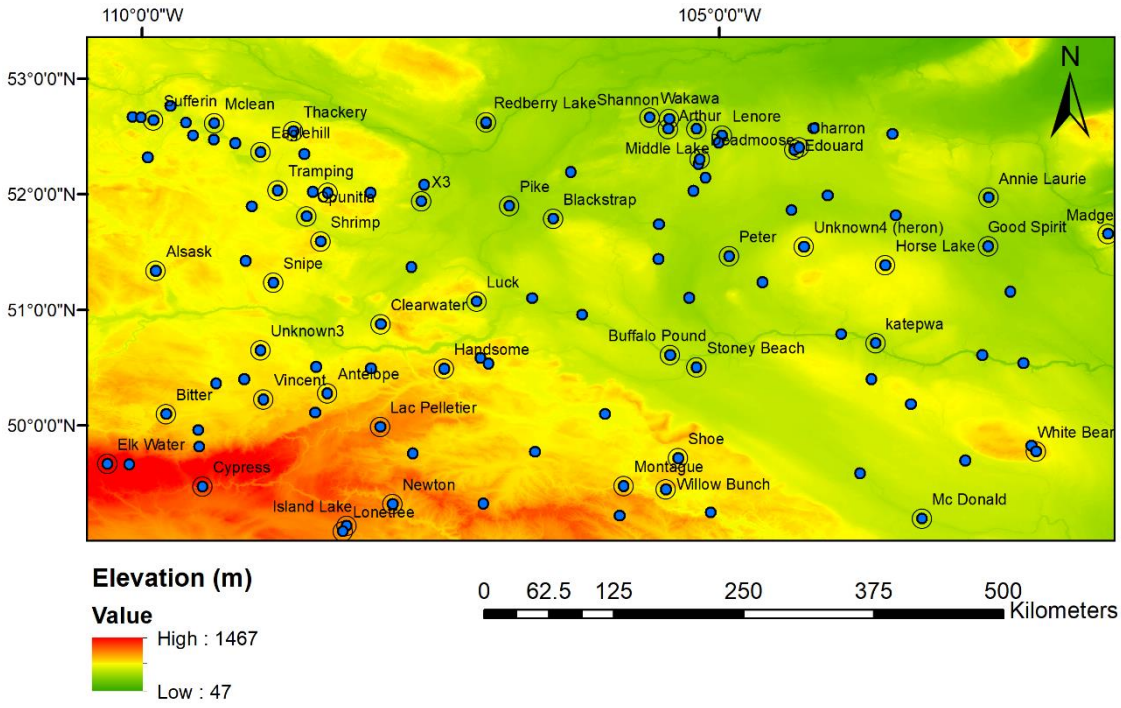


Figure 5: Map showing the study area and topography of the Prairies. Lake locations for which $C_{24}$ *n*-alkanoic acid was present and quantifiable are labelled and circled. Lakes for which $C_{24}$ was not quantifiable are represented by a blue circle.

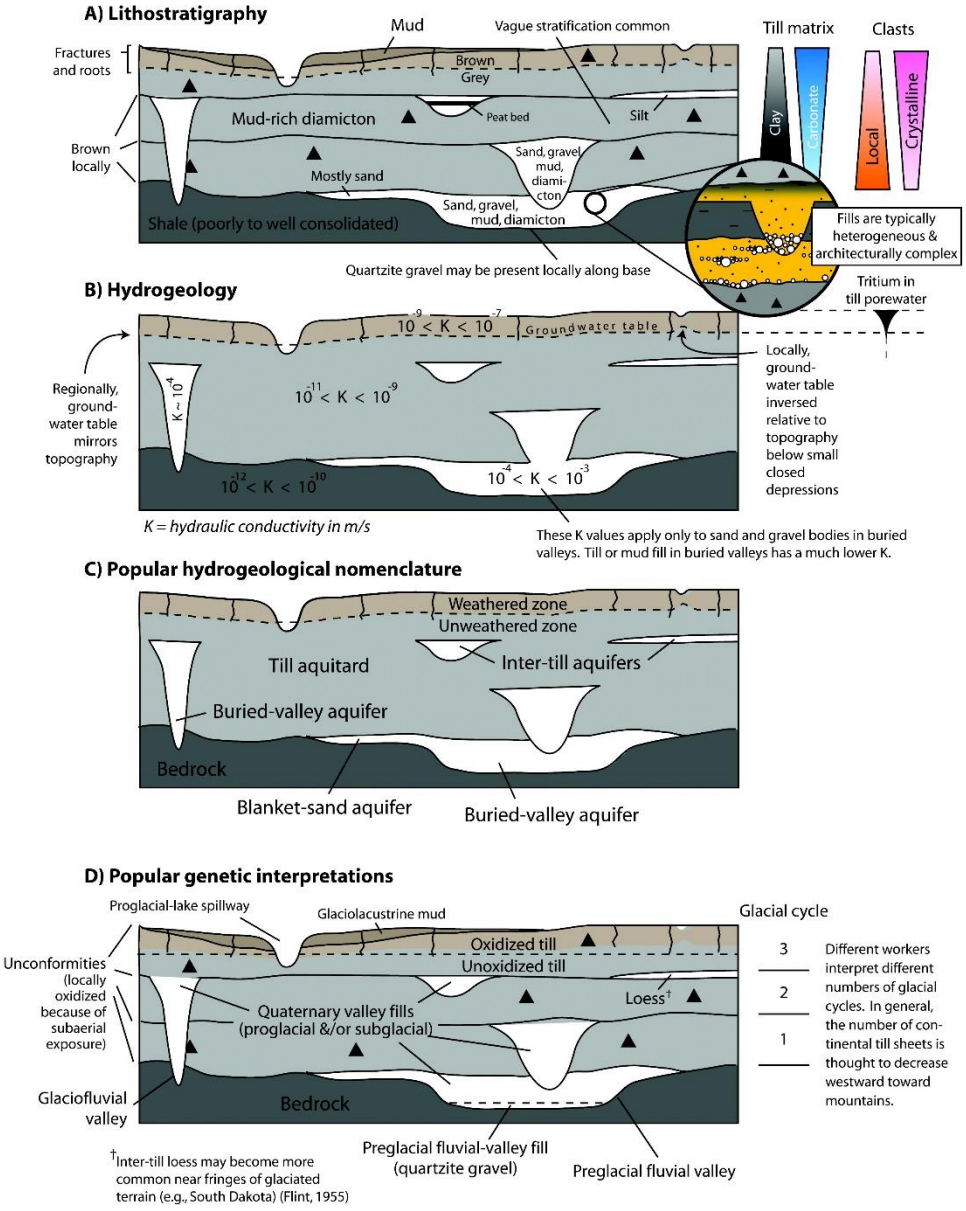


**Figure 6:** Diagram depicting the geology, hydrology and surficial sediment cover of the Canadian Prairies (Cummings et al., 2012).

The quaternary glacial deposits provide important mineral nutrients which support productive wildlife habitats, while closed basins facilitate nutrient recycling and prevent flushing by surface runoff (van der Kamp and Hayashi, 2009). As a result, 71% of wetlands in the Prairie Pothole Region have been drained for agricultural development (Euliss Jr et al., 2006) which has negative implications for ecology, groundwater recharge, flood prevention and the global cycling of nutrients (van der Kamp and Hayashi, 1998; Smith et al., 2011). Furthermore, drastic changes in the hydrologic regime, induced by climate change, will have negative implications for wildlife living in the Prairie wetlands and agriculture in the Canadian Prairies (Conly and van der Kamp, 2001; Bonsal and Regier, 2007).

### 1.2.3 Vegetation

The Pothole Region is constrained in the north east by progressively more humid conditions which have produced nutrient-poor peat bogs in permanent wetlands and lakes (Conly and van der Kamp, 2001). The western and southern limits are constrained by the Rocky Mountains and the extent of glacial deposits (Conly and van der Kamp, 2001). The region is characterised by arid grassland in the southwest, gradually transitioning into grassland with interspersed aspen groves, to boreal in the northeast (Raddatz, 2000). Summer/spring precipitation ratios are perhaps the most important control on Prairie vegetation distribution, with temperature and soil type playing a lesser role (Looman, 1983). The grasslands are treeless and composed of mid-height and short grasses (figure. 7) with lesser tall grasses and forbs (Shorthouse, 2010). Cool-season ($C_3$) grasses (wheat grass (*Agropyron spp.*) and speargrass (*Stipa spp.*)) and warm season ($C_4$) grasses (blue grama grass (*Bouteloua gracilis*)) dominate (Cui et al., 2017). Important differences between $C_3$ and $C_4$ grasses are photosynthetic pathways (Pearcy and Ehleringer, 1983) and leaf structure (Smith and Freeman, 2006) which may affect fractionation of hydrogen isotopes (Kahmen et al., 2008; Sachse et al., 2012). Furthermore, due to differences in leaf conductance to water vapour and transpiration at given photosynthetic capacities, $C_4$ grasses have higher water-use efficiencies (A/E) (ratio of photosynthesis to transpiration (Pearcy and Ehleringer, 1983).

## 1.2.4 Ecoregions

The Prairie Ecozone has been divided into seven ecoregions (Shorthouse, 2010), as with ecozones, ecoregions are defined based on interacting biotic and abiotic features (Bailey, 2004). The Prairie ecoregions, defined by The Canada Committee on Ecological Land Classification (Ironside, 1989), that are relevant to this study, are shown in figure 6 and described thereafter.

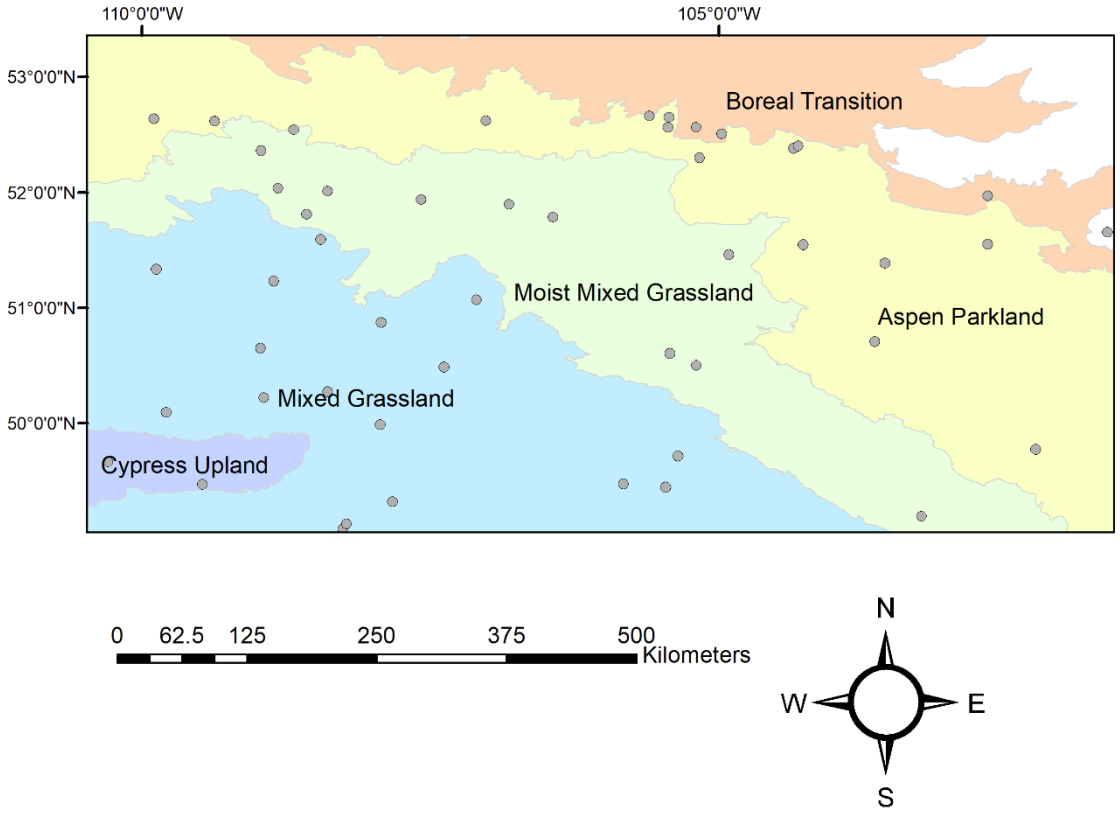


**Figure 7:** Map of Prairie Ecoregion boundaries within Saskatchewan. Lakes with the $C_{24}$ *n*-alkanoic acid are represented by grey dots. Software used – ArcMap.

.

The southernmost ecoregion, the Mixed Grassland ecoregion, is semi-arid and consists of Shortgrass prairie which is characterised by the presence of short and mid-sized grass species and sedges (Shorthouse, 2010). Mean annual temperatures can exceed 5˚C, while the mean summer and winter temperatures are 16˚C and -10˚C respectively (Shorthouse, 2010). Soils in this region mainly comprise chernozemic soils (dark surface soils with carbonate enrichment in the subsoil) and solonetzic soils (high percentage of sodium ions) (Agriculture Organization for the United Nations, 1998). About 50% of the region is cultivated for crops while

the remainder is used for pasture or rangeland (Shorthouse, 2010). Dominant grasses include blue grama, speargrass and western wheat grass (Shorthouse, 2010), and are therefore a mixture of $C_3$ and $C_4$ species (Cui et al., 2017).

The Cypress Upland Ecoregion is described by Shorthouse (2010) as 'an outlier of the Montane Vegetative Zone'. The upland region is located within the Mixed Grassland Ecoregion and is topographically isolated, sitting around 600m higher than the surrounding topography of the Mixed Grassland Ecoregion, and consists of a mixture of forests, grasslands, meadows, ranch lands and marshlands (Shourthouse, 2010). Higher precipitation rates facilitate the growth of conifer and deciduous trees at higher elevations. The mean annual temperature is 2.7˚C, while mean July and January temperatures are 16˚C and -12.1˚C (Shorthouse, 2010). These forests support a variety of plant species and grasses which are a mixture of $C_3$ and $C_4$ species (Shorthouse, 2010).

The Moist Mixed Grassland ecoregion forms a tilted arc, concentric to the Mixed Grassland ecoregion. Mean summer temperatures are 1-2˚C cooler than the Mixed Grassland ecoregion while the mean winter temperature is -11˚C (Shorthouse, 2010). Wetter conditions and cooler temperatures in the Moist Mixed Grassland ecoregion allow grasses and shrubs to thrive, therefore ca. 80% of the region is under cultivation (Shorthouse, 2010). $C_3$ species, such as wheat grass, favour cooler and moister conditions due to water use efficiency (Taylor et al., 2010) and are therefore more common than in the Mixed Grassland ecoregion (Shorthouse, 2010). However, blue grama grass ($C_4$) occurs on drier, more exposed areas (Shorthouse, 2010).

The Aspen Parkland ecoregion is a transition zone between the Prairie grasslands and the northern boreal forest (Shorthouse, 2010). The mean annual temperature is 3.5˚C while mean summer and winter temperatures are 14˚C and -8˚C respectively (Shorthouse, 2010). Vegetation is gradually taller, transitioning from grassland to forest in more northern regions. Aspen trees form groves with interspersed moist mixed grass prairie and plains rough fescues, in addition, groves of oak are common in south-eastern Saskatchewan (Shorthouse, 2010).

**Figure 8**: Examples of shortgrass prairie from the Mixed Grassland Ecoregion (Shorthouse, 2010).

## 1.3 Palaeohydrology and Considerations for the Interpretation of δD Measurements

### 1.3.1 Moisture Proxies

There have been many successful studies constraining the palaeohydrological cycle within the Canadian Prairies, however, it has been challenging to develop a high-resolution moisture proxy which is not restricted spatially or temporally by environmental factors such as the availability of fossils or pollin (Sachse et al., 2012). Prior to the development, and subsequent swift advancement, of compound specific isotope ratio mass spectrometry, the options available to palaeoclimatologists assessing past hydrologic change bore several disadvantages.

In addition to major improvements to the analytical methods available, several extremely valuable softwares have become freely accessible (e.g. ClimateWNA and Isoscapes, see Wang et al., 2012; Bowen and Revanaugh, 2003). This has made the analysis of past hydrologic change much less arduous than it was before the late 1990s (Sachse et al., 2012). In this section several multi-proxy qualitative approaches that allow inferences about palaeo-hydrologic change will be reviewed. Following this, some compound specific palaeo-hydrologic studies will be reviewed with a focus on *n*-alkyl compounds, calibration studies and Canada and North America. In what follows, many limitations of previous studies are highlighted, however, this is primarily due to the technology available at the time. New technological advancements have opened exciting doors for palaeoclimatology and our understanding of droughts, however without the existing work in place, such contemporary studies would not be possible.

#### 1.3.1.1 Dendrochronology

Edvardsson et al. (2016) acknowledge the lack of reliable, high resolution moisture proxies covering the Holocene, suggesting the study of living and subfossil peatland trees may provide further insight into past hyrological change. The tree ring patterns of excavated oak (*Quercus* spp.) and pine (*Pinus sylvestris* L.) are characterised by periods of depressed growth which reflects annual to decadal hydroclimatic changes (Edvardson et al., 2016). While a potential constraint of this method, particularly in drought prone areas, is the spatial distribution of tree cover, the spatio-temporal distribution may provide insight into decadal to centennial Holocene climate, and hydrological change (Edvardson et al., 2016). Furthermore, where tree cover is adequate over large geographical areas, synchronicity between tree-population dynamics and tree-ring chronologies can show periods of regional climate forcing (Edvardson et al., 2016). Therefore, given the correct circumstances, dendrochronology can provide useful spatio-temporal information about hydroclimatic conditions and palaeoclimate, however, since tree cover in the Canadian Prairies is sparse, this technique is largely limited to the forested margins of the Prairie Ecozone (Case and MacDonald, 1995; Sauchyn and Skinner, 2001). Nevertheless, dendrochronology has provided insight into drought within the Canadian Prairies. For example, dendrochronology has been used in conjunction with the Palmer Drought Severity Index (PDSI) (see section 4.2.1) in order to constrain periods of drought occurring

since 1597 (Sauchyn and Skinner, 2001). Tree-ring widths from white spruce (*Picea glauca*) and lodgepole pine (*Pinus contorta*) accounted for 47% and 39% of the variance in regional July PDSI (Sauchyn and Skinner, 2001). However, this study only utilised four species of tree from four sites, likely due to the scarcity of trees in the Prairie Ecozone. In order to obtain large enough sample numbers for reliable results, alternative proxies are more suitable for the Canadian Prairies. Furthermore, the temporal range of dendrochronology on the Great Plains is limited to around AD 1650 (Jacques et al., 2008).

#### 1.3.1.2 Canadian Dune fields

Past aeolian activity discerned from dune fields in the Canadian Prairies has been used to elucidate environmental change and infer periods of aridity e.g. Wolfe et al. (2006). While this approach has proved useful in discerning widespread periods of increased aeolian activity which are likely linked to periods of aridity, it is hard to quantify the severity of the dry period and whether it is linked to a drought. It should be noted that the authors intended to infer periods of aridity rather than periods of drought. As with all proxies, there are merits and constraints, a second limitation of using dune fields as a palaeoclimate or hydroclimatic proxy, recognised by Wolfe et al. (2006), is the dynamic nature of dune fields. Dune fields are not widespread, solid or permanent landscape features and can be easily reworked, causing the oldest evidence of aeolian activity to be overprinted, limiting them spatially and temporally. Furthermore, since little work has been done to improve dune mobility equations, predictions about how dunes may have moved are potentially inaccurate in comparison to other contemporary methods (Hugenholtz and Wolfe, 2005). However, dune fields may provide useful hydroclimatic and palaeoclimate information when used in conjunction with other proxies.

#### 1.3.1.3 Aragonite, Microfossils and Pollen

There is a moderate correlation between aragonite $\delta^{18}O/\delta^{13}C$ data and inferred $\delta^{18}O$ changes in the saline Redberry Lake, Saskatchewan (Van Stempvoort et al., 1993). The moderate correlation is interpreted as hydrologic fluctuations in lake level, however, due to the lack of a strong correlation between $\delta^{18}O$ and $\delta^{13}C$, clear conclusions about factors such as temperature and humidity could not be

drawn. This was caused by the involvement of other complicated contributors to the signal (Van Stempvoort et al., 1993). Unfortunately, fossil algal remains (diatoms), which may have complimented Van Stempvoort et al.'s (1993) results were not found in all sediment samples or were poorly preserved, highlighting another potential limitation and difficulty of attempting to reconstruct palaeohydrology and palaeoclimate. Furthermore, since lake water pH is more important than temperature in influencing the community composition of diatoms, diatom-inferred July temperatures appear to be less accurate when pH is variable (Bigler and Hall, 2003). Mechanisms for pH fluctuations are forest fires and erosional events causing sediment in-wash (Bigler and Hall, 2003), both of which are potentially applicable to lakes in the Canadian Prairies. It is possible certain lakes in the Canadian Prairies may experience pH fluctuations due to generally alkaline conditions being diluted by summer precipitation, conversely evaporation and drought may increase lake pH. Additional limitations that are commonly encountered when analysing fossil remains, namely diatoms, in order to interpret palaeoclimate, are summarised by Bigler and Hall (2003).

Fossil ostracods from Devils Lake, North Dakota, a closed basin lake in the Great Plains have allowed periods of salinity to be inferred from trace-element and bulk-carbonate geochemistry (Haskell et al., 1996). The 24m core allowed for salinity fluctuations to be observed and interpreted in terms of climatic changes, which are supported by pollen data (Haskell et al., 1996). Similarly, periods of high salinity have been correlated to intense and frequent droughts, supported by Mg/Ca data from ostracods (Fritz et al., 2000). While this allows inferences about periods of aridity, the data does not allow quantitative analysis of climatic factors such as temperature, precipitation or humidity. However, if used in conjunction with other studies, these inferences may prove valuable when assessing past climate regionally.

Alternatively, other methods such as the Mutual Ostracod Temperature Range (MOTR) allow estimates of past air temperatures based on the presence or absence of species in in a fossil assemblage (Horne, 2007). By using the present as an analogue for the past, estimates of temperature can be made based on the coexistence of certain species. However, complications arise when using such analogues due to the relationship between water and air temperatures and

assumptions about the climatic tolerances of living ostracod species (Horne, 2007). Furthermore, this method hinges on the presence of multiple ostracod species and their preservation.

Another multi-proxy approach utilises aragonite in conjunction with pollen (Poaceae) and charcoal to infer palaeohydrology (Grim et al., 2011). Endogenic aragonite precipitation was used to infer periods of groundwater recharge and by extension rain-fall, supported by charcoal and pollen data (Grimm et al., 2011). This approach may prove extremely useful in lakes which exhibit the appropriate climatic, hydrologic and limnologic conditions for endogenic aragonite precipitation, and in lakes that facilitate groundwater flow via coarse permeable materials such as glacial outwash (Grimm et al., 2011). However, complications may occur when attempting to elucidate precipitation variations in the Canadian Prairies, since groundwater flow is limited by low permeability glacial till (van der Kamp and Hayashi, 2009).

Pollen records have been used to support and infer past moisture change. However, pollen has also been used to infer temperature and effective moisture (Jacques et al., 2008). A study conducted in Lake Mina, west-central Minnesota, analysed pollen preserved in varved sediments. Results showed sub-centennial-scale climate changes were detectable by pollen. Detection at this resolution was possible at intersections between ecotones which facilitate fast vegetative responses (Jacques et al., 2008). Therefore, pollen records may document possible vegetation shifts, which in turn can provide information regarding available moisture (Sasche et al., 2012). However, while pollen records may provide important information about palaeohydrology, many shallow lakes in the Canadian Prairies have experienced episodic drying which is not conducive to pollen preservation (Grimm, 2001). Given this, pollen may provide an incomplete record when attempting to deduce periods of drought. Conversely, a lack of pollen data may indicate a period of drought, highlighting the importance of multi-proxy approaches.

#### 1.3.1.4 Sedimentary Structures

Hydrologic changes may be documented in down-core stratigraphic variations, geochemistry, sedimentary structures and unconformities (Anderson et al., 2005).

However, using these proxies to interpret hydrologic changes requires a hydrologically closed lake with adequate shelter, facilitating thermal stratification e.g. Marcella Lake, southwestern Yukon Territory (Anderson et al., 2005) and Little Manitou Lake, northern Great Plains (Sack and Last, 1994). Anderson et al. (2005) summarise that accumulations of calcium carbonate and organic matter at the sediment water interface depend on the position of the depositional site in relation to the thermocline, which is reconstructed using a model. The authors acknowledge the fact that interpretation of sedimentary properties hinges on the accuracy of the model, which if correct provides useful insight into past lake levels and hydrologic changes. Similarly, the use of subsurface sedimentary facies, identified from offshore cores in Little Manitou Lake have allowed the interpretation of periods of hydrologic change (Sack and Last, 1994). Unlike Anderson et al.'s (2005) study, Sack and Last (1994) rely purely on the interpretation of mineralogical and lithostratigraphic variations which reveal periods of limnological change. However, it is important to acknowledge the potential spatial limitations of this technique, as many lakes will not be adequately sheltered to allow such interpretations. Furthermore, in order to interpret climate change regionally, multiple closed basin lakes should be analysed.

As discussed above, there are many methods for reconstructing palaeoclimate and hydrologic change, each with their merits and limitations. Dendrochronology may give insight into periods of annual to decadal drought due to depressed growth, visible from growth rings, furthermore, spatio-temporal patterns of tree cover may elucidate periods of drought over longer time scales (Edvardson et al., 2016). Additionally, tree ring widths have been correlated to drought indices within the Canadian Prairies (Sauchyn and Skinner, 2001; suggesting dendrochronology has the potential to quantify past hydrologic change. Limitations occur where tree cover is sparse or when examining periods of drought extending beyond around AD 1650 (Jacques et al., 2008). Dune fields have the potential to infer periods of aridity, which may be linked to droughts, however, much like dendrochronology they are limited temporally due to their dynamic nature (Wolfe et al., 2006). However, dune fields may provide useful supporting evidence for droughts, particularly in the Canadian Prairies where aridity may have facilitated widespread aeolian activity. Conversely, microfossils have been used to infer and

quantify periods of hydrologic change over larger timescales but tend to be limited spatially due to their initial presence in lakes or by preservation (Haskell et al., 1996; Horne, 2007; Van Stempvoort et al., 1993). Pollen has also been used to infer past moisture changes, however, high resolution climate change may be limited spatially to ecotones which document fast vegetative change (Jacques et al., 2008). Furthermore, episodic drying of shallow lakes within the Canadian prairies impedes the preservation of pollen (Grimm, 2001). Each method discussed above has constraints however each have contributed significantly to palaeoclimatic research. However, in recent years it has become apparent that a method which facilitates high resolution spatial and temporal analysis is required in order to discern a clearer picture of past hydrologic change.

### 1.3.2 Compound-specific Analysis of Organic Compounds

In recent years, there has been a shift in focus from the moisture proxies discussed above to compound specific stable isotope analysis of organic compounds. Plant leaf waxes are an effective palaeoclimatic proxy as they are spatially and temporally abundant (Huang et al., 2004; Sachse et al., 2004; Yang and Huang, 2003), while an increasing number of studies have shown the δD values of plant leaf waxes reflect that of precipitation (Feakins et al., 2016; Hou et al., 2008; Huang et al., 2002). Previous work has shown there is a clear relationship between

the hydrogen isotopic value of plant leaf waxes in sediment and that of present marine and lacustrine water (Feakins et al., 2016; Huang et al., 2002; Huang et al., 2004; Makou et al., 2007). A constant apparent fractionation between environmental water and sediment denotes a viable proxy for palaeoclimatic reconstruction (Freimuth et al., 2017). This section aims to summarise important strengths, limitations and caveats highlighted by previous work in order to validate this study. Process

Surface sediments in 36 lakes in eastern North America were analysed in order to determine the hydrogen isotope ratio of modern lake water and of individual lipids (Huang et al., 2004). Lakes were selected in order to create north-south and east-west transects, while a variety of lipids were compared to assess which lipids best record the hydrogen isotopic values of surface sediments and are therefore the most useful palaeoenvironmental and palaeoclimatic proxies (Huang et al., 2004). Huang et al. (2004) conclude that free and ester-bound palmitic acid (16: 0 fatty acid), $C_{17}$ *n*-alkane and phytol all record the hydrogen isotope ratios of lake water and are therefore useful isotopic indicators. *n*-alkanoic acids were found to exhibit the same relationship to a lesser degree (Huang et al., 2004). Similarly, hydrogen isotope ratios of Palmitic Acid from 33 lake surface sediment transects in western North America have shown to record the δD of modern lake water (Huang et al., 2002). A smaller scale study consisting of 13 lakes spread across Europe found the δD of long chain *n*-alkanes paralleled that of meteoric water, with a mean fractionation factor of -128‰ (Sachse et al., 2004). Similarly, hydrogen isotope ratios from terrigenous alkanes, extracted from lake sediments across a north-south transect in the Tibetan Plateau have shown to correlate to the δD signal of precipitation (Xia et al., 2008).

Therefore, compound specific analysis of biomarkers preserved in lake sediments accurately record the δD of environmental water. However, there are considerably fewer studies which analyse the δD of *n*-alkanoic acids relative to those analysing *n*-alkanes (e.g. Bi et al., 2005; Collins et al., 2013; Hou et al., 2007; Liu et al., 2006; Liu and Huang, 2005; McInerney et al., 2011; Sachse et al., 2004; Seki et al., 2009). A potential limitation of using n-alkanoic acids may be that they are minor components in older sediments (Sachse et al., 2004). Given this, the stable isotope ratios of *n*-alkanes and *n*-alkanoic acids extracted from

leaf waxes within a single plant yield similar values, with small systematic differences in $\delta^{13}C$ and δD (Chikaraishi and Naraoka, 2007). Nonetheless, previous work has shown *n*-alkanoic acids record the δD of precipitation less accurately than n-alkanes (Feakins et al., 2016; Huang et al., 2002). However, since the fractionation between precipitation δD and leaf wax δD (apparent fractionation (εapp)) varies extensively between plant species and growth forms (Freimuth et al., 2017), the extent to which *n*-alkanoic acids may trace the δD of meteoric water in previously unexamined areas is unclear. Therefore, more literature comparing δD values of leaf wax compound classes is needed. This study will provide an indication of the extent to which *n*-alkanoic acids are useful in the Canadian Prairies.

Literature documenting the use of *n*-alkanoic acids is limited but positive in many respects as significant correlations are observed with environmental variables. For example, *n*-alkanoic acids extracted from lake sediments in the eastern Canadian Arctic have shown to correlate significantly with temperature (Shanahan et al., 2013). Additionally, the δD of precipitation, calculated using Bowen and Revanaugh's (2003) Online Isotopes in Precipitation Calculator (OIPC), showed a moderate correlation with the δD of *n*-alkanoic acids (Shanahan et al., 2013). A second study uses *n*-alkanoic acids ($C_{24}$-$C_{26}$) from terrestrial plants preserved in marine sediments, originating from vascular plant leaf waxes. This study concludes that changes in the δD of *n*-alkanoic acids parallel known changes in aridity over the timescale investigated (Makou et al., 2007).

Previous studies have concluded that δD values of plant leaf waxes are significantly correlated with source water (e.g. Berke et al. 2015; Garcin et al. 2012; Feakins et al. 2016; Vogts et al. 2016). Furthermore, Huang et al. (2004) advocate surface sediment testing as an effective method of validating isotopic proxies and encourage work establishing other lipids as proxies, such as *n*-alkanoic acids. While *n*-alkanoic acids are one of the least tested lipids, results from other lipids are promising as lipids in lake sediments accurately record environmental parameters such as precipitation δD and temperature. Variations in the δD of lipids cannot solely be accounted for by seasonal source water and a constant biosynthetic fractionation - relative humidity and temperature are important variables to consider (Berke et al. 2015). Furthermore, determining

the source organism of the chain length being analysed is another important variable that is critical when analysing plant leaf waxes with the intention of producing an effective calibration. Not only is it important to delineate aquatic and terrestrial species, certain chain lengths may have more than one source organism with differing biosynthetic pathways, this produces variations in the resultant isotopic value. For example, *n*-$C_{17}$ alkane may be produced by heterotrophs or photoautotrophs (Garcin et al. 2011). Finally, in many cases it is not possible to obtain a substantial number of samples which can limit the validity of a calibration. Where circumstances allow a large sample size, more robust calibrations can be developed (e.g. Feakins et al. 2016; Huang et al. 2004). Therefore, not only is it important to select a chain length with a known source that exhibits reliable characteristics on the chromatogram, it is imperative to select a chain length which is consistently visible in samples in order to maximise the reliability of results.

### 1.3.3 Previous use of 'Isoscapes'

Published literature citing Bowen and Revenaugh's (2003) isotope interpolation method has played an important role in advancing the understanding of stable isotope ratios. Bowen and Revenaugh (2003) have capitalised on early work which aimed to model the spatial variation in stable isotopic values of precipitation across continents. Since the development of this new method of interpolation, the opportunity for a wide range of scientific studies has been generated, primarily aiming to reconstruct palaeoclimate and palaeohydrology however other uses include archaeology and wildlife forensics (e.g. Mays, 2010; Bowen et al., 2005).

Previous work investigating leaf-wax *n*-alkane *δ*D values in terrestrial plants and broadleaf trees concluded leaf-wax *δ*D values successfully tracked Bowen and Revenaugh's (2003) interpolated precipitation *δ*D values (Sasche et al., 2006). In addition to this, a study investigating *n*-alkane isotopic ratios of $C_3$ and $C_4$ grasses on the Great Plains found isotopic ratios largely reflected precipitation *δ*D values (Smith and Freeman, 2006). This has important implications for this study as it suggests that lipids formed in the dominant vegetation types growing on the Canadian Prairies have been shown to track precipitation *δ*D values. Smith and Freeman (2006) conclude that since the apparent fractionation between *n*-alkanes and precipitation is not constant, annual precipitation and relative humidity are the climatic controls on lipid *δ*D values. In addition to this, the overall latitudinal trend seen in both precipitation and lipids suggests the *δ*D of precipitation is the primary influence on *δ*D of lipids. A similar trend is expected in this study. The interpolation method used by Bowen and Revenaugh (2003) and Bowen and Wilkinson (2002) has been scrutinised by some for its accuracy (e.g. Terzer et al. 2013). However, work by Hou et al. (2008) conclude the OIPC is pin-point accurate, as physical *δ*D values are extremely similar to the value predicted by the model.

### 1.3.4 Drought Indices

The SPEI drought index has predominantly been used in conjunction with carbon and oxygen stable isotopes in tree ring cellulose. However, there are significantly less publications that correlate hydrogen isotopic ratios with the SPEI Drought Index or with stable isotopes in plant leaf waxes. The SPEI and the stable isotopes ($\delta^{13}C$ and $\delta^{18}O$) have been correlated with varying degrees of success. The $\delta^{13}C$ from cellulose extracted from *Picea shrenkiana* was found to be negatively correlated with the SPEI during the growing season in north western China ($r^2$ = -0.38, $P < 0.01$). In addition to this, tree-ring $\delta^{18}O$ values were also negatively correlated with SPEI ($r^2$ = 0.54) (Xu et al., 2018). Similarly, a study in the Tianshan mountains of China found $\delta^{18}O$ was significantly positively correlated with the SPEI in November but negatively correlated with SPEI from May to July and throughout the growing season ($r^2$=-0.55, $r^2$=-0.51, $p<0.01$) (Xu et al., 2014). Therefore, changes in moisture can be inferred using stable isotopes and the SPEI. A third study in south western China has attributed increasingly weak correlations between tree ring $\delta^{18}O$ and SPEI and $\delta^{18}O$ and vapour pressure deficit to rising

central Pacific sea surface temperature, highlighting a critical effect of climate change (An et al., 2019). This shows how stable isotopes can be linked to the SPEI drought index in order to infer moisture change and make assumptions about larger atmospheric phenomena.

The Palmer Drought Severity Index (Palmer, 1965) is a widely used drought index which has been used to assess general moisture changes. As with the SPEI, most published applications of the PDSI used in conjunction with stable isotopes utilise tree ring cellulose as the source for stable isotopes (e.g. Sano et al., 2012; Szymczak et al., 2011; Xu et al., 2011). However, there is a lack of published work comparing the PDSI to hydrogen isotopes, possibly because hydrogen isotope ratio mass spectrometry is a relatively novel approach which is unlikely to be used in conjunction with an older drought index.

Tree ring cellulose analysed for $\delta^{18}O$ from Fujian cypress, *Fokienia hodginsii* in Laos has showed significant negative correlation with the May-October PDSI (Xu et al., 2011). Similarly, a study utilising cypress trees in Vietnam found the $\delta^{18}O$ from cellulose was significantly correlated with temperature, precipitation and the May-October PDSI (Sano et al., 2012). Therefore, the PDSI has been shown to correlate with stable isotopes extracted from vegetation and is a potentially useful index in elucidating droughts. Other work has used the PDSI and SPI to assess when the most severe droughts have occurred during the 20$^{th}$ century. This study found the PDSI and SPI to be generally in agreement but advises that because the PDSI calculation takes into account long term moisture conditions, the SPI is more applicable to current meteorological conditions (Bonsal and Regier, 2007).

Guttman (1991) published a study examining the sensitivity of the PDSI, concluding the time it took for the PDSI to reflect actual conditions could be more than four years. In addition to this, it was found the effects of temperature anomalies are insignificant in comparison to precipitation anomalies. This suggests that the PDSI may fail to explain some variance in stable isotopes. Furthermore, the inconsistent nature of the PDSI at various locations makes spatial comparisons of the PDSI unreliable (Wells et al., 2004). Work aiming to elucidate the appropriate circumstances in which to use certain drought indices (including the PSDI, SPEI and SPI) concluded that the multi-scalar nature of the SPEI gave it an advantage

over the PDSI, sc-PDSI (a revised version of the PDSI (Wells et al., 2004)) and SPI (Jiang et al., 2015).

In summary, studies which have utilised the PDSI have been predominantly concerned with tree ring cellulose therefore further work is required to investigate its use in conjunction with plant leaf waxes. In addition, the PDSI accounts for long term moisture changes therefore should not be considered for studies concerned with current meteorological conditions (Bonsal and Regier, 2007). The PDSI may prove useful to some studies if precipitation and temperature anomalies were weighted equally, improving the ability of the indice to explain variance in stable isotopes. While the SPI accounts for current meteorological conditions, it is limited by its inability to account for evapotranspiration. Improvements made to the SPI (SPEI), which now account for evapotranspiration, have resulted in a refined technique which is useful when considering the complexities associated with hydrogen isotope fractionation.

### 1.3.5 Climate WNA

Climate WNA (Western North America), now Climate NA (North America), is a software package developed by Wang et al. (2012) which provides a high-resolution climate database aimed at researchers and resource managers. As well as providing historical data and future projections, Climate WNA allows users to select specific locations for which a vast number of highly accurate estimates of climate variables are given. Wang et al. (2012) present a spatially expanded version of Climate WNA which covers North America west of 100˚longitude.

Climate WNA uses monthly climate data for the 1961-1990 normal period generated by PRISM (Parameter-elevation regressions on independent slopes model), to produce a reference climate grid (2.5 arc min) (Daly et al., 2002; Wang et al., 2012). The data developed by PRISM incorporates weather station data, a DEM (digital elevation model) and professional knowledge of climate patterns (Daly et al., 2002; Wang et al., 2012). Some data needed to produce the reference grid could not be provided by PRISM or were found by Wang et al. (2012) to be less accurate. In such cases the ANUSPLIN (Australian National University Spline) (Hutchinson, 1989) was used to interpolate weather station records, subsequently the datasets were integrated seamlessly (Wang et al., 2012).

The climate WNA dataset has been widely used for a variety of applications including agricultural studies (Muir and Angert, 2016), droughts (Zargar et al., 2014) and climate change (Shanley et al., 2015). The previous success observed in other scientific studies, particularly when used for correlation analysis, suggests the software is accurate and appropriate for this study. For example, strong correlations were achieved when the Climate WNA dataset was used to assess the hardiness of Douglas Fir trees to drought and cold (Bansal et al., 2016). Other successful applications include the use of the CMD (Hargreave's climate moisture deficit), calculated by the Climate WNA software, which was correlated to the productivity of birds (Saracco et al., 2018).

# Chapter 2 Methodology

## 2.1 Sample Collection

Surface sediment samples from 106 Lakes in southern Saskatchewan, Canada were sampled between July 29$^{th}$ and August 30$^{th}$, 2013 using an Ekman grab sampler. The top 10mm of collected sediments were taken as subsamples and freeze-dried at 0.01 Pa for 36 hours before analysis. Lakes span 4˚latitudinally and across 9˚longitude. The lakes comprise a range of salinities, from fresh to hypersaline and have a diverse ionic composition (Plancq et al., 2018).

## 2.2 *n*-Alkanoic Acid Analysis

Freeze-dried sediments were homogenised before the total lipid extract (TLE) was extracted using a Dionex model ASE350 accelerated solvent extractor with dichloromethane (DCM):methanol (MeOH) (9:1, v:v) (Plancq et al., 2018).

Following extraction, excess solvent was evaporated using a Turbovap before being weighed.

LC-$NH_2$ columns were washed with 3 bed-volumes (5-10ml) of DCM:isopropyl alcohol (1:1 v:v) before the total lipid extract was separated into a neutral and an acid fraction by eluting with DCM:isopropyl alcohol (1:1, v:v), followed by ether with 4% acetic acid (v:v) (Plancq et al., 2018). The neutral fraction was separated further by chromatography over a silica gel column, containing 35-70µm particles, into four fractions of increasing polarity. Fractions one to four were eluted using hexane, DCM, ethyl acetate:hexane (1:3, v:v) and MeOH, respectively. The acid fraction was derivatised by adding 100µl of MeOH with 12% $BF_3$ (v:v) (stored at -17.78˚C (0˚F)) before heating in an oven at 70˚C for one hour.

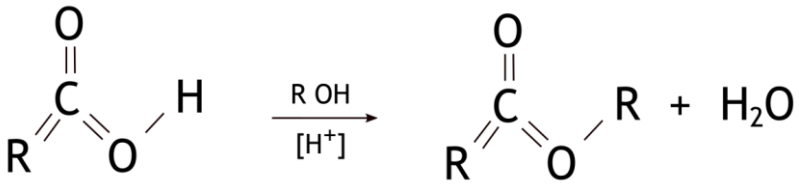


**Figure 9:** Fischer esterification of *n*-alkanoic acid.

A silica gel column was cleaned by eluting with 4ml of hexane before the acid fraction was added to the column. The column was eluted again with another 4ml of hexane then 4ml of DCM, both products were saved in case methylation did not work. The fatty acid methyl esters (FAMEs) produced by elution with DCM were transferred to a GC vial with an insert due to low concentrations of organic material.

25µl of hexane was added to each insert containing organic material before running on the IsoPrime GC-5 GC-IRMS (Gas Chromatography-Isotope-ratio Mass Spectrometry). The GC-IRMS was equipped with an Agilent Technologies 7890B system which has accurate temperature and injection control as well as reliability. An in-house standard (see section 2.2.1) was used to quantify the concentration of samples. Samples were run in duplicates with one standard mixture before and after every three sample injections. An HP5 30m long column with an internal diameter of 0.32mm and film thickness of 0.25µm was used in constant flow mode

with a flow rate of 1.2ml/minute. Helium was the carrier gas, and samples were run at 60°C for 2 minutes, thereafter the temperature increased at 30°C/minute until 120°C, and 5°C/minute until 325°C, at which point the temperature remained steady for 16 minutes. Hydrogen isotope results were expressed as δD, in per mil (‰), relative to VSMOW (Vienna Standard Mean Oceanic Water) (Eqn 1).

$$\delta D_{sample} = 1000\ x\ (R_{sample}\ x\ R_{VSMOW}^{-1})\ - 1$$

Equation 1: δD sample calculation, where R is the ratio of deuterium to protium ($^2H$ :$^1H$).

The long chain *n*-alkanoic acids were identified by comparison of retention times with the in-house standard mixture (figure 9).

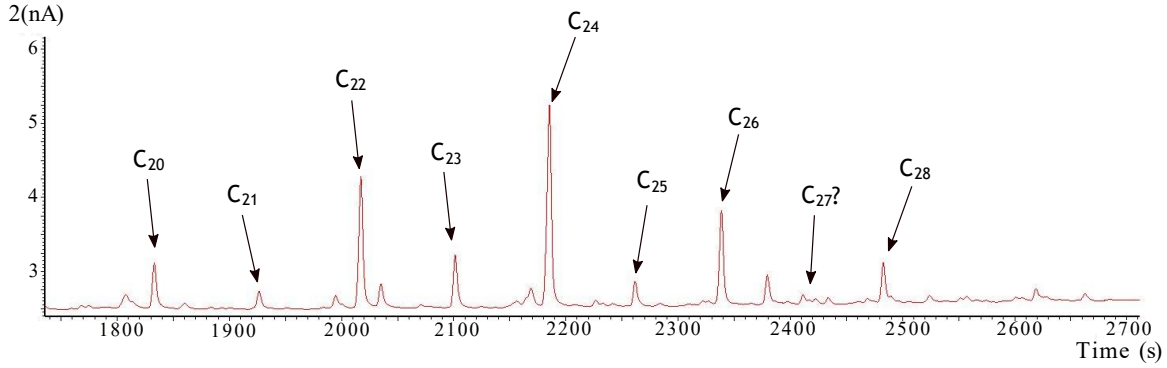


**Figure 10:** Example chromatogram showing $C_{20}$ to $C_{28}$.

## 2.2.1 Standard Preparation

Straight chain alkanes were used as standards and consisted of six chain lengths; $C_{18}$, $C_{19}$, $C_{20}$, $C_{23}$, $C_{26}$ and $C_{30}$. Each straight chain alkane was dissolved in 50mL of hexane; table 1 summarises the mass of each chain length that was dissolved in hexane.

| Straight Chain Alkane | Mass (mg) |
|---|---|
| $C_{18}$ | 15.37 |

| | |
|---|---|
| $C_{19}$ | 27.7 |
| $C_{20}$ | 42.53 |
| $C_{23}$ | 70.23 |
| $C_{26}$ | 15.46 |
| $C_{30}$ | 70.6 |

Table 1: The mass in milligrams of each straight chain alkane dissolved in 50mL of hexane.

8mL of each solution containing the alkane was transferred to a combusted 60mL vial in order to mix the solutions, subsequently the solvent was evaporated using a gentle stream of nitrogen from a turbovap until dry. The solid was then added to an 8mL vial using a small amount of hexane before being dried. Finally, 8ml of hexane was added to the 8ml vial.

## 2.3 Calculation of Environmental Variables

The environmental variables that are correlated with δD data were calculated using several types of software. Each software allowed site specific data to be generated in order for accurate correlations with δD data. Information on how to access the software used in this calibration is detailed below.

### 2.3.1 Climate WNA

The Climate WNA v4.62 zip file was downloaded from https://sites.ualberta.ca. The executable file was run in conjunction with the latitude, longitude and elevation data which was gathered with samples. This generated a vast amount of site-specific data for each lake including average seasonal temperatures, precipitation amount (including quantity of snow) and CMD (Climatic Moisture Deficit) (Appendix C).

### 2.3.2 Precipitation δD Data

Site-specific precipitation δD data was obtained using Bowen and Revenaugh's (2003) 'isoscape', accessible at www.waterisotopes.org. Average annual and monthly data was collected by entering the latitude, longitude and elevation for individual lakes. This data was combined into averages for seasons (winter, spring, summer, autumn and growing season) before being correlated with δD data (Appendix A).

### 2.3.3 SPEI

The SPEI (Standard Precipitation Evapotranspiration Index) was calculated using the Global SPEI Database, accessible at https://spei.csic.es/database.html, which offers multiscalar timescales (1-48 months) covering the period January 1901 to December 2015. Site specific 12-month averages were generated using elevation, temperature and precipitation data for each site. This data was combined to produce annual averages over different timespans including 1980 – 2015 and 2010 – 2015. See section 1.3.4 and 4.2.1 for more information on SPEI and drought indices.

## 2.4 Analysis of Chain Lengths

Initially, it was hypothesised that the chain lengths $C_{24}$, $C_{26}$ and $C_{28}$ were of terrestrial origin, and therefore of interest (e.g. Otto and Simpson, 2005; Sauer et al., 2001). Following initial analysis, $C_{28}$ showed no clear correlations with environmental variables (see section 2.3 for details on environmental variables), this prompted close examination of each chromatogram. $C_{28}$ regularly exhibits co-elution on either side of the chromatogram peak, therefore there is a high probability that the δD values associated with these peaks are inaccurate. Subsequently, the $C_{24}$ and $C_{26}$ peaks were examined in more detail, since the $C_{24}$ peak was present in higher concentrations, was present in more samples and displayed co-elution in fewer samples than $C_{26}$, $C_{24}$ was used thereafter.

## 2.5 Data Analysis Framework

During the initial analysis of δD $C_{24}$ data it became apparent that correlations with environmental variables were underpinned by a strong spatial component.

However, deciphering what caused lakes to differ spatially and therefore how they should be separated required a large amount of environmental data with respect to the study area and trial and error. This section lays the framework for the spatial separation of lakes which allowed δD $C_{24}$ to be correlated to environmental variables.

### 2.5.1 Spatial Separation of Lakes

Initial attempts at correlating environmental variables and other calculated parameters, such as SPEI and estimated precipitation δD values, with the calculated δD $C_{24}$ of all 49 lakes showed no significant correlations. It was hypothesised that the main air masses carrying water vapour south to north and west to east may be reflected by Raleigh distillation, thus an increasingly lighter isotopic signature would be seen inland. However, no significant correlations were observed with δD $C_{24}$ values and latitude or longitude (figure 10). In addition, there was no relationship between δD $C_{24}$ and temperature or precipitation.

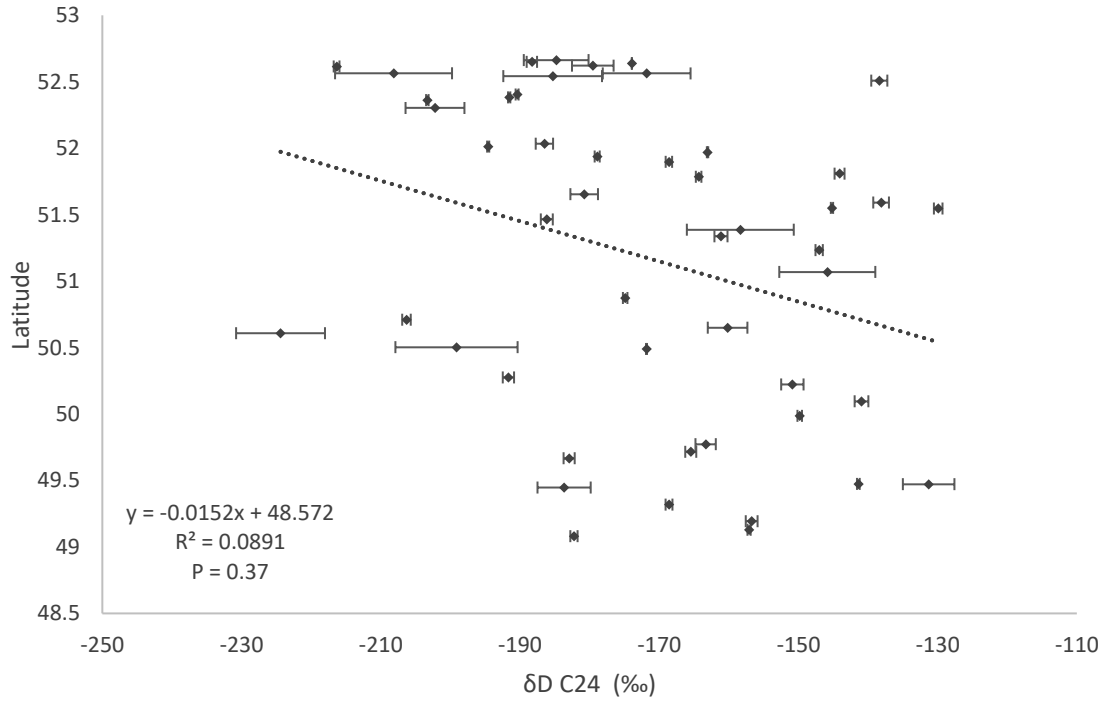


**Figure 2:** Relationship between δD $C_{24}$ and latitude before spatial separation. Relative standard errors are below 5%.

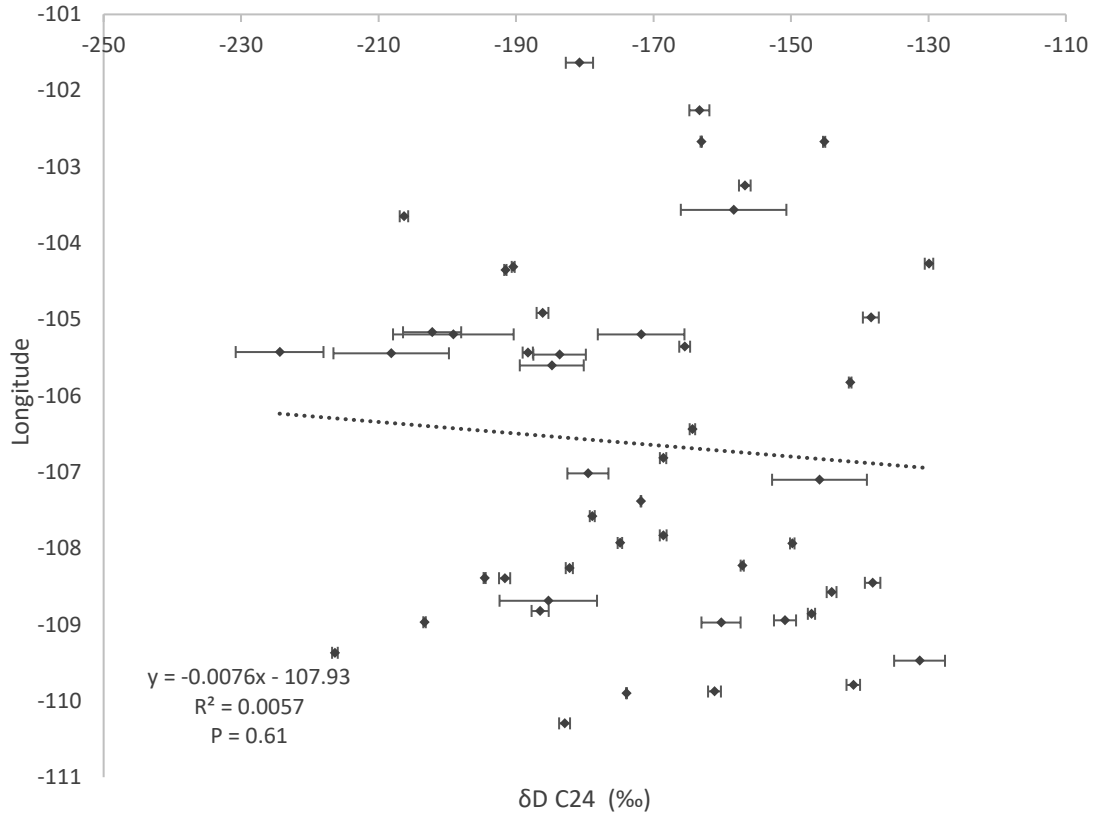


**Figure 3:** Relationship between δD $C_{24}$ and longitude before spatial separation. Relative standard errors are below 5%.

Since the water plants use to synthesise leaf wax lipids is ultimately sourced from precipitation, it was hypothesised that the δD value of precipitation would be reflected in leaf wax δD $C_{24}$ values, even after various fractionations. No correlation was observed with δD $C_{24}$ and the estimated δD value of precipitation (figure 12).

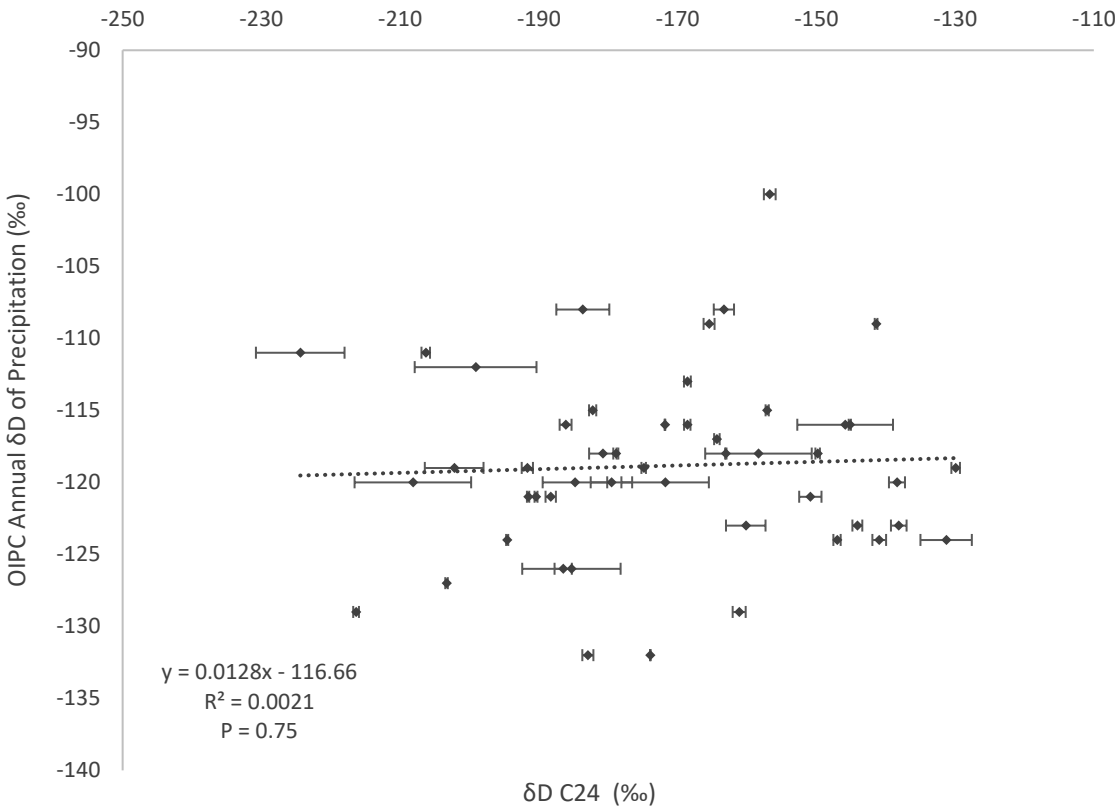


**Figure 4:** δD $C_{24}$ correlation with the δD estimated from Bowen and Revenaugh's (2003) OIPC (Online Isotopes in Precipitation Calculator).

Since no correlations were observed with climatic factors, it was assumed there were variables which were not being accounted for. Therefore, the SPEI, which considers potential evaporation and precipitation (Vicente-Serrano, 2010), was calculated and plotted against the δD $C_{24}$ values obtained from sediment samples. Once more, no clear relationships were observed.

No patterns could be discerned between the above stated variables and the δD of alkanoic acids, therefore attempts were made to group sample locations into smaller groups geographically. Initially, lakes were grouped as geographically close clusters. While correlations improved slightly, it was hypothesised that correlations were being affected by vegetation changes occurring where clusters of lakes encompassed several ecoregions. Therefore, lakes were separated into groups based on the ecoregion in which they were encompassed. This method produced particularly poor correlations with all environmental variables. Figure 13 illustrates one example of the results produced when lakes were grouped based on the ecoregion in which they are included.

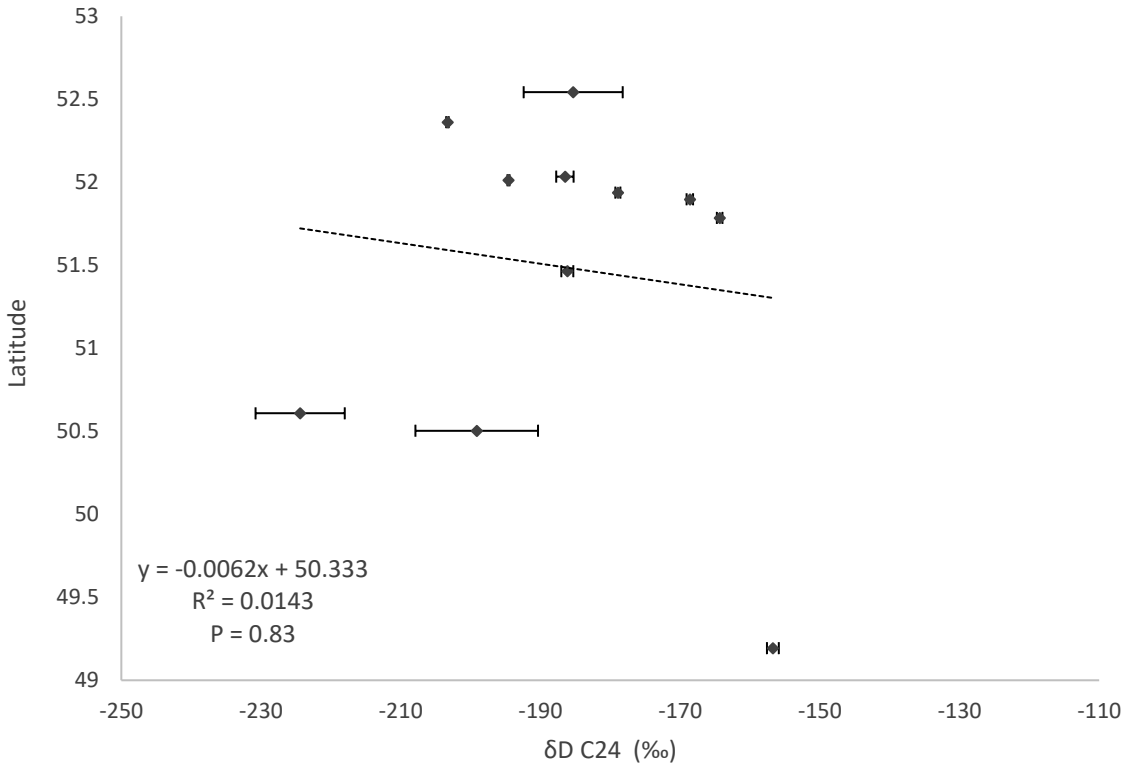


**Figure 5:** Lakes within the Moist Mixed Grassland ecoregion. δD $C_{24}$ plotted against latitude.

Figures 14 and 15 show Bowen and Revenaugh's (2003) online isotopes in precipitation calculator results plotted against the SPEI values for all lakes containing $C_{24}$. Three distinct positive correlations were produced showing an increase in δD of water is related to a higher SPEI score. This is expected as higher SPEI predicts more deuterium within lake water. Groups were not distinguished based purely on the correlations shown in figure 14, however the relationship below was used to inform latitudinal boundaries which are likely a function of other physical factors which change with latitude and longitude (see chapter 4). Groups separated by latitude will be referred to as Group XA, groups separated by longitude will be referred to as Group XB, where 'X' refers to the group number within the separation.

| Lake | Latitude | Longitude | Water δD | SPEI 2010-2015 |
|---|---|---|---|---|
| Lonetree | 49.081 | -108.258 | -115 | 0.75 |
| Island Lake | 49.129 | -108.22 | -115 | 0.75 |
| Mc Donald | 49.193 | -103.243 | -100 | 0.81 |
| Newton | 49.318 | -107.829 | -113 | 0.74 |
| Willow Bunch | 49.447 | -105.461 | -108 | 0.77 |
| Cypress | 49.472 | -109.473 | -124 | 0.68 |
| Montague | 49.474 | -105.826 | -109 | 0.65 |
| Elk Water | 49.667 | -110.294 | -132 | 0.72 |
| Shoe | 49.715 | -105.356 | -109 | 0.80 |
| White Bear | 49.773 | -102.257 | -108 | 0.96 |
| Lac Pelletier | 49.98 | -107.935 | -118 | 0.79 |
| Bitter | 50.096 | -109.789 | -124 | 0.6 |
| Vincent | 50.222 | -108.944 | -121 | 0.74 |
| Antelope | 50.275 | -108.391 | -119 | 0.77 |
| Handsome | 50.489 | -107.383 | -116 | 0.75 |
| Stoney Beach | 50.50 | -105.194 | -112 | 0.93 |
| Buffalo Pound | 50.608 | -105.426 | -111 | 0.93 |
| Unknown3 | 50.649 | -108.971 | -123 | 0.7 |
| katepwa | 50.709 | -103.646 | -111 | 0.96 |
| Clearwater | 50.873 | -107.929 | -119 | 0.82 |
| Luck | 51.069 | -107.100 | -116 | 1.00 |
| Snipe | 51.233 | -108.858 | -124 | 0.85 |
| Alsask | 51.337 | -109.876 | -129 | 0.71 |
| Horse Lake | 51.387 | -103.561 | -118 | 0.99 |
| Porter | 51.464 | -104.913 | -116 | 0.99 |
| Unknown4 (heron) | 51.546 | -104.268 | -119 | 1.13 |
| Good Spirit | 51.551 | -102.670 | -116 | 0.77 |
| Shrimp | 51.591 | -108.451 | -123 | 0.99 |
| Madge | 51.654 | -101.634 | -118 | 0.9 |
| Blackstrap | 51.785 | -106.438 | -117 | 1.09 |
| Opunitia | 51.808 | -108.573 | -123 | 0.93 |
| Pike | 51.897 | -106.816 | -116 | 1.09 |
| X3 | 51.93 | -107.577 | -118 | 1.04 |
| Annie Laurie | 51.970 | -102.668 | -118 | 0.77 |
| Springwater | 52.012 | -108.388 | -124 | 1.0 |
| Tramping | 52.034 | -108.820 | -126 | 0.97 |
| Deadmoose | 52.302 | -105.167 | -119 | 1.16 |
| Eaglehill | 52.362 | -108.968 | -127 | 0.93 |
| Edouard | 52.382 | -104.350 | -121 | 1.15 |
| Charron | 52.404 | -104.310 | -121 | 1.15 |
| Lenore | 52.508 | -104.974 | -120 | 1.22 |
| Thackery | 52.542 | -108.686 | -126 | 1.09 |
| Middle Lake | 52.562 | -105.194 | -120 | 1.27 |
| Arthur | 52.563 | -105.4 | -120 | 1.27 |
| Mclean | 52.615 | -109.369 | -129 | 0.98 |
| Redberry Lake | 52.621 | -107.01 | -120 | 1.22 |
| Sufferin | 52.637 | -109.898 | -132 | 0.92 |
| Shannon | 52.649 | -105.433 | -121 | 1.27 |
| Wakawa | 52.663 | -105.601 | -120 | 1.28 |

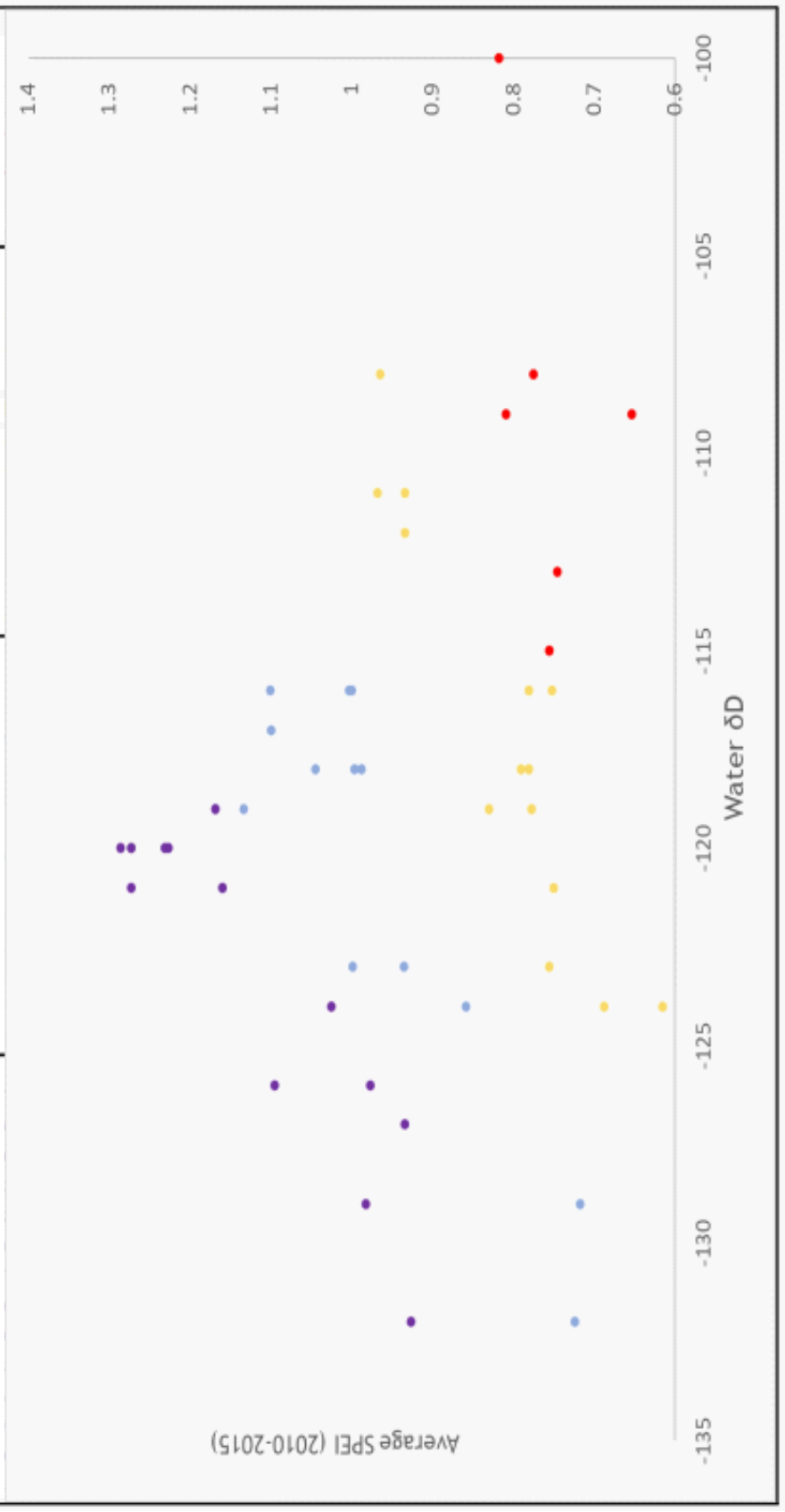


**Figure 6:** The graph on right shows clusters of data used to produce latitudinal separations, which are illustrated by colour on the left. Clusters of data were not exact functions of latitude but were used to distinguish latitudinal boundaries. Colours are coded in conjunction with figures X, except light blue which was divided further into smaller groups. Water δD = Bowen and Revenaugh's (2003) Online Isotopes in Precipitation Calculations.

| Lake | Latitude | Longitude | Water δD | SPEI 2010-2015 |
|---|---|---|---|---|
| Elk Water | 49.667 | -110.294 | -132 | 0.72 |
| Sufferin | 52.637 | -109.898 | -132 | 0.92 |
| Alsask | 51.337 | -109.876 | -129 | 0.71 |
| Bitter | 50.096 | -109.789 | -124 | 0.6 |
| Cypress | 49.472 | -109.473 | -124 | 0.68 |
| Mclean | 52.615 | -109.369 | -129 | 0.98 |
| Unknown3 | 50.649 | -108.971 | -123 | 0.7 |
| Eaglehill | 52.362 | -108.968 | -127 | 0.93 |
| Vincent | 50.222 | -108.944 | -121 | |
| Snipe | 51.233 | -108.858 | -124 | 0.85 |
| Tramping | 52.034 | -108.820 | -126 | 0.97 |
| Thackery | 52.542 | -108.686 | -126 | 1.09 |
| Opunitia | 51.808 | -108.573 | -123 | 0.93 |
| Shrimp | 51.591 | -108.451 | -123 | 0.99 |
| Antelope | 50.275 | -108.391 | -119 | 0.77 |
| Springwater | 52.012 | -108.388 | -124 | 1.0 |
| Lonetree | 49.081 | -108.258 | -115 | 0.75 |
| Island Lake | 49.129 | -108.22 | -115 | 0.75 |
| Lac Pelletier | 49.98 | -107.935 | -118 | 0.79 |
| Clearwater | 50.873 | -107.929 | -119 | 0.82 |
| Newton | 49.318 | -107.829 | -113 | 0.74 |
| X3 | 51.93 | -107.577 | -118 | 1.04 |
| Handsome | 50.489 | -107.383 | -116 | 0.75 |
| Luck | 51.069 | -107.100 | -116 | 1.00 |
| Redberry Lake | 52.621 | -107.01 | -120 | 1.22 |
| Pike | 51.897 | -106.816 | -116 | 1.09 |
| Blackstrap | 51.785 | -106.438 | -117 | 1.09 |
| Montague | 49.474 | -105.826 | -109 | 0.65 |
| Wakawa | 52.663 | -105.601 | -120 | 1.28 |
| Willow Bunch | 49.447 | -105.461 | -108 | 0.77 |
| Arthur | 52.563 | -105.4 | -120 | 1.27 |
| Shannon | 52.649 | -105.433 | -121 | 1.27 |
| Buffalo Pound | 50.608 | -105.426 | -111 | 0.93 |
| Shoe | 49.715 | -105.356 | -109 | 0.80 |
| Stoney Beach | 50.50 | -105.194 | -112 | 0.93 |
| Middle Lake | 52.562 | -105.194 | -120 | 1.27 |
| Deadmoose | 52.302 | -105.167 | -119 | 1.16 |
| Lenore | 52.508 | -104.974 | -120 | 1.22 |
| Porter | 51.464 | -104.913 | -116 | 0.99 |
| Edouard | 52.382 | -104.350 | -121 | 1.15 |
| Charron | 52.404 | -104.310 | -121 | 1.15 |
| Unknown4 (heron | 51.546 | -104.268 | -119 | 1.13 |
| katepwa | 50.709 | -103.646 | -111 | 0.96 |
| Horse Lake | 51.387 | -103.561 | -118 | 0.99 |
| Mc Donald | 49.193 | -103.243 | -100 | 0.81 |
| Good Spirit | 51.551 | -102.670 | -116 | 0.77 |
| Annie Laurie | 51.970 | -102.668 | -118 | 0.77 |
| White Bear | 49.773 | -102.257 | -108 | 0.96 |
| Madge | 51.654 | -101.634 | -118 | 0.9 |

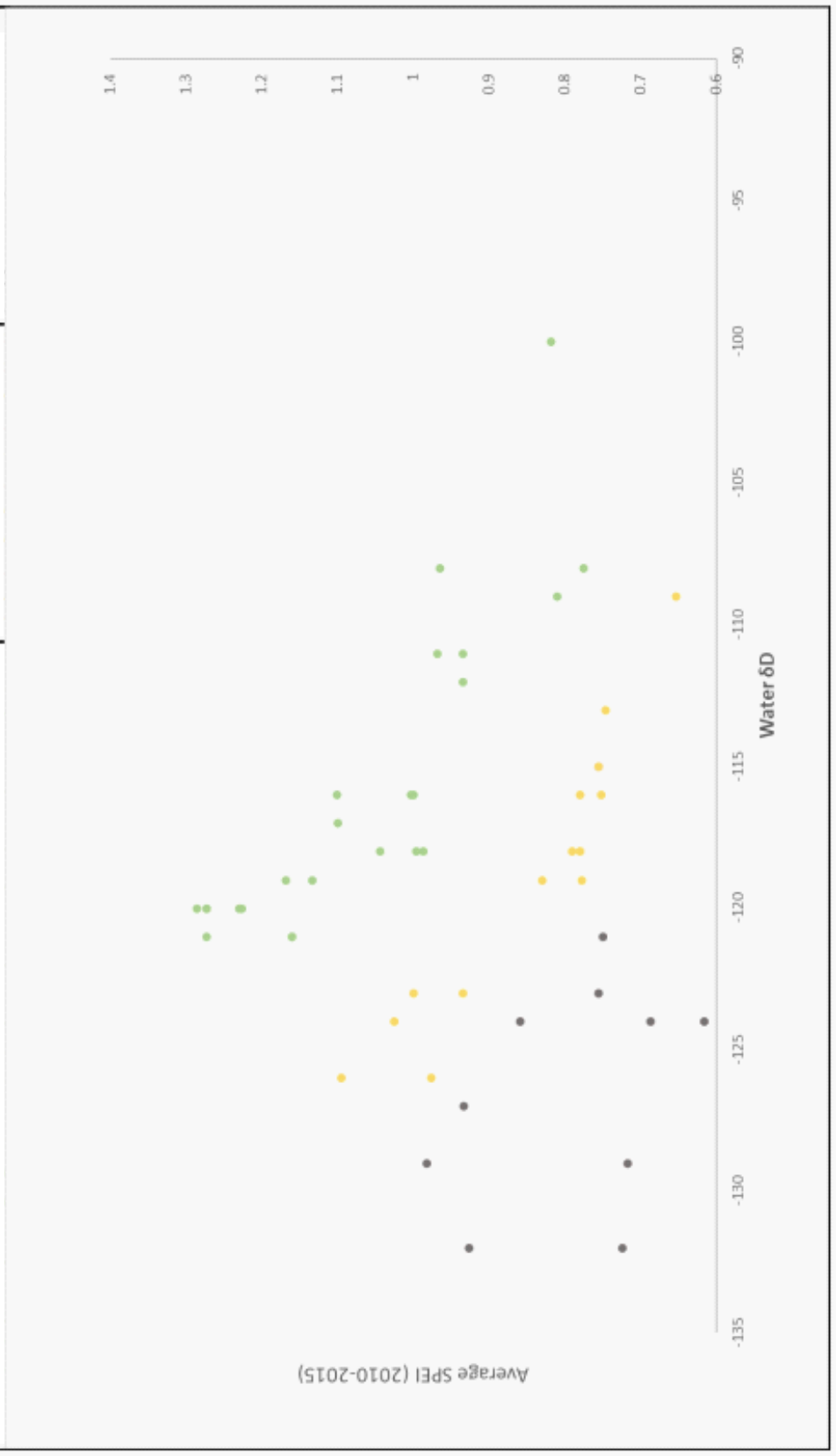


**Figure 7:** The graph on right shows clusters of data used to produce longitudinal separations, groups are coded by the same colour on the left. Clusters of data were not exact functions of longitude but were used to distinguish longitudinal boundaries. Colours are coded in conjunction with figures 18 and 19, except green which was divided further into smaller groups. Water δD = Bowen and Revenaugh's (2003) Online Isotopes in Precipitation Calculator results.

Following spatial separation by latitude and longitude, δD $C_{24}$ yielded strong correlations with SPEI, estimated precipitation δD, latitude, longitude, precipitation amount, temperature and elevation to varying degrees in five out of eight groups. The remaining three groups produced poor or no correlations.

The third group resultant of the latitudinal separation yielded no obvious relationships. Therefore, this group was divided further by longitude using two gradients produced when δD $C_{24}$ was plotted against precipitation (figure 16).

| Lake | Average δD | Latitude | Longitude | Elevation (m | Annual Ppt (mm) |
|---|---|---|---|---|---|
| Alsask | -161.13 | 51.34 | -109.88 | 638 | 306 |
| Snipe | -147.02 | 51.23 | -108.86 | 654 | 311 |
| Opunitia | -144.09 | 51.81 | -108.57 | 594 | 362 |
| Shrimp | -138.12 | 51.59 | -108.45 | 672 | 348 |
| X3 | -178.91 | 51.94 | -107.58 | 546 | 360 |
| Luck | -145.85 | 51.07 | -107.10 | 585 | 349 |
| Pike | -168.61 | 51.90 | -106.82 | 489 | 355 |
| Blackstrap | -164.34 | 51.79 | -106.44 | 534 | 367 |
| Porter | -186.15 | 51.46 | -104.91 | 519 | 379 |
| Heron | -129.92 | 51.55 | -104.27 | 648 | 432 |
| Horse Lake | -158.35 | 51.39 | -103.56 | 669 | 461 |
| Good Spirit | -145.18 | 51.55 | -102.67 | 485 | 454 |
| Annie Laurie | -163.05 | 51.97 | -102.67 | 508 | 467 |
| Madge | -180.78 | 51.65 | -101.63 | 614 | 485 |

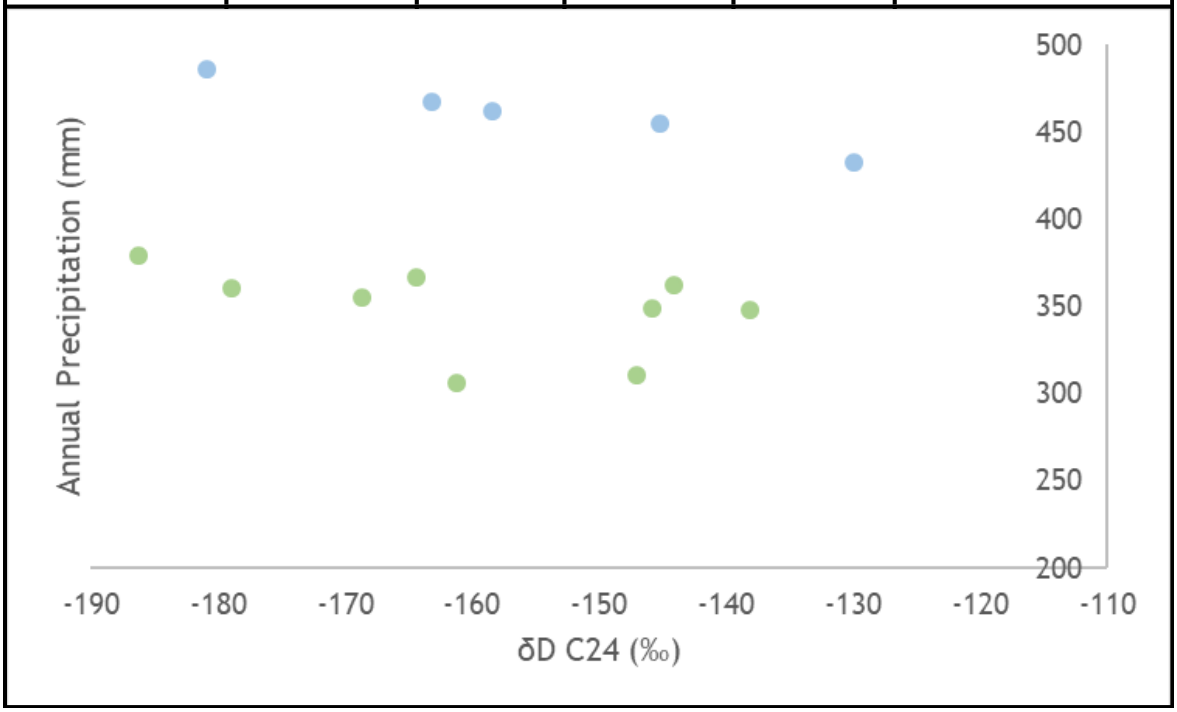


**Figure 8:** The graph on the bottom shows the two clusters of points produced by precipitation and δD $C_{24.}$ Clusters of points produced the longitudinal separations shown in the table. Colours are coded in conjunction with figures 18 and 19.

The third group from the longitudinal separation was divided into smaller groups using clusters of data produced when δD $C_{24}$ was plotted against latitude (figure 17). Data below 51˚degrees latitude produced reliable correlations; however, data above 51˚degrees latitude was divided further into an eastern and western section. Figure 18 shows the final separation of Group B lakes. Lake co-ordinates have been plotted on ArcMap over a topographical map.

| Lake | δD C24 | Latitude | Longitude | Water δD |
|---|---|---|---|---|
| Mc Donald | -156.7162924 | 49.193596 | -103.243156 | -100 |
| Willow Bunch | -183.6636886 | 49.447147 | -105.461304 | -108 |
| Montague | -141.3892244 | 49.474371 | -105.826202 | -109 |
| Shoe | -165.4658941 | 49.715906 | -105.356316 | -109 |
| White Bear | -165.4658941 | 49.773227 | -102.257477 | -108 |
| Handsome | -171.8250311 | 50.489624 | -107.383293 | -116 |
| Stoney Beach | -199.1193416 | 50.50326 | -105.194847 | -112 |
| Buffalo Pound | -224.3990682 | 50.608245 | -105.426537 | -111 |
| katepwa | -206.3072198 | 50.709939 | -103.646446 | -111 |
| Luck | -145.8495146 | 51.069232 | -107.100616 | -116 |
| Horse Lake | -158.3470183 | 51.387156 | -103.561981 | -118 |
| Porter | -186.1477891 | 51.464382 | -104.913696 | -116 |
| Unknown4 (heron) | -129.9178834 | 51.546535 | -104.268456 | -119 |
| Good Spirit | -145.1769966 | 51.551032 | -102.670776 | -116 |
| Madge | -180.7777307 | 51.654347 | -101.634552 | -118 |
| Blackstrap | -164.3375611 | 51.785259 | -106.438293 | -117 |
| Pike | -168.6089339 | 51.897708 | -106.816895 | -116 |
| X3 | -178.9093633 | 51.93777 | -107.577721 | -118 |
| Annie Laurie | -163.0545779 | 51.970037 | -102.668182 | -118 |
| Deadmoose | -202.2095619 | 52.302819 | -105.167259 | -119 |
| Edouard | -191.5531243 | 52.382578 | -104.350311 | -121 |
| Charron | -190.4119289 | 52.404288 | -104.310143 | -121 |
| Lenore | -138.3799532 | 52.508747 | -104.974167 | -120 |
| Middle Lake | -171.8000954 | 52.562869 | -105.194595 | -120 |
| Arthur | -208.1627133 | 52.563928 | -105.4431 | -120 |
| Redberry Lake | -179.5406138 | 52.621283 | -107.01889 | -120 |
| Shannon | -188.2932708 | 52.649965 | -105.433426 | -121 |
| Wakawa | -184.8012689 | 52.663265 | -105.601006 | -120 |

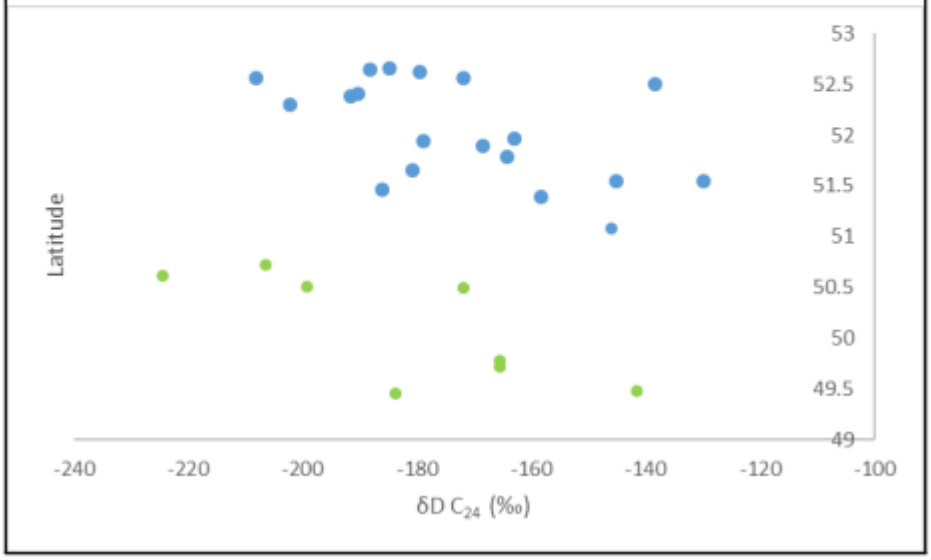


**Figure 9: The** graph shows the two groups produced by latitude and δD $C_{24}$.

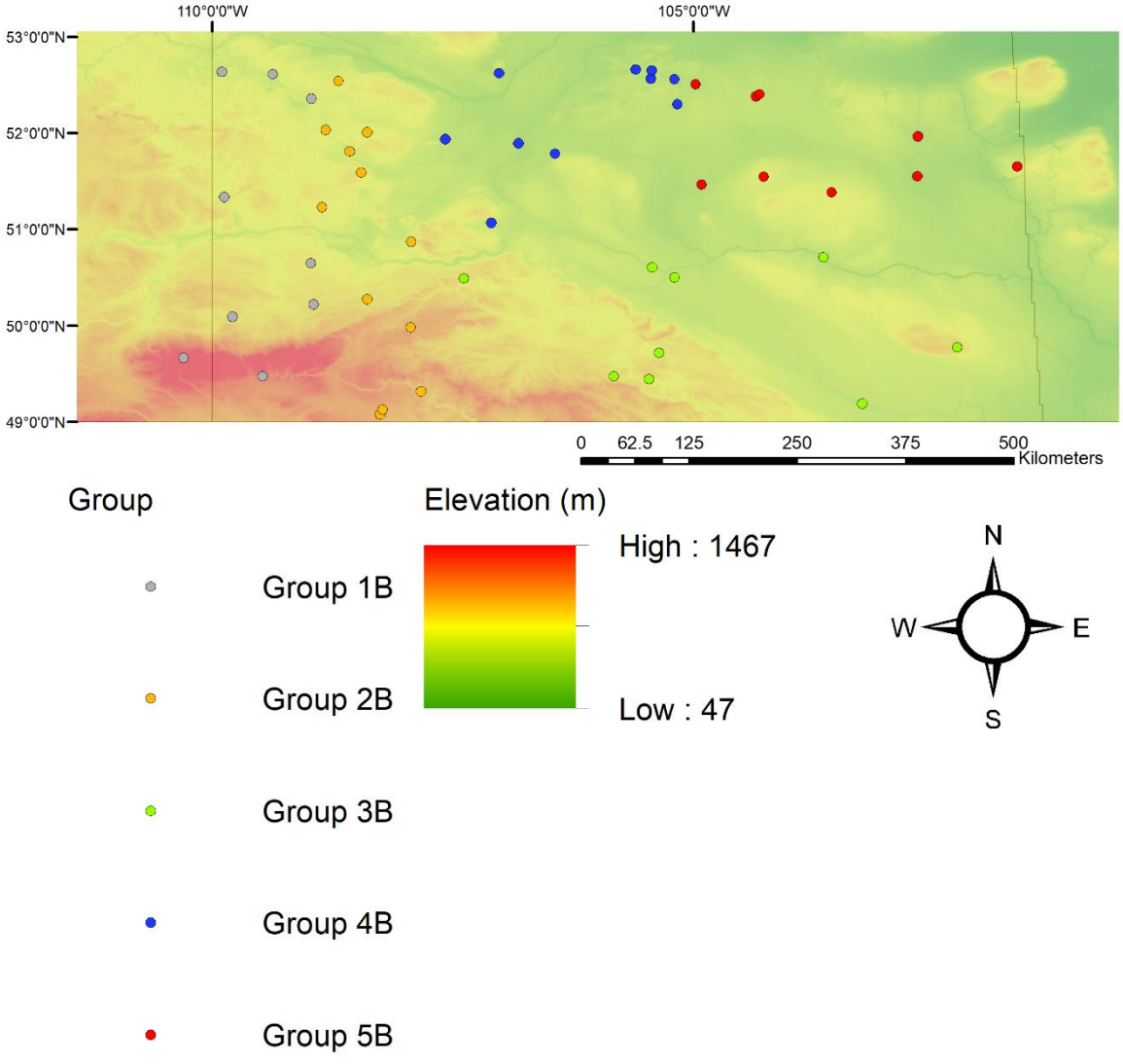


**Figure 10:** The final spatial separation of lakes in Group B.

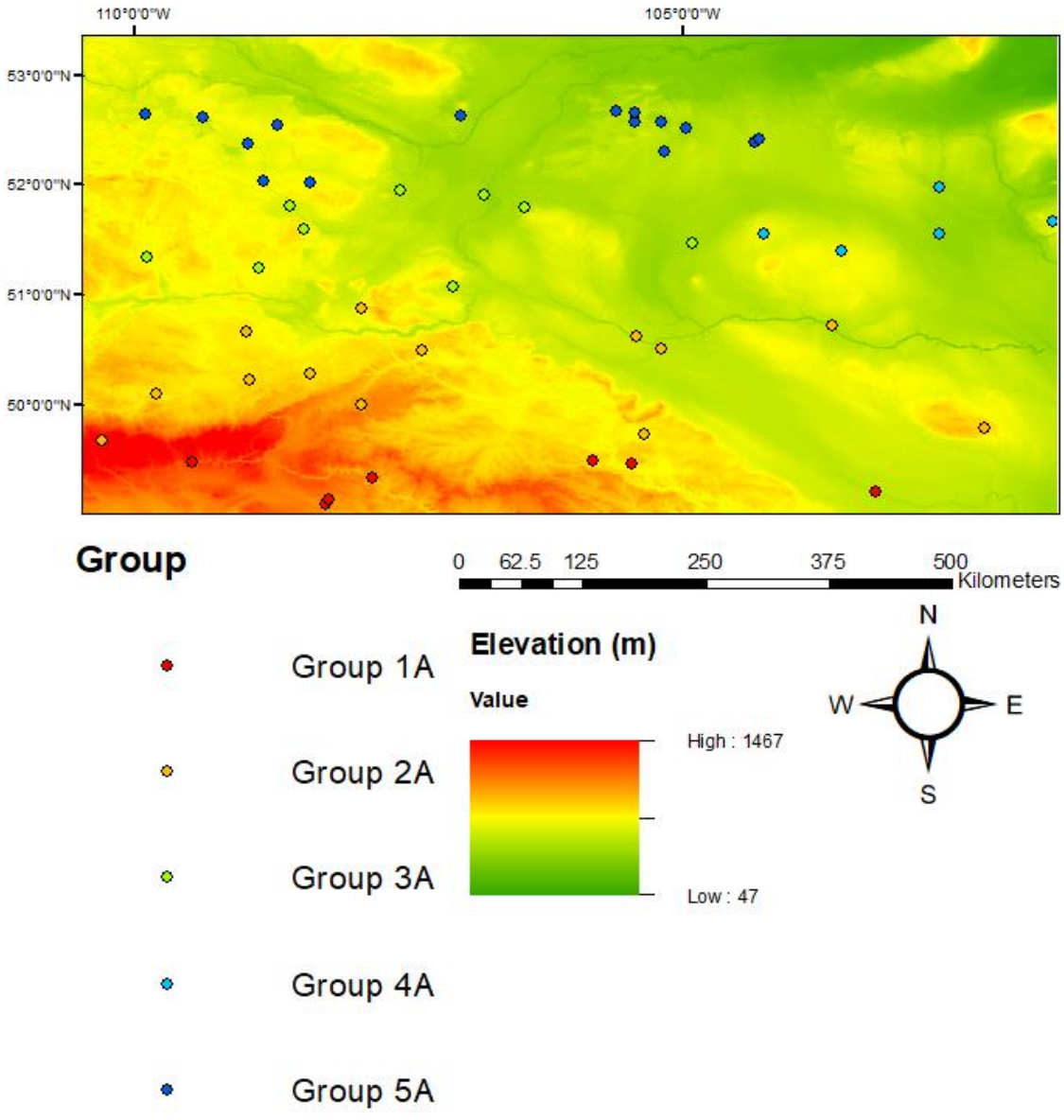


**Figure 11:** Final Spatial separation for Group A lakes.

### 2.5.2 ArcGIS

Once the environmental variables for each lake with quantifiable measures of $C_{24}$ were gathered, they were compiled into an excel spreadsheet. This was then transferred to ArcMap, a geospatial processing program that is a component of ArcGIS. Shapefiles were downloaded from the Government of Canada website [accessable at https://open.canada.ca/]. Each shapefile was set to the coordinate reference system WGS1984 in order to correctly position each lake on the map.

# Chapter 3 Results

This study finds there is a strong link between the δD $C_{24}$ of lake surface sediment samples and various environmental variables such as SPEI, the δD of precipitation, precipitation amount, temperature, latitude, longitude and elevation. Figures 21-24 show linear regression analysis for selected environmental variables, table 2 and table 3 summarise all analysis undertaken within groups.

### 3.1.1 Outlier Analysis

Clear correlations exist between δD $C_{24}$ and environmental variables when lakes are grouped into spatial zones. Despite the overall identification of correlations, some data did not fit a linear regression model. However, statistical analysis using the software 'R' (R Core Team, 2013), undertaken to prove the validity of the model highlighted several data points were outliers. Elkwater Lake, Whitebear Lake and Peter Lake all have a poor fit to linear regression models and were each statistically identified as outliers during statistical outlier analysis. The environmental reasons causing these lakes to differ are discussed in section 4.4.1.

### 3.1.2 Long Chain *n*-alkanoic Acids

*n*-alkanoic acids were quantifiable in 76 out of the 89 samples analysed, ranging in chain lengths from $C_{14}$ to $C_{32}$ with a strong even over odd predominance, suggesting they have not been degraded and reflect terrestrial sources. Long chain *n*-alkanoic acids dominate with $C_{24}$ as the most abundant chain length, found in 59 samples. Samples in which $C_{24}$ could not be identified usually have large contaminate peaks which are formed at approximately the same time as $C_{24}$ *n*-alkanoic acid. Co-elution is most common in lower chain lengths, particularly around $C_{16}$ and $C_{18}$ where chromatograms are noisy. However, chain lengths $C_{24}$, $C_{26}$ and $C_{28}$ were of interest as they are of terrestrial origin and produced by characteristic Prairie grasses (Otto and Simpson, 2005). Conversely, short-chain *n*-alkanoic acids ($C_{12}$ to $C_{18}$) are synthesised by both plants and microorganisms and may have convoluted sources which may complicate analysis (Harwood and Russel, 1984).

### 3.1.3 *n*-$C_{28}$ Alkanoic Acid

The $C_{28}$ acid occurred in 42 out of 76 (55%) samples, in the lowest concentrations of the three chain lengths of interest, with frequent co-elution occurring on either side of the $C_{28}$ peak. Samples with poorly defined peaks, and therefore lots of co-elution, often exhibited atypical δD values relative to other chain lengths.

### 3.1.4 *n*-$C_{26}$ Alkanoic Acid

The $C_{26}$ acid was present in 53 out of 76 (70%) samples and was generally well defined showing much less co-elution than the $C_{28}$ acid but more co-elution than the $C_{24}$ acid. In addition, the $C_{26}$ acid was also present in much higher concentrations than the $C_{28}$ acid but generally lower concentrations than the $C_{24}$ acid.

### 3.1.5 *n*-$C_{24}$ Alkanoic Acid

The $C_{24}$ acid was present in 59 out of 76 (78%) samples, however only 49 of those samples were used after 10 were omitted for reasons discussed in section 4.1.3. $C_{24}$ was consistently well defined and only occasionally showed minor co-elution. Concentrations of $C_{24}$ were higher than those of $C_{26}$ and $C_{28}$.

### 3.1.6 Linear Regression Analysis

δD $C_{24}$ values ranged from -224.4‰ to -129.9‰ with northerly lakes tending to exhibit lighter δD $C_{24}$ values. When considering the study area as a whole, spatial patterns in δD $C_{24}$ are particularly ambiguous and much harder to discern than in the results obtained from the OIPC calculations. Average annual δD precipitation ($\delta D_{ppt}$) values, calculated from the OIPC, ranged from -132‰ to -100‰, with a clear and gradual shift from heavy in the south east to light in the north west. Similarly, the results calculated for the average SPEI from 2010 to 2015 showed a distinct pattern of low (arid) in the south west transitioning into higher (humid) values in the northeast. SPEI values ranged from 0.6 to 1.3. See section 2.3.3 for information on SPEI calculation.

δD $C_{24}$ produced moderate to strong negative correlations with SPEI in 5 out of 10 groups with aridity resulting in more positive δD $C_{24}$. Correlations with the SPEI occurred to varying degrees in both the latitudinal and longitudinal separations.

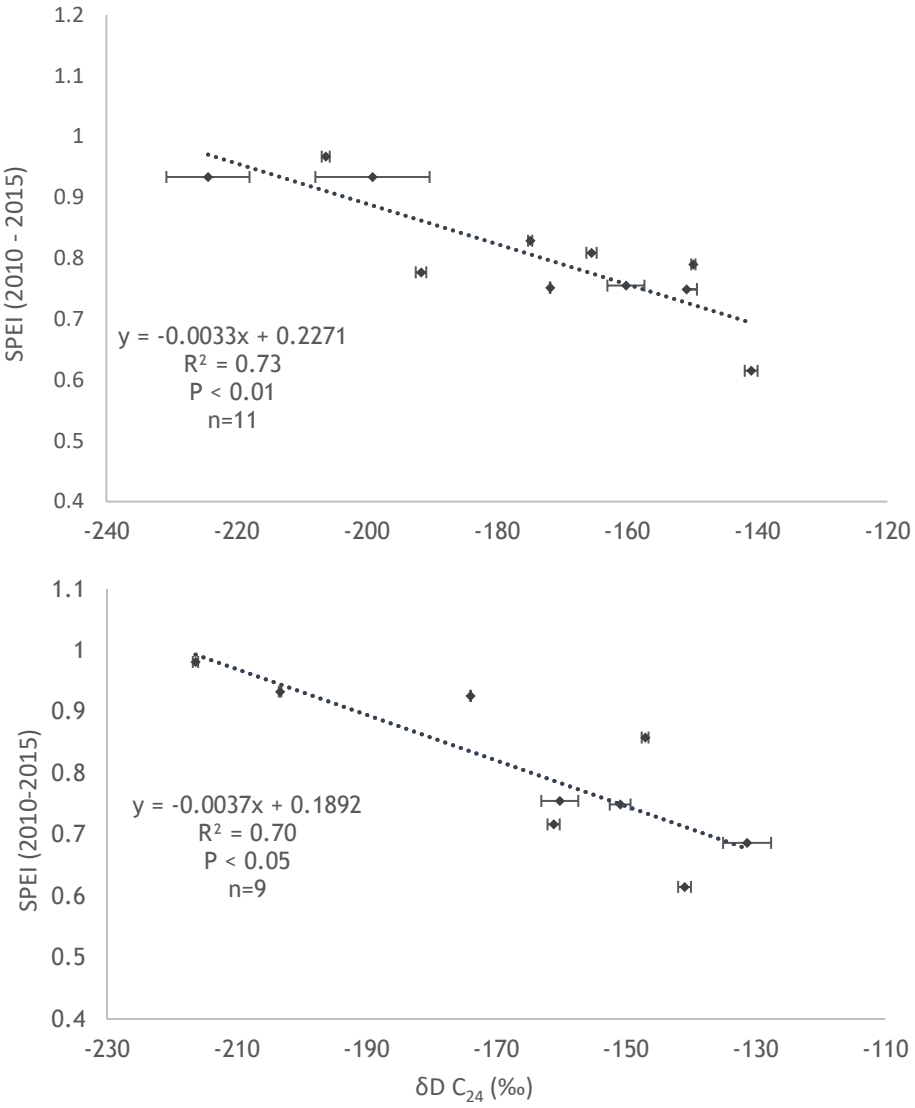


**Figure 12:** Linear regression analysis for δD $C_{24}$ vs SPEI (2010-2015) in Group 2A (top) and Group 1B (bottom). Lower SPEI indicates aridity.

Linear regression analysis of δD $C_{24}$ vs the δD of precipitation exhibited strong but complex relationships. The δD of precipitation was strongly negatively correlated with δD $C_{24}$ in some groups and strongly positively correlated with δD $C_{24}$ in others. Nevertheless, there was a significant relationship between the δD of precipitation and δD $C_{24}$. In addition to this, strong negative correlations were found with precipitation amount. As with the δD of precipitation, the strength of correlation with precipitation amount varies between seasons, but is weakest in spring (table 1). Groups correlating with a seasonal precipitation amount do not always correlate with the equivalent seasonal precipitation δD.

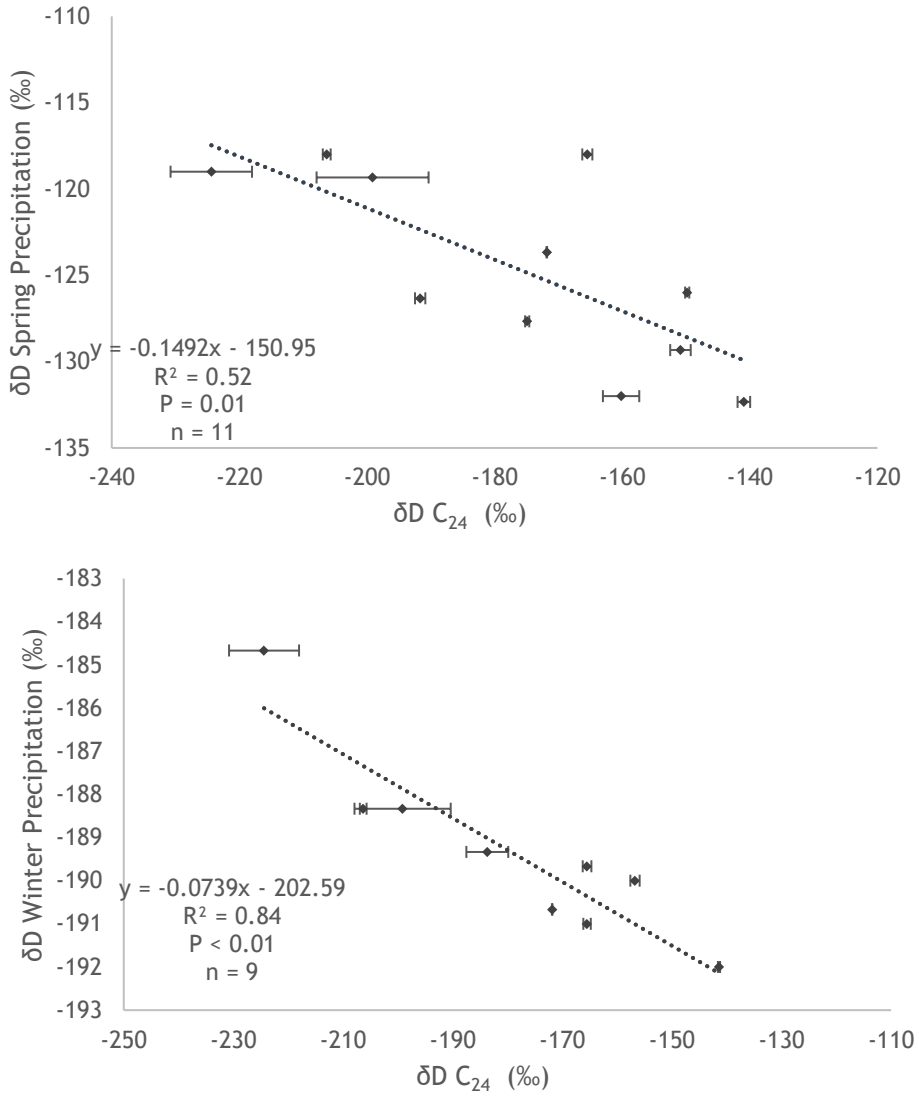


**Figure 13:** Linear regression analysis showing the relationship between the δD of precipitation and δD $C_{24}$ in Group 2A (top) and Group 3B (bottom).

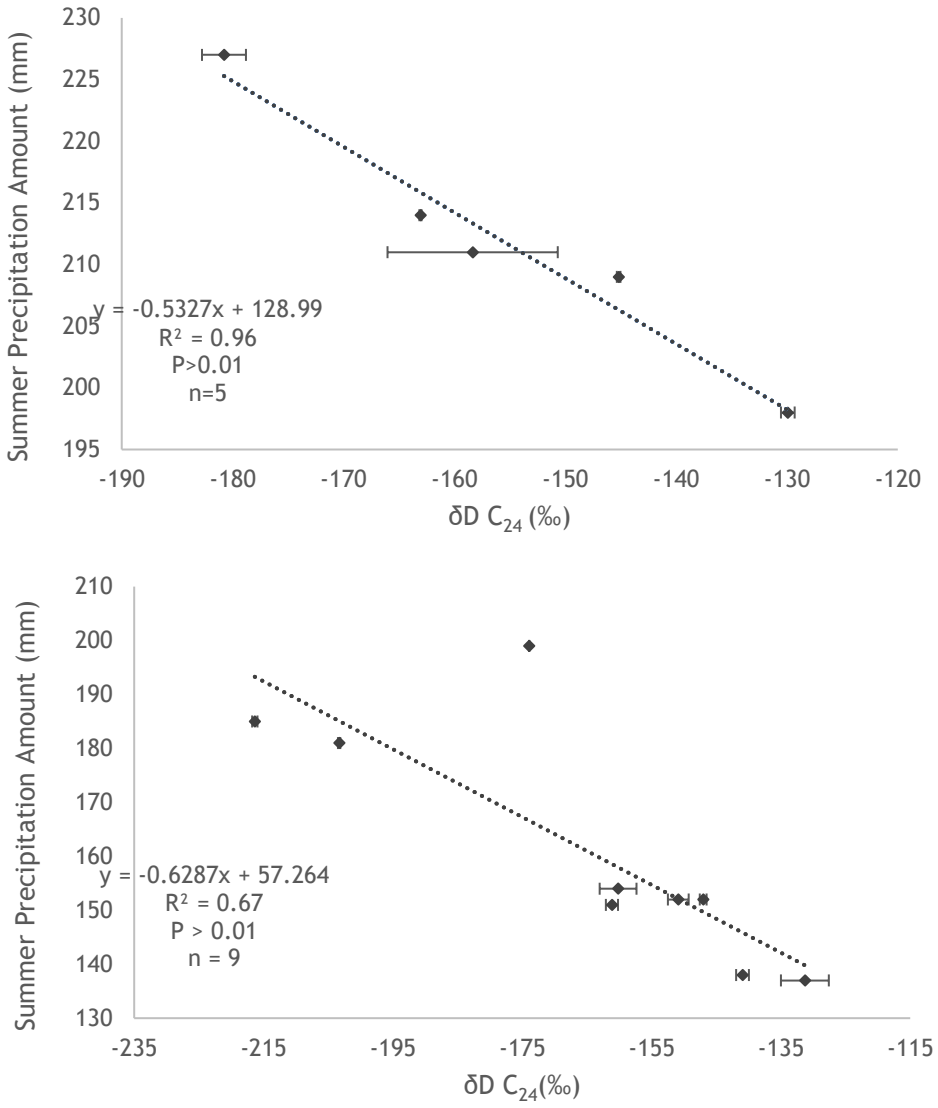


**Figure 14:** Linear regression analysis showing the relationship between precipitation amount and $\delta D\ C_{24}$ for Group 4A (top) and Group 1B (bottom).

Strong relationships exist between δD $C_{24}$ and seasonal temperature. In all cases higher temperatures are associated with more positive δD $C_{24}$. The strongest relationships exist within Group 4A, for which δD $C_{24}$ produced significant correlations with temperatures in all seasons, in particular winter and autumn (fig. 23).

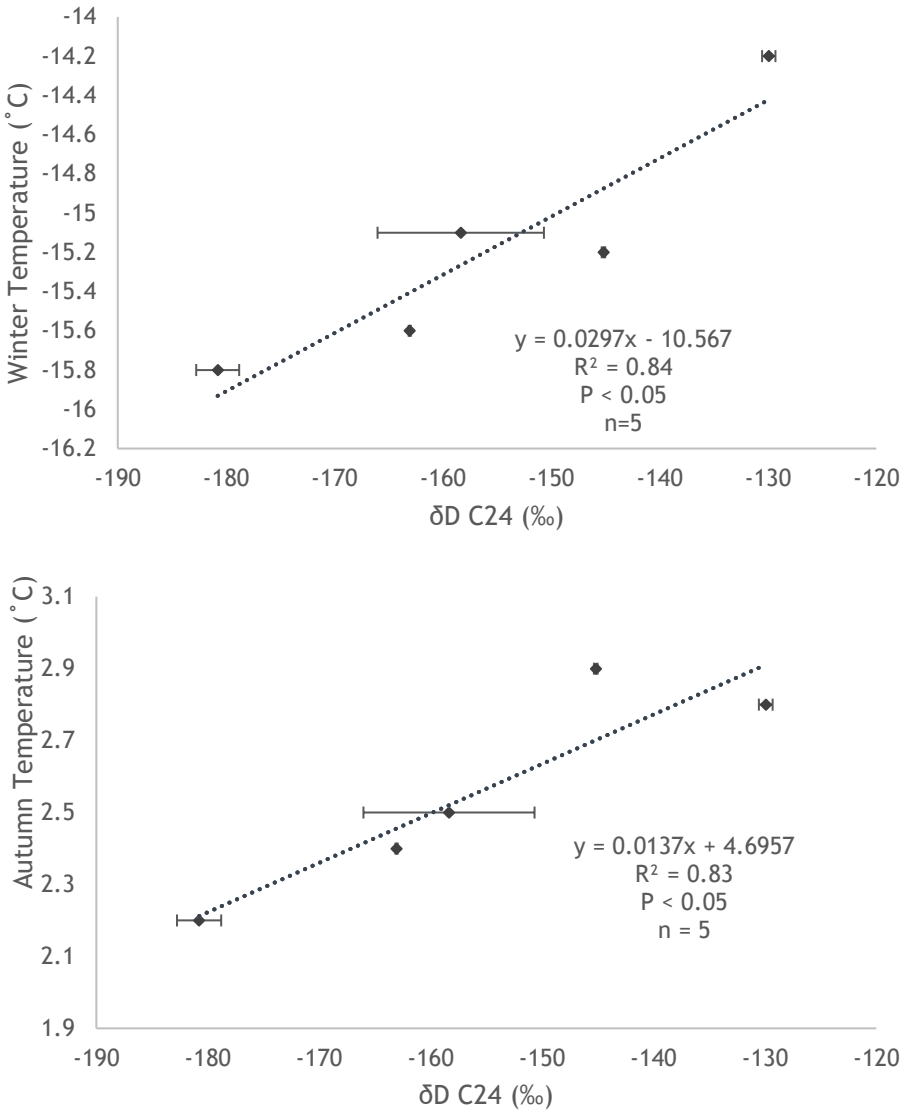


**Figure 15:** Linear regression analysis showing the relationship between winter and autumn temperature and δD $C_{24}$ in Group 4A.

Latitude and longitude produce moderate to strong correlations with δD $C_{24}$. Groups show a relationship with either latitude or longitude, however relationships with latitude are stronger and occur more frequently (tables 2 and 3). All groups in which there is a relationship with latitude or longitude show δD $C_{24}$ decreasing with distance from source. Finally, strong positive correlations exist between δD $C_{24}$ and elevation (fig. 24). This is unexpected as most literature reports stable isotopic ratios decreasing with increasing elevation. Tables X and X below report all results obtained from linear regression analysis.

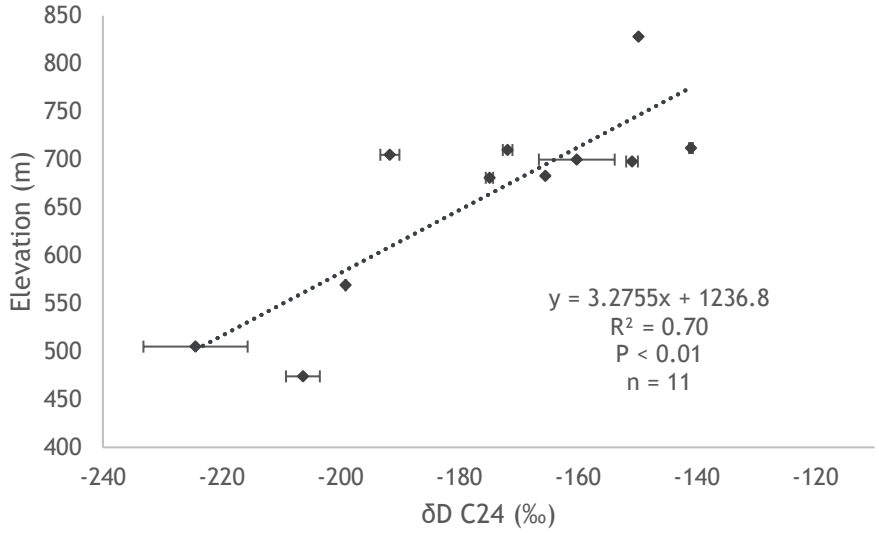


**Figure 16:** Linear regression analysis showing the relationship between elevation and δD $C_{24}$ within Group 2A

| Group | Winter precipitation amount (mm) | Spring precipitation amount (mm) | Summer precipitation amount (mm) | Autumn precipitation amount (mm) | Winter precipitation δD (‰) | Spring precipitation δD (‰) | Summer precipitation δD (‰) | Autumn precipitation δD (‰) |
|---|---|---|---|---|---|---|---|---|
| **1A** | $R^2$=0.11, P=0.04 | $R^2$=0, P=0.03 | R2=0, P=0.06 | R2=0, P=0.06 | R2=0.17, P=0.36 | R2=0.07, P=0.56 | R2=0.08, P=0.54 | R2=0.08, P=0.55 |
| **2A** | $R^2$=0.25, P=0.12 | $R^2$=0.25, P=0.12 | **$R^2$=0.62, P=>0.01** | **$R^2$=0.41, P=0.03** | $R^2$=0, P=0.91 | **$R^2$=0.52, P=0.01** | **$R^2$=0.41, P=0.04** | **$R^2$=0.46, P=0.02** |
| **3A** | R2=0.04, P=0.59 | R2=0, P=0.82 | R2=0.22, P=0.2 | R2=0.42, 0.06 | R2=0, P=0.96 | R2=0, P=0.64 | R2=0.02, P=0.64 | R2=0.01, P=0.78 |
| **4A** | **$R^2$=0.82, P=0.03** | $R^2$=0.02, P=0.81 | **$R^2$=0.95, P=0.004** | **$R^2$=0.91, P=0.01** | $R^2$=0.32, P=0.30 | $R^2$=0, P=0.95 | $R^2$=0.05, P=0.71 | $R^2$=0.05, 0.72 |
| **5A** | $R^2$=0.09, P=0.27 | $R^2$=0.03, P=0.54 | $R^2$=0.08, P=0.31 | $R^2$=0.08, P=0.33 | $R^2$=0.01, P=0.78 | $R^2$=0.03, P=0.55 | $R^2$=0.03, P=0.57 | $R^2$=0.03, P=0.55 |
| **1B** | $R^2$=0.02, P=0.75 | $R^2$=0.05, P=0.56 | **$R^2$=0.67, P=0.007** | $R^2$=0.22, P=0.20 | **$R^2$=0.56, p=0.02** | $R^2$=0.42, P=0.06 | **$R^2$=0.44, P=0.05** | **$R^2$=0.51, P=0.03** |
| **2B** | $R^2$=0, P=0.098 | $R^2$=0.02, P=0.69 | $R^2$=0.05, P=0.52 | $R^2$=0.02, P=0.20 | $R^2$=0.01, P=0.78 | $R^2$=0.02, P=0.69 | $R^2$=0.02, P=0.70 | $R^2$=0.01, P=0.73 |
| **3B** | $R^2$=0, P=0.87 | $R^2$=0.03, P=0.66 | $R^2$=0, P=0.97 | $R^2$=0, P=0.88 | **$R^2$=0.84, P=0** | $R^2$=0.35, P=0.09 | **$R^2$=0.5, P=0.03** | **$R^2$=0.55, P=0.02** |
| **4B** | **$R^2$=0.43, P=0.04** | $R^2$=0.31, P=0.10 | **$R^2$=0.56, P=0.01** | **$R^2$=0.50, P=0.02** | **$R^2$=0.59, P=0.01** | $R^2$=0.39, P=0.06 | **$R^2$=0.50, P=0.02** | **$R^2$=0.58, P=0.01** |
| **5B** | $R^2$=0.30, P=0.16 | $R^2$=0.05, P=0.60 | $R^2$=0.01, P=0.41 | $R^2$=0.49, P=0.06 | **$R^2$=0.61, P=0.02** | $R^2$=0.15, P=0.34 | $R^2$=0.12, P=0.41 | $R^2$=0.14, P=0.36 |

Table 2: Linear regression model results for δD $C_{24}$ with precipitation amount and precipitation δD calculated from the OIPC (Bowen and Revenaugh, 2003). Unshaded numbers in bold represent significant correlations.

| Group | Latitude | Longitude | Elevation | SPEI (2010 – 2015) | Average Winter Temperature (˚C) | Average Spring Temperature (˚C) | Average Summer Temperature (˚C) | Average Autumn Temperature (˚C) |
|---|---|---|---|---|---|---|---|---|
| **1A** | $R^2$=0.19, P=0.33 | $R^2$=0.03, P=0.73 | $R^2$=0.08, P=0.53 | $R^2$=0.39, P=0.13 | $R^2$=0.05, P=0.88 | $R^2$=0.27, R=0.23 | $R^2$=0.30, P=0.21 | $R^2$=0.30, P=0.21 |
| **2A** | $R^2$=0.27, P=0.1 | **$R^2$=0.55, P=0.01** | **$R^2$=0.70, 0.001** | **$R^2$=0.73, P=0.001** | **$R^2$=0.67, P=0.002** | $R^2$=0.25, P=0.12 | **$R^2$=0.62, P=0.004** | **$R^2$=0.44, 0.03** |
| **3A** | $R^2$=0.13, P=0.35 | $R^2$=0.38, P=0.08 | **$R^2$=0.56, P=0.02** | $R^2$=0.08, P=0.47 | $R^2$=0.42, P=0.06 | **$R^2$=0.45, P=0.05** | $R^2$=0.05, P=0.86 | $R^2$=0.07, P=0.5 |
| **4A** | $R^2$=0.11, P=0.59 | $R^2$=0.71, P=0.07 | $R^2$=0, P=0.96 | $R^2$=0.02, P=0.66 | **$R^2$=0.84, P=0.03** | **$R^2$=0.72, P=0.07** | **$R^2$=0.48, P=0.2** | **$R^2$=0.83, P=0.03** |
| **5A** | $R^2$=0.03, P=0.56 | $R^2$=0.05, P=0.42 | $R^2$=0.04, P=0.46 | $R^2$=0.08, P=0.31 | $R^2$=0.07, P=0.34 | $R^2$=0.08, P=0.31 | $R^2$=0.02, P=0.60 | $R^2$=0.03, P=0.54 |
| **1B** | **$R^2$=0.75, P=0.002** | $R^2$=0.09, P=0.81 | **$R^2$=0.47, P=0.04** | **$R^2$=0.70, P=0.005** | **$R^2$=0.73, P=0.004** | **$R^2$=0.50, P=0.03** | $R^2$=0.28, P=0.14 | **$R^2$=0.52, P=0.03** |
| **2B** | $R^2$=0.02, P=0.70 | $R^2$=0.04, P=0.54 | $R^2$=0.02, P=0.71 | $R^2$=0.01, P=0.75 | $R^2$=0.02, P=0.72 | $R^2$=0.08, P=0.79 | $R^2$=0.01, P=0.78 | $R^2$=0.02, P=0.69 |
| **3B** | **$R^2$=0.60, P=0.03** | $R^2$=0.01, P=0.79 | **$R^2$=0.51, P=0.05** | **$R^2$=0.75, P=0.01** | $R^2$=0.43, P=0.08 | $R^2$=0.24, P=0.22 | $R^2$=0.15, P=0.34 | **$R^2$=0.60, 0.02** |
| **4B** | $R^2$=0.56, P=0.01 | $R^2$=0.36, P=0.07 | $R^2$=0.14, 0.30 | $R^2$=0.41, P=0.05 | $R^2$=0.62, P=0.01 | $R^2$=0.58, P=0.01 | $R^2$=0.53, P=0.02 | $R^2$=0.56, P=0.01 |
| **5B** | $R^2$=0.15, P=0.35 | $R^2$=0.03, P=0.67 | $R^2$=0, P=0.94 | $R^2$=0.01, P=0.82 | $R^2$=0.45, P=0.07 | $R^2$=**0.**41, P=0.09 | $R^2$=**0.**42, 0.08 | **$R^2$=0.74, P=0.01** |

Table 3: Linear regression results for δD $C_{24}$ with seasonal temperature variables, SPEI, latitude, longitude and elevation. Unshaded numbers in bold are significant correlations.

# Chapter 4 Discussion

## 4.1 Long Chain *n*-alkanoic Acids

### 4.1.1 *n*-$C_{28}$ Alkanoic Acid

Initially *n*-$C_{28}$ was tested with each environmental parameter as it is a long chain alkanoic acid typically produced by terrestrial higher plants (Makou et al., 2007) and therefore is likely to have a slightly less complicated signal than lower chain lengths produced by aquatic plants. In most samples for which the $C_{28}$ acid was present, co-elution occurred before and after the peak suggesting the hydrogen isotope signature was likely convoluted and not the true δD $C_{28}$ value. Due to the large number of samples with this specific pattern, it can be hypothesised that this is likely caused by other compounds with a similar retention time which are commonly found in Canadian lakes.

### 4.1.2 *n*-$C_{26}$ Alkanoic Acid

The $C_{26}$ acid exhibited generally reliable characteristics, therefore it can be postulated that a successful calibration would be possible with the $C_{26}$ alkanoic acid in the Canadian Prairies. However, due to time constraints and the reliability of results produced using the $C_{24}$ alkanoic acid this hypothesis was not tested.

### 4.1.3 *n*-$C_{24}$ Alkanoic Acid

The $C_{24}$ acid produces significant correlations with all environmental parameters. Previous literature (e.g. Gao et al., 2011) reports mid chain lengths ($C_{20}$ to $C_{24}$) as being characteristic of submerged and floating aquatic plants. However, the findings of Thomas et al. (2012) show that turbidity in lakes, caused by glacial inflows, inhibit the growth of aquatic plants, therefore terrestrial plants can produce chain lengths as low as $C_{22}$. Other studies in the U.S. Northern Great Plains analysed grasses growing in the catchment of prairie lakes, results showed that $C_{24}$ dominates in the fresh grass material (Toney, 2011). Furthermore, it is reasonable to conclude that, due to strong correlations with precipitation amount and precipitation δD, $C_{24}$ is derived from terrestrial plants. Had $C_{24}$ been derived from aquatic plants the effect of evaporation would have likely meant that correlations would have been stronger with indices accounting for evaporation.

## 4.2 Drought Indices

### 4.2.1 PDSI, CMD, SPI and SPEI

For the purpose of this study, the Palmer Drought Severity Index (PDSI) (Palmer, 1965) was investigated as a potential parameter to be compared with δD $C_{24}$. The PDSI is a previously widely used index that addresses the intensity and timing of droughts (Alley, 1984), and was one of the first successful methods of quantifying the severity of droughts across different climates (Wells et al., 2004). As with the SPEI, the PDSI is based on a water balance model, however, while the PDSI has the potential to correlate with the measured δD $C_{24}$ of surface sediments, it has been criticised for its random nature due to its inability to account for variability in precipitation between locations (Wells et al., 2004). Other limitations of the PDSI are that it is more qualitative than quantitative (Heddinghaus and Sabol, 1991) and is not comparable between diverse climatological regions (Wells et al., 2004). The PDSI was a widely used, but now dated drought index, which has provided an important steppingstone for contemporary, quantitative drought indices to be developed. Comparatively, the SPEI has a higher spatial resolution than the PDSI (0.5˚ compared to 2.5˚), is easier to calculate and allows different types of drought to be characterised due to its multi-scalar nature (Beguería et al., 2014; Vicente-Serrano, 2010). Therefore, the PDSI was discounted as a parameter that would be correlated with $C_{24}$ δD values.

The Climatic Moisture Deficit (CMD) is an aridity metric that accounts for precipitation and evapotranspiration and is primarily used in agriculture as it denotes the moisture required to be delivered by other sources such as irrigation to meet the requirements of vegetation growth (Girvetz and Zganjar, 2014). The CMD was calculated using ClimateWNA (see Wang, 2012) and is the sum of the difference between reference atmospheric evaporative demand ($E_{ref}$) and precipitatioin. If $E_{ref}$ is less than precipitation then the monthly CMD is zero, and the precipitation minus the $E_{ref}$ is the Climatic Moisture Surplus (CMS) (Wang, 2012). However, the CMD is primarily used for agricultural purposes and has the potential to produce measurements of 0 which would not be conducive to producing a successful linear regression model. Therefore, the CMD was discounted as a parameter.

The Standardised Precipitation Index (SPI) is a probability index that aimed to improve on the Palmer Indices (Guttman, 1999). The SPI is a well-tested index of drought severity, which measures accumulated precipitation (Stagge et al., 2015), however it is also advocated as a useful indicator of wetness and aridity (Guttman, 1999). In comparison, the Standardised Precipitation-Evapotranspiration Index (SPEI) is a more contemporary index measuring climatic water balance and accounts for the difference between precipitation and potential evapotranspiration (PET) (eqn. 2) (Vicente-Serrano, 2010). Therefore, the SPEI is a multi-temporal and simplistic index, that accounts for variables that the SPI does not such as humidity, wind speed and temperature (Stagge et al., 2015), thus the SPEI accounts for vital factors which have the potential to affect the δD $C_{24}$ of surface sediments.

$$D = P - \mathrm{PET}$$

Equation 2: SPEI Calculation where *D* is the difference between precipitation and PET (potential evapotranspiration), *P* is the monthly precipitation (mm) and PET (mm) is calculated using Thornthwaite's (1948) method using mean monthly temperature and the location of interest (Vicente-Serrano, 2010).

A detailed account of the calculation method can be found in Vicente-Serrano et al. (2010). A goodness of fit of a global SPEI dataset concludes the SPEI calculation is appropriate for most regions, independent of the month and timescale of analysis. Exceptions are regions in which there is poor data availability (Greenland, the Himalayas and northern Siberia) (Vicente-Serrano, 2010). After careful consideration of each of the investigated drought indices, it was apparent that the SPEI was the most appropriate index for the purpose of this study.

### 4.2.2 Choosing the 'right' SPEI

The SPEI produced strong correlations with δD $C_{24}$ in several groups (see section 2.3.3 for SPEI calculation). Furthermore, it was central in understanding regional climatic conditions and ultimately helped explain some of the challenges presented by the data. It is important to acknowledge that the values presented here for the SPEI were calculated as an annual average between 2010 and 2015, thus it is important to consider:

1. Depending on the sediment accumulation rate of each individual lake, the sediment sample taken could potentially represent organic matter that is a composite of a considerably longer period than 5 years. Therefore, it is highly likely that many of the sediment samples taken from the sampled lakes consist of sediment that is older than the period for which the SPEI was calculated. However, calculating sediment accumulation rates for 49 lakes and adjusting the SPEI calculation accordingly would be extremely time consuming, furthermore such data was not available for this study. Unless the method above is used, which requires a large amount of data, an estimation of the period over which to calculate the SPEI must be made. This estimation will never accurately account for all lakes. Following the initial 2010 to 2015 SPEI calculation, the average SPEI between 1980 and 2015 was calculated. This SPEI calculation yielded particularly poor correlations, therefore, it was assumed the initial 5-year period is likely more appropriate for the lakes examined.

2. The SPEI was calculated as an annual average. Despite moderate to strong correlations with δD $C_{24}$, if the SPEI was calculated as seasonal averages, it is highly likely that much stronger correlations would have been produced. For example, the SPEI could be calculated for the growing season alone, and values for the rest of the year neglected. In addition to this, seasonal SPEI values would provide a better understanding of climatic seasonal variation at specific sites and for the study area. However, in order to produce a calibration with seasonal averages, such as δD with growing season, a different methodology should be used to separate lakes that considers lake hydrology as opposed to the method used in this study. For

example, lakes which are predominantly supplied with spring meltwater or groundwater are unlikely to correlate with growing season SPEI.

## 4.3 Spatial Interpolation of Isotopic Precipitation Data

There are several potential influences on the δD recorded in plant leaf waxes. Influences are linked to the source water that the plants use, for instance, direct local precipitation is an important source of water for vegetation growth, although certain areas are also influenced by indirect precipitation via spring meltwater and subsurface water flow (Pham et al., 2009). In addition, secondary effects of evaporative fractionation on soil moisture and lakewater may influence the δD of the vegetation source water and ultimately the δD of the leaf wax. Here, we find that even after fractionation occurring in soil moisture and transpiration, the δD value of precipitation produced strong correlations with the δD value of sediment samples. In this study, Bowen and Revenaugh's (2003) and Bowen et al.'s (2005) precipitation interpolation model is used to estimate the δD value of precipitation for each lake.

An estimate for the δD value of precipitation at a given location is calculated by interpolating data from Global Network of Isotopes in Precipitation (GNIP) Stations (accessible at https://nucleus.iaea.org/wiser). While previous work has utilised spatial interpolation methods such as triangulation, contouring and inverse distance methods (Bowen and Revenaugh, 2003), or simply by reference to the nearest station (Bowen and Wilkinson, 2002), a more contemporary method developed by Bowen and Revenaugh (2003) accounts for the factors which control Rayleigh distillation. The fractionation of isotopes occurring as air masses move over land is primarily driven by temperature change. Bowen and Revenaugh (2003) incorporate changes in geographic location and altitude, which ultimately control the temperature changes driving Raleigh distillation, to improve the accuracy of their model. The length and origin of vapour-transport pathways, which affect isotopic values, is affected by large-scale patterns of atmospheric vapour transport (Amundson et al., 1996; Bowen and Revenaugh, 2003). This causes regional deviations from the predictions based on location and altitude but are subsequently accounted for by spatially interpolating the residuals from the altitude and location model and including them in the calculation (Bowen and Wilkinson, 2002). Terzer et al. (2013) present a more recent model, using a cluster-based water isotope prediction (RCWIP) approach, which explains more isotopic variance (>67% compared to 58-61%) than Bowen and Revenaugh's (2003) model (Terzer et al., 2013). Terzer et al. (2013) aimed to improve predictive

accuracy, producing a spatially continuous global stable isotope ratio map. While predictive accuracy may have been improved, a limitation of this approach is the ability to obtain isotopic data from a specific location with ease. It is apparent Bowen and Revenaugh's (2003) spatial interpolation model is an accurate method of estimating isotopic values of precipitation while remaining easy to use and accessible. A potential limitation of Bowen and Revenaugh's (2003) model, highlighted by Terzer et al. (2013), is poorer performance in areas such as the tropics, particularly in predicting monthly δD values (Terzer et al., 2013). However, this effect is irrelevant when considering the Canadian Prairies. Bowen and Revenaugh's (2003) 'isoscape' model can be accessed at www.waterisotopes.org. Terzer et al.'s (2013) model can be accessed at www-naweb.iaea.org/napc/ih/IHS_resources_rcwip.html.

## 4.4 Spatial Separation and Outlier Analysis

Separating lakes spatially is vital when trying to discern hydrogen isotopic response to environmental parameters. The successful spatial separation of lakes appears to be determined by specific weather patterns that are functions of latitude, longitude or both. The weather patterns, which are controlled by the Pacific and Tropical air masses, as well as physical factors such as elevation, drive the isotopic differences observed in latitude and longitude, which in turn provide useful spatial boundaries for lake separations. Vegetation appears to have a lesser role in determining δD $C_{24}$, evident from the poor correlations produced when lakes are separated as a function of ecoregion. This is unsurprising as the Canadian Prairies is predominantly a mixture of $C_3$ and $C_4$ grasses (Cui et al., 2017). However, vegetation will play a more significant role when lakes in the Mixed Grassland and Moist Mixed Grassland ecoregions are compared with those in the Aspen parkland and Boreal Transition Zone due to significant differences in biosynthetic fractionation between grasses and trees (Sachse et al.,2012).

The initial hypothesis that δD $C_{24}$ values would record Rayleigh distillation was complicated by the confluence of air masses, evident from the δD values of precipitation. Interestingly, the δD of precipitation calculated from the OIPC behaves in a manner differing to what was expected and does not exhibit Rayleigh distillation across the study area in an east-west or north-south direction. Instead, the isotopic signal in the east of the study area is heavier than that in the west. This can be explained by the convergence of the Pacific and Tropical air masses. Since the tropical air mass is enriched in deuterium relative to the Pacific air mass, and dominates the eastern section of the study area, precipitation signals are lighter in the west and heavier in the east which complicates the interpretation of δD $C_{24}$ values with respect to δD precipitation values.

Finally, there is not a clear answer as to whether the latitudinal or longitudinal separation is superior, as groups in both separations have different strengths depending on the parameter in question. Therefore, both separations should be used in conjunction, depending on the objectives of the study.

### 4.4.1 Outlier Analysis

Linear regression analysis showed 3 lakes which appeared to have abnormal values that did not conform to the normal distribution of points within the model. These points were investigated using outlier analysis to confirm whether the data was distorting the regression model.

Elkwater Lake lies in the South West of the study area, coordinates [49.668, -110.294], at 1217masl, which is around 250m above the next highest elevation lake, and approximately double that of the average lake elevation. Consequently, vegetation surrounding Elkwater lake differs significantly from others within the spatial grouping. Therefore, Elkwater Lake was excluded from all linear regression analysis on the grounds it is anomalously high in elevation and therefore will be influenced differently by environmental variables relative to other lakes.

Spatially, Whitebear Lake is isolated from other lakes, positioned in the South East of the study area, therefore it can be reasoned it is likely subjected to different climatic influences. Given the distance between Whitebear Lake and other lakes used to produce the calibration, Whitebear Lake will be excluded from the calibration.

Peter Lake is a long 's' shaped lake orientated north-south, positioned in the Moist Mixed Grassland ecoregion, in a catchment which is isolated from other lakes being analysed. Peter Lake has been identified as a statistical outlier, however the reason for this is not clear. Factors which may affect $\delta D\ C_{24}$ values of Peter Lake such as precipitation levels and temperature are normal, given its geographic location. Furthermore, there is little research concerning the hydrology, geomorphology or characteristics of Peter Lake that may cause it to behave as an outlier. $\delta D\ C_{24}$ values of Peter Lake are particularly negative given its geographic location, therefore, it can by postulated there may be a significant influx of water, besides precipitation, that is influencing $\delta D\ C_{24}$. Ingress of water from northern lakes via sub-surface flow or fill-spill relationships, with typically more negative $\delta D\ C_{24}$ values, may cause a more negative isotopic signature in Peter Lake. This hypothesis is difficult to test as there is no available $\delta D\ C_{24}$ data for nearby lakes which may experience similar hydrologic conditions. However, close examination of river networks in Saskatchewan suggest there is potential inflow from the north-

east and north-west by meltwater with a particularly negative δD $C_{24}$ value into Peter Lake. Given the δD $C_{24}$ signature of more northern lakes relative to Peter Lake, significant water ingress with a particularly negative δD $C_{24}$ signature is a likely environmental factor causing Peter Lake to deviate isotopically from geographically close lakes.

## 4.5 Interpretation of δD $C_{24}$ Linear Regression Analysis

Figure 18 and figure 19 show each spatial separation as defined in section 2.5.1. Below, linear regression analysis for δD $C_{24}$ with environmental variables for each group will be discussed separately, with the aim of clarifying the effect such variables have on hydrogen isotopic ratios spatially within the Canadian Prairies.

### 4.5.1 Group 1A – Southern-most sites

Overall Group 1A lakes are divided into east-west transects. Lakes in the Group 1A transect are the southernmost sites in the study area. Here, δD values for leaf waxes exhibit no correlation with latitude or longitude, therefore Raleigh distillation is unlikely to have significantly influenced δD $C_{24}$ values. In addition, weak correlations are produced with all seasonal precipitation variables (table 2). Precipitation and longitude are strongly correlated, such that precipitation amount is higher at eastern longitudes. More precipitation typically produces more negative δD values, however this is not the case. Therefore, it is possible large variations in the amount of evaporation occurring between sites may be affecting the δD $C_{24}$ value prior to uptake. Alternatively, the heavier tropical δD $C_{24}$ signal max be affecting eastern lakes more than that of western lakes.

### 4.5.2 Group 2A – 50 degrees North transect

The Group 2A transect runs across the study area around 50 degrees north. A strong negative correlation between SPEI and δD $C_{24}$ is produced due to more arid conditions in the west. The trend is likely due to more evaporation relative to precipitation causing deuterium enrichment of soil water or plant leaf water. This agrees with published data that report the association of drier conditions with more positive δD values in living plants, see Sachse et al. (2012) for a dataset compiling studies globally.

Lakes in Group 2A are separated based on a very small range of latitudes (49.7˚N to 50.9˚N), therefore δD $C_{24}$ has no correlation with latitude. δD $C_{24}$ has a moderate to strong correlation with longitude which initially could appear to reflect Raleigh distillation. This would be explained by the Pacific air mass moving east over the Prairies during winter, preferentially precipitating more deuterium, such that a progressively lighter isotopic signal is prevalent inland. However, the δD value estimated by the OIPC, predicts more positive δD values inland with a strong but opposite correlation with longitude, compared to δD $C_{24}$. Therefore, Raleigh distillation does not affect the meteoric water in these lakes and is not what is driving the trend seen in δD $C_{24}$. In addition to this OIPC precipitation δD values for spring, summer and autumn are moderately negatively correlated with δD $C_{24}$, such that more positive δD precipitation values for a particular location exhibit more negative δD $C_{24}$ values further east (figures 25, 26 and 27).

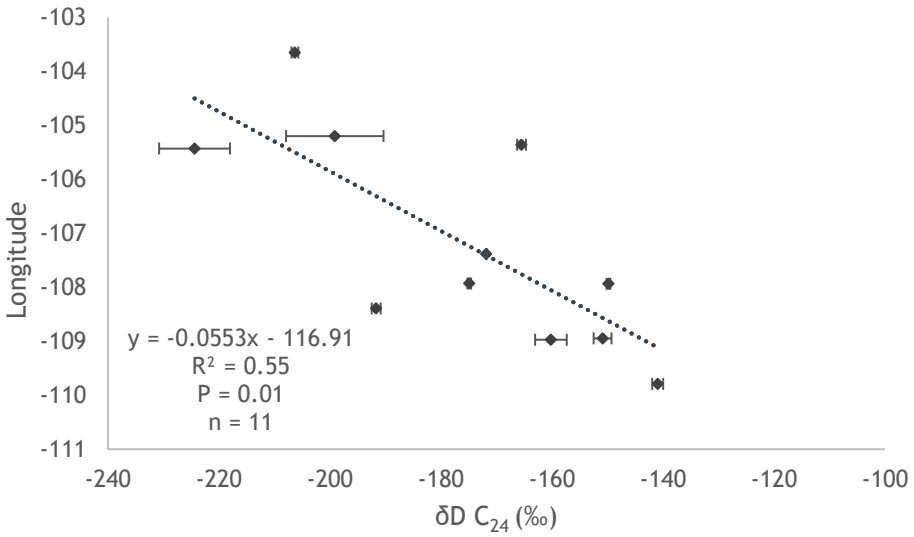


**Figure 17**: Group 2A - The relationship between δD C24 and longitude, δD C24 becomes increasingly negative eastward.

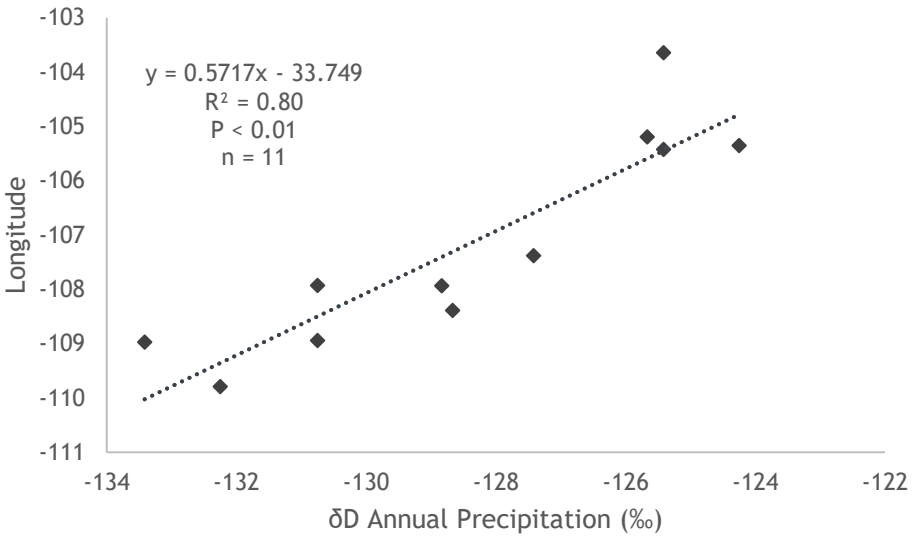


**Figure 18:** Group 2A - The relationship between the δD of average annual precipitation and longitude, the δD of precipitation becomes increasingly positive eastward. Error bars were not calculated using the OIPC.

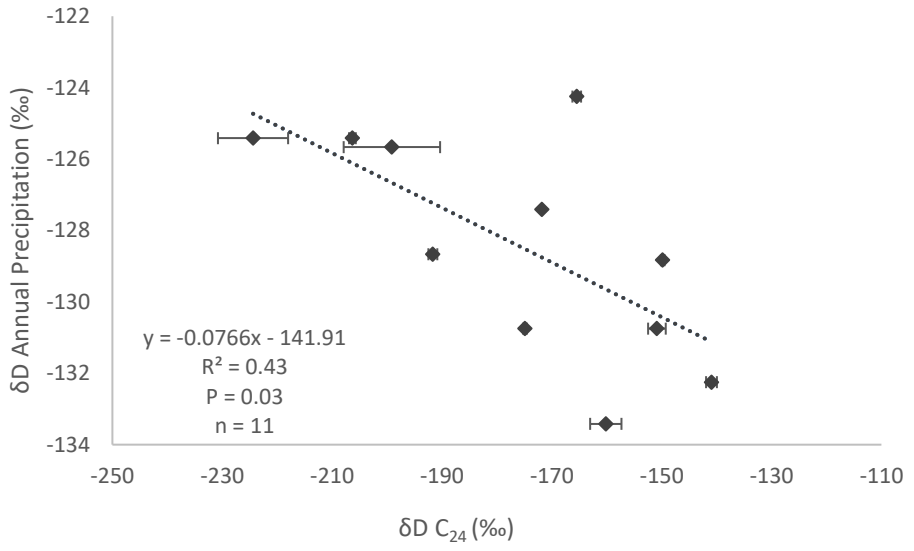


**Figure 19: Group 2A -** Relationship between δD C24 (‰) and the average δD of annual precipitation. The average of annual precipitation has been used to illustrate this relationship however this relationship exists in all seasons except winter.

The negative correlation between δD precipitation and δD $C_{24}$ wax is unexpected, but points to more complex controls on δD $C_{24}$ than just direct influence from precipitation. Here we discuss several potential reasons for the negative correlation between δD precipitation and δD $C_{24}$:

1. Isotopically light rainwater precipitates in the western section of the study area. Warm arid conditions cause evaporation from the soil/lake water, and evapotranspiration from leaf water, before photosynthesis, producing a heavier δD $C_{24}$ signal.

2. This may also be accompanied by the isotopically heavy rain falling in the eastern section of the study area being diluted by residual meltwater and isotopically light precipitation which has not evaporated due to colder humid conditions.

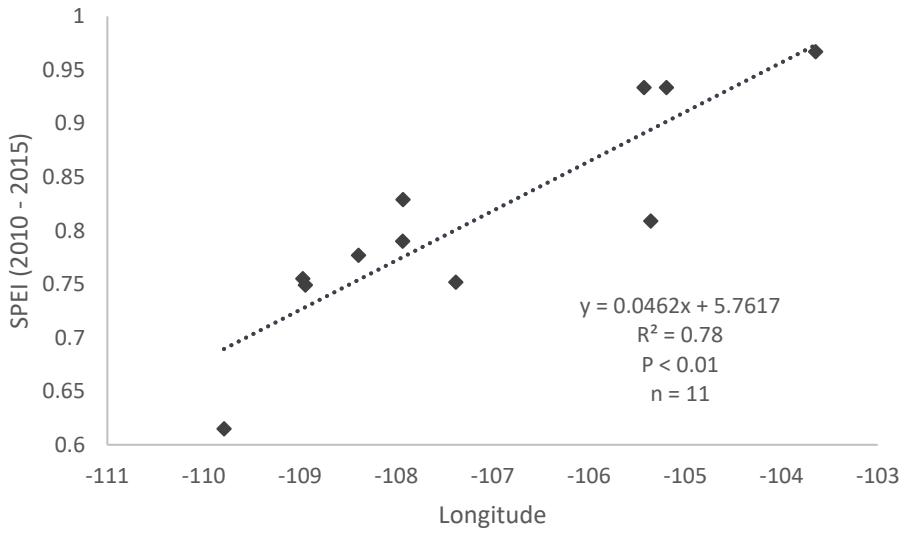


**Figure 20:** Group 2A **-** The relationship between SPEI (2010 – 2015) and Longitude showing a gradual change from aridity in the west to humid conditions in the east.

Generally, $\delta D_{ppt}$ becomes progressively more negative with altitude, therefore higher altitude sites in the western part of the Prairies have lighter isotopic precipitation signatures than the lower altitude sites in the east. Conversely, δD $C_{24}$ lake sediment values increase with increasing altitude. This is likely due to higher temperatures at higher elevations during the summer, spring and autumn (Environmental variables for each lake are displayed in appendix B). Therefore, despite a good correlation between elevation and δD $C_{24}$ the relationship is likely a function of temperature and aridity. Moderate to strong positive correlations are produced with δD $C_{24}$ and all temperature variables except summer. This is expected as all seasonal temperatures, except summer, progressively decrease eastward. Summer temperature and longitude have no relationship because the dominant air mass during summer comes from the Gulf of Mexico northward. Therefore, it is likely that the dominant control on the spatial distribution of dD in this group is temperature.

### 4.5.3 Group 3A – a 51 degree North transect

There is little correlation between δD $C_{24}$ and latitude. This may be because higher latitudes are harder for tropical air to reach from the south during summer and/or because the Cypress Hills block warm air from reaching western sites. Furthermore, western lakes are likely to be partially influenced by the Pacific air mass during summer as well, convoluting a tropical signal. In addition to this, Group 3A encompasses only a few latitudinal degrees, therefore a correlation between δD $C_{24}$ and latitude would not be expected. A moderate correlation exists between longitude and δD $C_{24}$, with a progressively lighter signature eastward. As with Group 2A, this does not match the precipitation δD signal. Since western lakes experience more arid conditions than eastern lakes, a humidity gradient may explain why δD $C_{24}$ values show a different pattern to the δD of precipitation. Furthermore, the lack of negative correlation between δD $C_{24}$ and the δD of precipitation can be explained by a much less gradual transition from arid to humid (figures 29 and 30).

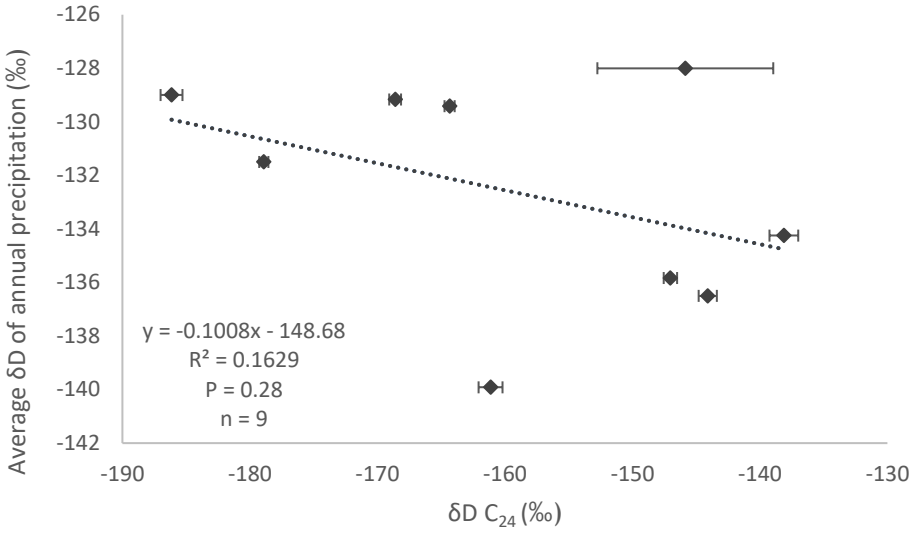


**Figure 21:** Group 3A - Relationship between δD $C_{24}$ and the average δD of annual precipitation in Group 3A.

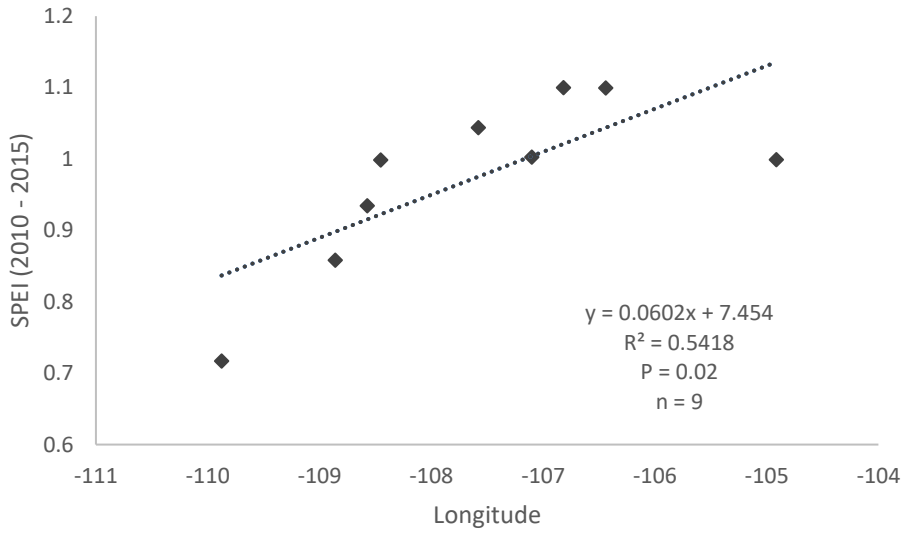


**Figure 22:** Group 3A - Relationship between Longitude and SPEI in Group 3A. Although the relationship is still significant, Group 3A exhibits a much weaker correlation than in Group 2A which may result in a weak correlation between δD $C_{24}$ and $\delta D_{ppt}$.

A moderate correlation exists between δD $C_{24}$ and spring temperature such that higher spring temperatures are related to more positive δD $C_{24}$. Higher spring temperatures occur at high elevation western sites, therefore the relationship between δD $C_{24}$ and elevation is likely related to temperature. There are no significant correlations between δD $C_{24}$ and precipitation however this may be due

to the small variability in rainfall across the lakes in Group 3A. Similarly, there is a very small range of SPEI values in Group 3A lakes comparative to groups in which strong correlations are produced. This may account for a poor correlation between δD $C_{24}$ and SPEI.

### 4.5.4 Group 4A – Eastern sites

Lake sediment δD $C_{24}$ in Group 4A correlate poorly with latitude but strongly with longitude, such that a lighter δD $C_{24}$ signal is observed in eastern lakes. δD $C_{24}$ correlates poorly with elevation, however, in topographically flat regions, it is unlikely elevation will have any significant effect on δD $C_{24}$. This may be due to the fact elevation has no significant effect on temperature or precipitation.

δD $C_{24}$ correlates strongly with winter, spring and autumn temperatures and moderately with summer temperature. In all cases, higher temperatures in the west, produce more positive δD $C_{24}$ values. Furthermore, Winter, summer and autumn precipitation are all strongly correlated to δD $C_{24}$ such that higher precipitation rates inland produce more negative δD $C_{24}$ values. Both temperature and precipitation amount are strongly correlated with longitude, therefore this likely explains the correlation between $C_{24}$ and longitude. Conversely, spring precipitation produces no correlation with δD $C_{24}$, for one of two reasons, or a combination of both:

1. Spring precipitation varies the least across lakes in Group 4A, therefore other variables may have more influence on scatter of the linear regression model.

2. Snowmelt during spring will infiltrate ground water meaning spring precipitation is not the only source of water used by plants for photosynthesis. This is supported by a strong correlation with winter precipitation amount and δD $C_{24}$.

### 4.5.5 Group 5A – Northernmost sites

Group 5A did not produce any significant correlations. Group 5A has the largest number of samples and encompasses the largest area, with lakes in three different ecoregions, furthermore eastern sample locations are sparse and very condensed.

Lakes located in different ecoregions will accumulate $C_{24}$ from a variety of plants with different photosynthetic pathways. Furthermore, it is possible $C_{24}$ has been transported by wind or by water and is therefore not autochthonous to the sediment in some lakes. If $C_{24}$ is the product of many different biosynthetic pathways it is unlikely to correlate with the environmental variables from the study area. After separating Group 5A further, by longitude, into two groups either side of Redberry lake, no significant correlations are produced. This may be because sample locations in both groups still span two ecoregions. Some eastern lakes are located very close to, or within, the Boreal transition. Since this ecoregion encompasses very different vegetation, including trees, it is unsurprising these lakes produce no correlation. Similarly, western lakes are located across the Moist Mixed Grassland and the Aspen Parkland. Taller grasses and small trees will have significantly different biosynthetic pathways impeding any correlation between $C_{24}$ values and environmental variables. In addition, the location of western lakes may cause them to be affected less by moving air masses, this may encourage more precipitation recycling thus altering the δD $C_{24}$.

### 4.5.6 Group 1B – Westernmost lakes

Group 1B lakes are characterised by colder temperatures at higher latitudes. Colder temperatures are also strongly correlated with more negative δD precipitation values. This signal appears to be recorded in the δD $C_{24}$ values of lake sediments, evident in the moderate to strong correlation with δD $C_{24}$ and seasonal precipitation δD. Since there is likely to be very little, if any, influence from the tropical air mass, and therefore little variation in evaporation, the correlation produced is positive. Furthermore, since temperature appears to control the δD of precipitation and δD $C_{24}$, the moderate correlation between δD $C_{24}$ and latitude is likely a function of temperature. Similarly, the correlation observed between elevation and δD $C_{24}$ can be interpreted as a result of temperature increasing with elevation. No correlation exists between δD $C_{24}$ and longitude, this is expected as Group 1B lakes span just 1 degree of longitude. Moderate correlations exist between δD $C_{24}$ and summer, autumn and winter precipitation δD. This may be explained by autumn and winter precipitation freezing before being used during the growing season as meltwater, and therefore overprinting any signal that may have been produced with spring precipitation δD.

A moderate to strong correlation with SPEI shows aridity produces more positive δD $C_{24}$ values, which reflects stronger evaporation of protium. In addition, winter spring and autumn temperatures produce moderate to strong positive correlations with δD $C_{24}$. Therefore, higher temperatures, and more aridity, in the in southerly lakes produce more positive δD $C_{24}$. There is a particularly strong positive correlation between δD $C_{24}$ and winter temperature but no correlation with summer temperature. The strong correlation with winter temperature may be because winter temperature varies the most across lakes, conversely less variation in autumn and spring temperatures produces weaker correlations. Furthermore, temperatures during winter, spring and autumn are strongly correlated with latitude, such that northern lakes generally experience lower temperatures. This relationship does not exist during summer, which may explain the poor correlation with δD $C_{24}$ and summer temperature. A strong negative correlation between δD $C_{24}$ and summer precipitation shows higher precipitation rates are related to more protium rainout. Since good correlations exist between the δD of seasonal precipitation and δD $C_{24}$, poor correlations with precipitation amount during winter, spring and autumn is likely due to a lack of variation in precipitation amount during these seasons.

### 4.5.7 Group 2B – A southeast-northwest transect

Group 2B produced no significant correlations with environmental factors. This may be because Group 2B produces a general Southeast to Northwest transect which opposes the combined direction of air masses and thus temperature and precipitation gradients. This is supported by results from Group 4B, which produced the strongest correlations, and forms a general southwest to norteast transect.

### 4.5.8 Group 3B – South-eastern lakes

δD $C_{24}$ values are strongly negatively correlated with winter precipitation δD. This may explain the poor relationship with spring precipitation δD, if predominantly snowmelt water is used for photosynthesis relative to spring precipitation. A moderate correlation with δD $C_{24}$ and summer precipitation δD is likely due to the tropical air mass exerting a stronger influence on lakes during the summer months.

Minor influence of the Pacific air mass during summer would explain why the summer signal is weaker than that observed with winter precipitation δD.

A significant correlation between δD $C_{24}$ and SPEI shows more arid conditions produce more positive δD $C_{24}$. In addition to this, increasing humidity northward may also explain the steady decrease in δD $C_{24}$ values with latitude, given OIPC results exclude Rayleigh distillation as a possible explanation.

### 4.5.9 Group 4B – Central northern lakes

δD $C_{24}$ values of Group 4B produced moderate to strong correlations with latitude, longitude, Precipitation δD, SPEI and nearly all seasonal temperature and precipitation variables. Furthermore, moderate to strong positive correlations are produced between δD $C_{24}$ and the δD value of seasonal precipitation, except during spring. The strongest correlations are produced during autumn (September, October, November) and winter (December, January, Febuary). This may be because snow, gathered over the autumn and winter months, is melting in spring and subsequently being used by terrestrial plants. Weaker correlations during the summer and spring months may be due to other variables such as variable evaporation rates across sites and the use of snowmelt for photosynthesis. Similarly, δD $C_{24}$ produces moderate correlations with precipitation amount during all seasons except spring.

SPEI is moderately correlated with δD $C_{24}$, furthermore SPEI is strongly correlated with latitude and moderately correlated with longitude, such that aridity in the south west produces more positive δD $C_{24}$ due to evaporation of protium. In addition, warmer temperatures in all months produce more positive δD $C_{24}$.

### 4.5.10 Group 5B – North-eastern lakes

Group 5B produced moderate to strong correlations with all temperature variables. A strong positive correlation exists between the δD of winter precipitation (December, January, February) and δD $C_{24}$, however this correlation does not exist in any other months. This is likely due to large volumes of winter snow melting during the growing season, as seen in Group 4B. Group 4B and Group 5B are high latitude north eastern lakes. Interestingly, these results disagree with

data reported by Pham et al. (2009), which supports summer precipitation as the most important source of water for lakes in the north east of the Prairies. However, 5 out of 9 lakes in Group 5B were not included in the data presented by Pham et al. (2009). Furthermore, Pham et al. (2009) analysed 9 out of 10 lakes encompassed in Group 4B, which produced a correlation with summer precipitation δD as well as winter precipitation δD, suggesting precipitation from both seasons influence the hydrology of these lakes.

### 4.5.11 An Overview of δD $C_{24}$ Correlations

Overall, Group B lakes produced particularly strong correlations with seasonal precipitation δD values compared with Group A lakes, with the strongest correlations produced during winter. Both Group A and Group B lakes correlated well with seasonal precipitation amounts, with the strongest correlations produced during summer and autumn. This may be due to a lack of variation between sites in the amount of precipitation falling during spring and winter. Strong correlations with temperature are produced in both separations, with no season or seasons dominating, however poor correlations appear to be associated with a lack of variation in temperatures between sites. Groups in both separations correlate with latitude and longitude, correlations are produced where there is a large variation in latitude or longitude and are likely a function of another variable e.g. temperature. Similarly, correlations produced in Group A and Group B with elevation may be attributed to one or more other environmental variables that change with elevation. Both Group A and Group B lakes correlated with SPEI, strong correlations were produced in 3/10 Groups analysed, however this would likely be improved if seasonal values for SPEI were calculated (see section 4.2.2).

## 4.6 Prairie Lake Hydrology

The recharge mechanisms of Prairie lakes may provide important information about ENSO events due the effect such events have on snowpack (Pham et al., 2009). For example, lakes which correlate with all seasonal precipitation δD are likely to show much weaker correlations with winter precipitation δD, relative to the δD of other seasons, during El Nino events. Therefore, it is important to quantify the relative importance of seasonal precipitation on Prairie lakes.

The primary controls on Prairie lake hydrology have been debated e.g. (Pham et al., 2009; Su et al., 2000). Some isotopic analysis has suggested that winter precipitation is the most important control on Prairie lake hydrology, whether directly via runoff or indirectly as subsurface flow (Pham et al., 2009). Other studies suggest spring snowmelt and summer precipitation are of roughly comparable magnitude (Su et al., 2000). However, subsurface water flow tends to be a minor component of Prairie lake water balance due to the impermeable nature of the clay rich glacial deposits (Van der Kamp and Hayashi, 1998). Nevertheless, some conclusions may be drawn with respect to Prairie lake hydrology when considering the correlations between δD $C_{24}$ and the δD of precipitation. For example, δD $C_{24}$ in group 4B produced good correlations with summer and winter precipitation δD, results suggest spring snowmelt is marginally more important with regards to water source for these lakes. However, δD $C_{24}$ also correlates with autumn precipitation δD to a lesser degree, this may be due to the lesser role of snowfall during the later months of autumn. Conversely, δD $C_{24}$ in group 2A produces a particularly poor correlation with the δD of winter precipitation, however a strong correlation is produced with spring and summer precipitation δD. This suggests that for these lakes, all of which are located below 51° latitude, spring snowmelt is less significant with respect to lake re-charge, while spring and summer precipitation are more influential. This may be due to lower latitude lakes being subjected to greater influence from the tropical air mass. δD $C_{24}$ in Group 1A showed very little correlation with the δD of precipitation. This may be due to subsurface flow from a distant source travelling through fractures or through sections of slightly coarser material. While subsurface flow is a minor component, it may cause still cause Prairie lake water δD to become offset from that of local precipitation δD. Furthermore, transpiration in wetland margins can encourage lateral flow of shallow

groundwater which exerts a strong influence on wetland hydrology (van der Kamp and Hayashi, 2009).

## 4.7 Downcore Analysis

Vegetation change in response to moisture change, particularly during periods of drought, is a challenging aspect of using a stable isotope calibration due to different plant species having different levels of biosynthetic fractionation. However, downcore pollen analysis should allow for correction of δD values, when faced with a major vegetation change, in order to produce an accurate palaeohydrologic or palaeoclimatic calculation. Where vegetation changes occur in an area in response to climatic changes over time e.g. trees replace grasses, the average difference in δD between species should be applied accordingly.

As discussed above, the area surrounding lakes 'Thackery', 'Springwater' and 'Tramping' is not calibrated. Conversely, in areas where latitudinal and longitudinal separations overlap, measurements can be taken using both calibrations. For example, 'Stoney Beach' and 'Buffalo Pound' are part of Group 2A and Group 3B, therefore one downcore δD $C_{24}$ measurement may provide results for several environmental parameters.

## 4.8 ArcGIS

ArcMap allowed for detailed analysis of the physical environment surrounding specific lakes. Shapefiles depicting ecoregions, rivers, basins, elevation and vegetation made making specific inferences about groups and individual lakes possible. For example, ArcMap is particularly useful following statistical outlier analysis. While a lake may be an outlier statistically, ArcMap allows assumptions regarding the environmental reason for this. Furthermore, the ability to colour specific points, which represent lakes, based on specific environmental variables allows large scale patterns, which are difficult to distinguish when looking at raw data, to be easily visualised. Identifying which ecoregion a lake was located within proved particularly important during the analysis stage, it was possible to query this instantly with ArcMap. Therefore, when conducting calibration studies such as this, which involve a large amount of data and require spatio-temporal thinking, ArcMap is an extremely useful tool.

# Chapter 5 Conclusion and Further Research

This study has presented a series of calibrations covering a large area of the Canadian Prairies using the $C_{24}$ *n*-alkanoic acid and multiple environmental variables. The calibrations presented in this study provide confirmation that the $C_{24}$ *n*-alkanoic acid is a viable moisture proxy on par with other *n*-alkyl compounds. This calibration can now be used in conjunction with sediment cores to discern past moisture changes, with the aim of gaining a better understanding of droughts, in order to mitigate the future effects of drought in light of a changing climate.

This study uses the novel approach of compound specific analysis of hydrogen isotopes in *n*-alkanoic acids. The data presented above employs the fundamental laws of stable isotope fractionation, used in conjunction with knowledge of the weather patterns occurring in the Prairie atmosphere to demonstrate that there is a strong correlation between δD *n*-$C_{24}$ and the hydrogen isotope ratio of precipitation, SPEI, precipitation amount, temperature, latitude and longitude. This will allow quantification of these variables in the past, and ultimately a more complete picture of past climate in the Canadian Prairies to be pieced together.

## 5.1 Prairie Lake Hydrology

There is some ambiguity surrounding the most influential source of water for Prairie lake hydrology e.g. Pham et al., 2009; Su et al., 2000, see section 1.2.1. Following analysis of δD $C_{24}$ results with respect to seasonal δD precipitation values, there appears to be no universal rule as to the control of Prairie lake hydrology. Most lakes seem to be heavily influenced by spring snowmelt, evident from strong correlations between δD $C_{24}$ and the δD of winter precipitation, however, correlations with other seasonal precipitation δD values suggest winter snowmelt cannot be held solely accountable for lake water hydrology at these sites. Furthermore, lakes which show no correlation with winter precipitation δD values but strong correlations with summer and spring precipitation δD suggest spring and summer precipitation exerts the primary control on lake water hydrology. Since the controls on prairie lake hydrology differ considerably depending on the area in question, this study offers a comprehensive explanation as to the method of recharge across lakes in the Prairies.

## 5.2 Contribution to the Knowledge Gap

The lack of a high-resolution, ubiquitous moisture proxies spanning adequate timescales has prevented a clear picture of palaeo-hydrologic change from being discerned in the Canadian Prairies. Many previous studies have analysed a series of lakes which form a transect across a continent (e.g. Huang et al., 2002; Huang et al., 2004; Xia et al., 2008), however, this study presents a hydrogen isotope calibration using lakes spread across the Canadian Prairies. Furthermore, there has been some uncertainty surrounding the feasibility of *n*-alkanoic acids as moisture proxies with respect to other organic compounds such as *n*-alkanes (Huang et al., 2004). This study presents a particularly large amount of data that demonstrates *n*-alkanoic acids are a suitable proxy that successfully trace the δD of environmental water among other environmental parameters. Here, a calibration is presented that can be used ubiquitously within the Canadian Prairie study area in order to help build a clear understanding of palaeo-hydrologic change. In addition to this, δD $C_{24}$ results have allowed inferences about the re-charge mechanism for lakes which may offer the potential to infer past ENSO events.

## 5.3 Further Research

The carbon chain length *n*-$C_{28}$ produced unreliable results in this study, however, it is clear *n*-$C_{28}$ produced poor correlations with environmental variables due to frequent co-elution with other compounds. It is possible the compounds present that cause the co-elution with *n*-$C_{28}$ are resultant of sampling or lab practices. Therefore, future research focussing on a calibration using the *n*-$C_{28}$ compound, if a reliable chromatogram is produced, may yield results similar to this study. Conversely, *n*-$C_{26}$ produced reliable peaks in relatively high concentrations, therefore more work using *n*-$C_{26}$ in the Canadian Prairies may also prove successful. In addition, this study focusses on long chain *n*-alkanoic acids and neglects shorter chain lengths, largely because terrestrial *n*-alkyl compounds are more likely to avoid certain complications associated with the evaporation of lacustrine water. However, short-chain *n*-alkanoic acids may produce an effective calibration within the Prairie region and is therefore a subject of interest for future research. The chromatograms analysed in this study suggest that *n*-$C_{18}$ may be a reliable option as it regularly exhibits well defined peaks and is present in high concentrations.

Secondly, as discussed in section 1.3, there are large gaps in the palaeo-hydrologic record due to lack of a proxy that is universally applicable to all lakes. It is now possible to begin to fill these gaps using the calibration presented in this study. Using sediment cores from around the Canadian Prairies, past hydrologic change can be quantified. In addition to this, results can be cross-examined in order to highlight any potential discrepancies or to confirm the reliability of results. The data acquired may then be used in climate models to predict future hydrologic changes in order to appropriately prepare for flooding or drought.

Finally, this study adds to the growing evidence that compound specific analysis of *n*-alkyl compounds can quantify past hydrologic change and that this methodology can be used ubiquitously and facilitates high-resolution results spanning adequate timescales. Furthermore, flooding and drought is a world-wide problem which is on the rise (Gan, 1988). Considering this, calibration studies using *n*-alkyl compounds should be encouraged globally in order to develop a complete understanding of global hydrologic change in order to mitigate the effects of flooding and drought.

# References

Agriculture Organization for the United Nations, 1998. *World reference base for soil resources* (Vol. 3). Food & Agriculture Org..

Alley, W.M., 1984. The Palmer drought severity index: limitations and assumptions. *Journal of Applied Meteorology and Climatology*, *23*(7), pp.1100-1109.

Amundson, R., Chadwick, O., Kendall, C., Wang, Y. and DeNiro, M., 1996. Isotopic evidence for shifts in atmospheric circulation patterns during the late Quaternary in mid–North America. *Geology*, *24*(1), pp.23-26.

An, W., Liu, X., Hou, S., Zeng, X., Sun, W., Wang, W., Wang, Y., Xu, G. and Ren, J., 2019. Unstable relationships between tree ring δ 18 O and climate variables over southwestern China: possible impacts from increasing central Pacific SSTs. *Theoretical and Applied Climatology*, *136*(1-2), pp.391-402.

Anderson, L., Abbott, M.B., Finney, B.P. and Edwards, M.E., 2005. Palaeohydrology of the Southwest Yukon Territory, Canada, based on multiproxy analyses of lake sediment cores from a depth transect. *The Holocene*, *15*(8), pp.1172-1183.

Avato, P., Bianchi, G. and Salamini, F., 1985. Absence of long chain aldehydes in the wax of the Glossy II mutant of maize. *Phytochemistry*, *24*(9), pp.1995-1997.

Bailey, R.G., 2004. Identifying ecoregion boundaries. *Environmental management*, *34*(1), pp.S14-S26.

Bansal, S., Harrington, C.A. and St. Clair, J.B., 2016. Tolerance to multiple climate stressors: a case study of Douglas-fir drought and cold hardiness. *Ecology and evolution*, *6*(7), pp.2074-2083.

Beguería, S., Vicente-Serrano, S.M., Reig, F. and Latorre, B., 2014. Standardized precipitation evapotranspiration index (SPEI) revisited: parameter fitting, evapotranspiration models, tools, datasets and drought monitoring. *International Journal of Climatology*, *34*(10), pp.3001-3023.

Berke, M.A., Tipple, B.J., Hambach, B. and Ehleringer, J.R., 2015. Life form-specific gradients in compound-specific hydrogen isotope ratios of modern leaf waxes along a North American Monsoonal transect. Oecologia, 179(4), pp.981-997.

Bi, X., Sheng, G., Liu, X., Li, C. and Fu, J., 2005. Molecular and carbon and hydrogen isotopic composition of n-alkanes in plant leaf waxes. *Organic Geochemistry*, *36*(10), pp.1405-1417.

Bigler, C. and Hall, R.I., 2003. Diatoms as quantitative indicators of July temperature: a validation attempt at century-scale with meteorological data from northern Sweden. *Palaeogeography, Palaeoclimatology, Palaeoecology*, *189*(3-4), pp.147-160.

Bonsal, B.R., Aider, R., Gachon, P. and Lapp, S., 2013. An assessment of Canadian prairie drought: past, present, and future. Climate Dynamics, 41(2), pp.501-516.

Bonsal, B.R. and Lawford, R.G., 1999. Teleconnections between El Niño and La Niña events and summer extended dry spells on the Canadian

Prairies. *International Journal of Climatology: A Journal of the Royal Meteorological Society*, *19*(13), pp.1445-1458.

Bonsal, B. and Regier, M., 2007. Historical comparison of the 2001/2002 drought in the Canadian Prairies. *Climate Research*, *33*(3), pp.229-242.

Bonsal, B.R., Zhang, X. and Hogg, W.D., 1999. Canadian Prairie growing season precipitation variability and associated atmospheric circulation. *Climate Research*, *11*(3), pp.191-208.

Bowen, G. J. (2017) The Online Isotopes in Precipitation Calculator, version 3.1. http://www.waterisotopes.org.

Bowen, G.J. and Revenaugh, J., 2003. Interpolating the isotopic composition of modern meteoric precipitation. *Water Resources Research*, *39*(10).

Bowen, G.J., Wassenaar, L.I. and Hobson, K.A., 2005. Global application of stable hydrogen and oxygen isotopes to wildlife forensics. *Oecologia*, *143*(3), pp.337-348.

Bowen, G.J. and Wilkinson, B., 2002. Spatial distribution of δ18O in meteoric precipitation. *Geology*, *30*(4), pp.315-318.

Brown, K.J., Clark, J.S., Grimm, E.C., Donovan, J.J., Mueller, P.G., Hansen, B.C.S. and Stefanova, I., 2005. Fire cycles in North American interior grasslands and their relation to prairie drought. *Proceedings of the National Academy of Sciences*, *102*(25), pp.8865-8870.

Case, R.A. and MacDonald, G.M., 1995. A dendroclimatic reconstruction of annual precipitation on the western Canadian prairies since AD 1505 from Pinus flexilis James. *Quaternary Research*, *44*(2), pp.267-275.

Chikaraishi, Y. and Naraoka, H., 2007. δ13C and δD relationships among three n-alkyl compound classes (n-alkanoic acid, n-alkane and n-alkanol) of terrestrial higher plants. Organic Geochemistry, 38(2), pp.198-215.

Chakravarti, A.K., 1972. The June-July precipitation pattern in the prairie provinces of Canada. *Journal of Geography*, *71*(3), pp.155-160.

Cheesbrough, T.M. and Kolattukudy, P.E., 1984. Alkane biosynthesis by decarbonylation of aldehydes catalyzed by a particulate preparation from Pisum sativum. *Proceedings of the National Academy of Sciences of the United States of America*, *81*(21), p.6613.

Chen, X., Liu, X., Jia, H., Jin, J., Kong, W. and Huang, Y., 2021. Inverse hydrogen isotope fractionation indicates heterotrophic microbial production of long-chain n-alkyl lipids in desolate Antarctic ponds. Geobiology, 19(4), pp.394-404.

Collins, J.A., Schefuß, E., Mulitza, S., Prange, M., Werner, M., Tharammal, T., Paul, A. and Wefer, G., 2013. Estimating the hydrogen isotopic composition of past precipitation using leaf-waxes from western Africa. *Quaternary Science Reviews*, *65*, pp.88-101.

Conly, F.M. and Van Der Kamp, G., 2001. Monitoring the hydrology of Canadian prairie wetlands to detect the effects of climate change and land use changes. *Environmental Monitoring and Assessment*, *67*(1-2), pp.195-215.

Covich, A.P., Fritz, S.C., Lamb, P.J., Marzolf, R.D., Matthews, W.J., Poiani, K.A., Prepas, E.E., Richman, M.B. and Winter, T.C., 1997. Potential effects of climate change on aquatic ecosystems of the Great Plains of North America. *Hydrological Processes*, *11*(8), pp.993-1021.

Craig, H. and Gordon, L.I., 1965. Deuterium and oxygen 18 variations in the ocean and the marine atmosphere.

Cummings, D.I., Russell, H.A. and Sharpe, D.R., 2012. Buried-valley aquifers in the Canadian Prairies: geology, hydrogeology, and origin. *Canadian Journal of Earth Sciences*, *49*(9), pp.987-1004.

Cui, T., Martz, L. and Guo, X., 2017. Grassland phenology response to drought in the Canadian prairies. *Remote Sensing*, *9*(12), p.1258.

Daly, C., Gibson, W.P., Taylor, G.H., Johnson, G.L. and Pasteris, P., 2002. A knowledge-based approach to the statistical mapping of climate. *Climate research*, *22*(2), pp.99-113.

Dansgaard, W., 1964. Stable isotopes in precipitation. *Tellus*, *16*(4), pp.436-468.

Ecological Stratification Working Group (Canada), Center for Land, Biological Resources Research (Canada) and Canada. State of the Environment Directorate, 1996. *A national ecological framework for Canada*. Centre for Land and Biological Resources Research; Hull, Quebec: State of the Environment Directorate.

Edvardsson, J., Stoffel, M., Corona, C., Bragazza, L., Leuschner, H.H., Charman, D.J. and Helama, S., 2016. Subfossil peatland trees as proxies for Holocene palaeohydrology and palaeoclimate. Earth-Science Reviews, 163, pp.118-140.

Eglinton, G. and Hamilton, R.J., 1967. Leaf epicuticular waxes. Science, 156(3780), pp.1322-1335.

Environment: Proceedings of the Royal Irish Academy (pp. 47-64). Royal Irish Academy.

Environmental Sampling. 2022. Stable Isotope Primer and Some Hydrological Applications. [online] Available at: <https://serc.carleton.edu/microbelife/research_methods/environ_sampling/stableisotopes.html> [Accessed 5 October 2022].

Euliss Jr, N.H., Gleason, R.A., Olness, A., McDougal, R.L., Murkin, H.R., Robarts, R.D., Bourbonniere, R.A. and Warner, B.G., 2006. North American prairie wetlands are important nonforested land-based carbon storage sites. *Science of the Total Environment*, *361*(1-3), pp.179-188.

Feakins, S.J., Bentley, L.P., Salinas, N., Shenkin, A., Blonder, B., Goldsmith, G.R., Ponton, C., Arvin, L.J., Wu, M.S., Peters, T. and West, A.J., 2016. Plant

leaf wax biomarkers capture gradients in hydrogen isotopes of precipitation from the Andes and Amazon. *Geochimica et Cosmochimica Acta*, *182*, pp.155-172.

Feakins, S.J., Bentley, L.P., Salinas, N., Shenkin, A., Blonder, B., Goldsmith, G.R., Ponton, C., Arvin, L.J., Wu, M.S., Peters, T. and West, A.J., 2016. Plant leaf wax biomarkers capture gradients in hydrogen isotopes of precipitation from the Andes and Amazon. *Geochimica et Cosmochimica Acta*, *182*, pp.155-172.

Freimuth, E.J., Diefendorf, A.F. and Lowell, T.V., 2017. Hydrogen isotopes of n-alkanes and n-alkanoic acids as tracers of precipitation in a temperate forest and implications for paleorecords. *Geochimica et Cosmochimica Acta*, *206*, pp.166-183.

Fritz, S.C., Ito, E., Yu, Z., Laird, K.R. and Engstrom, D.R., 2000. Hydrologic variation in the northern Great Plains during the last two millennia. *Quaternary Research*, *53*(2), pp.175-184.

Gan, T.Y., 1998. Hydroclimatic trends and possible climatic warming in the Canadian Prairies. Water resources research, 34(11), pp.3009-3015.

Gao, L., Hou, J., Toney, J., MacDonald, D. and Huang, Y., 2011. Mathematical modeling of the aquatic macrophyte inputs of mid-chain n-alkyl lipids to lake sediments: Implications for interpreting compound specific hydrogen isotopic records. *Geochimica et Cosmochimica Acta*, *75*(13), pp.3781-3791.

Garcin, Y., Schwab, V.F., Gleixner, G., Kahmen, A., Todou, G., Séné, O., Onana, J.M., Achoundong, G. and Sachse, D., 2012. Hydrogen isotope ratios of lacustrine sedimentary n-alkanes as proxies of tropical African hydrology: insights from a calibration transect across Cameroon. *Geochimica et Cosmochimica Acta*, *79*, pp.106-126.

Girvetz, E.H. and Zganjar, C., 2014. Dissecting indices of aridity for assessing the impacts of global climate change. *Climatic change*, *126*(3-4), pp.469-483.

Gamarra, B., Sachse, D. and Kahmen, A., 2016. Effects of leaf water evaporative 2H-enrichment and biosynthetic fractionation on leaf wax n-alkane δ2H values in C3 and C4 grasses. *Plant, cell & environment*, *39*(11), pp.2390-2403.

Gat, J.R., 1996. Oxygen and hydrogen isotopes in the hydrologic cycle. Annual Review of Earth and Planetary Sciences, 24(1), pp.225-262.

González-Cásares, M., Pompa-García, M. and Camarero, J.J., 2017. Differences in climate–growth relationship indicate diverse drought tolerances among five pine species coexisting in Northwestern Mexico. *Trees*, *31*(2), pp.531-544.

Grimm, E.C., 2001, December. Trends and palaeoecological problems in the vegetation and climate history of the northern Great Plains, USA. In *Biology and Environment: Proceedings of the Royal Irish Academy* (pp. 47-64). Royal Irish Academy.

Grimm, E.C., Donovan, J.J. and Brown, K.J., 2011. A high-resolution record of climate variability and landscape response from Kettle Lake, northern Great Plains, North America. Quaternary Science Reviews, 30(19-20), pp.2626-2650.

Gullett, D.W. and Skinner, W.R., 1992. The state of Canada's climate: temperature change in Canada 1895-1991.

Guttman, N.B., 1991. A sensitivity analysis of the palmer hydrologic drought index 1. *Jawra Journal of the American Water Resources Association*, *27*(5), pp.797-807.

Guttman, N.B., 1999. Accepting the standardized precipitation index: a calculation algorithm 1. *JAWRA Journal of the American Water Resources Association*, *35*(2), pp.311-322.

Harwood, J.L. and Russell, N.J., 1984. Lipids in Plants and Microbes, George Allen and Unwin.

Haskell, B.J., Engstrom, D.R. and Fritz, S.C., 1996. Late Quaternary paleohydrology in the North American Great Plains inferred from the geochemistry of endogenic carbonate and fossil ostracodes from Devils Lake, North Dakota, USA. *Palaeogeography, Palaeoclimatology, Palaeoecology*, *124*(3-4), pp.179-193.

Hayashi, M., van der Kamp, G. and Rudolph, D.L., 1998. Water and solute transfer between a prairie wetland and adjacent uplands, 1. Water balance. *Journal of Hydrology*, *207*(1-2), pp.42-55.

He, X., Pan, M., Wei, Z., Wood, E.F. and Sheffield, J., 2020. A global drought and flood catalogue from 1950 to 2016. *Bulletin of the American Meteorological Society*, *101*(5), pp.E508-E535.

Heddinghaus, T.R. and Sabol, P., 1991, September. A review of the Palmer Drought Severity Index and where do we go from here. In *Proc. 7th Conf. on Applied Climatology* (pp. 242-246). Boston, MA: American Meteorological Society.

Huang, Y., Shuman, B., Wang, Y. and Webb III, T., 2002. Hydrogen isotope ratios of palmitic acid in lacustrine sediments record late Quaternary climate variations. *Geology*, *30*(12), pp.1103-1106.

Huang, Y., Shuman, B., Wang, Y. and Webb, T., 2004. Hydrogen isotope ratios of individual lipids in lake sediments as novel tracers of climatic and environmental change: a surface sediment test. *Journal of Paleolimnology*, *31*(3), pp.363-375.

Hou, J., D'Andrea, W.J., MacDonald, D. and Huang, Y., 2007. Hydrogen isotopic variability in leaf waxes among terrestrial and aquatic plants around Blood Pond, Massachusetts (USA). *Organic Geochemistry*, *38*(6), pp.977-984.

Hou, J., D'Andrea, W.J. and Huang, Y., 2008. Can sedimentary leaf waxes record D/H ratios of continental precipitation? Field, model, and experimental assessments. Geochimica et Cosmochimica Acta, 72(14), pp.3503-3517.

Horne, D.J., 2007. A mutual temperature range method for Quaternary palaeoclimatic analysis using European nonmarine Ostracoda. *Quaternary Science Reviews*, *26*(9-10), pp.1398-1415.

Hugenholtz, C.H. and Wolfe, S.A., 2005. Biogeomorphic model of dunefield activation and stabilization on the northern Great Plains. *Geomorphology*, *70*(1-2), pp.53-70. B

Hutchinson, M.F., 1989. A new objective method for spatial interpolation of meteorological variables from irregular networks applied to the estimation of monthly mean solar radiation, temperature, precipitation and windrun.

IAEA/WMO (2015). Global Network of Isotopes in Precipitation. The GNIP Database. Accessible at: https://nucleus.iaea.org/wiser.

Ironside, G., 1989. *Canada Committee on Ecological Land Classification*. Ottawa: The Committee.

Jacques, J.M.S., Cumming, B.F. and Smol, J.P., 2008. A 900-year pollen-inferred temperature and effective moisture record from varved Lake Mina, west-central Minnesota, USA. *Quaternary Science Reviews*, *27*(7-8), pp.781-796.

Jiang, R., Xie, J., He, H., Luo, J. and Zhu, J., 2015. Use of four drought indices for evaluating drought characteristics under climate change in Shaanxi, China: 1951–2012. *Natural Hazards*, *75*(3), pp.2885-2903.

Kahmen, A., Simonin, K., Tu, K.P., Merchant, A., Callister, A., Siegwolf, R., Dawson, T.E. and Arndt, S.K., 2008. Effects of environmental parameters, leaf physiological properties and leaf water relations on leaf water δ18O enrichment in different Eucalyptus species. *Plant, Cell & Environment*, *31*(6), pp.738-751.

Kolattukudy, P.E., 1976. *Chemistry and biochemistry of natural waxes*. Elsevier Scientific Pub. Co..

Levy, K., Woster, A.P., Goldstein, R.S. and Carlton, E.J., 2016. Untangling the impacts of climate change on waterborne diseases: a systematic review of relationships between diarrheal diseases and temperature, rainfall, flooding, and drought. Environmental science & technology, 50(10), pp.4905-4922.

Liu, W. and Huang, Y., 2005. Compound specific D/H ratios and molecular distributions of higher plant leaf waxes as novel paleoenvironmental indicators in the Chinese Loess Plateau. *Organic Geochemistry*, *36*(6), pp.851-860.

Liu, W., Yang, H. and Li, L., 2006. Hydrogen isotopic compositions of n-alkanes from terrestrial plants correlate with their ecological life forms. *Oecologia*, *150*(2), pp.330-338.

Looman, J., 1983. Distribution of plant species and vegetation types in relation to climate. *Vegetatio*, *54*(1), pp.17-25.

Makou, M.C., Hughen, K.A., Xu, L., Sylva, S.P. and Eglinton, T.I., 2007. Isotopic records of tropical vegetation and climate change from terrestrial vascular plant biomarkers preserved in Cariaco Basin sediments. *Organic Geochemistry*, *38*(10), pp.1680-1691.

Mays, S., 2010. *The archaeology of human bones*. Routledge.

McCabe, G.J., Palecki, M.A. and Betancourt, J.L., 2004. Pacific and Atlantic Ocean influences on multidecadal drought frequency in the United States. *Proceedings of the National Academy of Sciences*, *101*(12), pp.4136-4141.

McInerney, F.A., Helliker, B.R. and Freeman, K.H., 2011. Hydrogen isotope ratios of leaf wax n-alkanes in grasses are insensitive to transpiration. *Geochimica et Cosmochimica Acta*, *75*(2), pp.541-554.

Muir, C.D. and Angert, A.L., 2016. Grow with the flow: a latitudinal cline in physiology is associated with more variable precipitation in Mimulus cardinalis. *bioRxiv*, p.080952.

Otto, A. and Simpson, M.J., 2005. Degradation and preservation of vascular plant-derived biomarkers in grassland and forest soils from Western Canada. *Biogeochemistry*, *74*(3), pp.377-409.

Ehleringer, J. and Pearcy, R.W., 1983. Variation in quantum yield for CO2 uptake among C3 and C4 plants. *Plant physiology*, *73*(3), pp.555-559.

Palmer, W.C., 1965. *Meteorological drought* (Vol. 30). US Department of Commerce, Weather Bureau.

Pennock, D., Bedard-Haughn, A., Kiss, J. and van der Kamp, G., 2014. Application of hydropedology to predictive mapping of wetland soils in the Canadian Prairie Pothole Region. *Geoderma*, *235*, pp.199-211.

Pham, S.V., Leavitt, P.R., McGowan, S. and Peres-Neto, P., 2008. Spatial variability of climate and land-use effects on lakes of the northern Great Plains. *Limnology and Oceanography*, *53*(2), pp.728-742.

Pham, S.V., Leavitt, P.R., McGowan, S., Wissel, B. and Wassenaar, L.I., 2009. Spatial and temporal variability of prairie lake hydrology as revealed using stable isotopes of hydrogen and oxygen. Limnology and Oceanography, 54(1), pp.101-118.

Plancq, J., Cavazzin, B., Juggins, S., Haig, H.A., Leavitt, P.R. and Toney, J.L., 2018. Assessing environmental controls on the distribution of long-chain alkenones in the Canadian Prairies. *Organic geochemistry*, *117*, pp.43-55.

Post-Beittenmiller, D., 1996. Biochemistry and molecular biology of wax production in plants. *Annual review of plant biology*, *47*(1), pp.405-430.

Quiring, S.M. and Papakyriakou, T.N., 2005. Characterizing the spatial and temporal variability of June–July moisture conditions in the Canadian prairies. *International Journal of Climatology: A Journal of the Royal Meteorological Society*, *25*(1), pp.117-138.

Raddatz, R.L., 2000. Summer rainfall recycling for an agricultural region of the Canadian prairies. *Canadian journal of soil science*, *80*(2), pp.367-373.

R Core Team., 2013. R: A language and environment for statistical computing. R Foundation for Statistical Computing, Vienna, Austria. URL http://www.R-project.org/.

Sachse, D., Billault, I., Bowen, G.J., Chikaraishi, Y., Dawson, T.E., Feakins, S.J., Freeman, K.H., Magill, C.R., McInerney, F.A., Van Der Meer, M.T. and Polissar, P., 2012. Molecular paleohydrology: interpreting the hydrogen-isotopic composition of lipid biomarkers from photosynthesizing organisms. *Annual Review of Earth and Planetary Sciences*, *40*, pp.221-249.

Sachse, D., Radke, J. and Gleixner, G., 2004. Hydrogen isotope ratios of recent lacustrine sedimentary n-alkanes record modern climate variability. *Geochimica et Cosmochimica Acta*, *68*(23), pp.4877-4889.

Sachse, D., Radke, J. and Gleixner, G., 2006. δD values of individual n-alkanes from terrestrial plants along a climatic gradient–Implications for the sedimentary biomarker record. *Organic Geochemistry*, *37*(4), pp.469-483.

Sack, L.A. and Last, W.M., 1994. Lithostratigraphy and recent sedimentation history of Little Manitou lake, Saskatchewan, Canada. *Journal of Paleolimnology*, *10*(3), pp.199-212.

Sano, M., Xu, C. and Nakatsuka, T., 2012. A 300-year Vietnam hydroclimate and ENSO variability record reconstructed from tree ringδ18O. *Journal of Geophysical Research: Atmospheres*, *117*(D12).

Saracco, J.F., Fettig, S.M., San Miguel, G.L., Mehlman, D.W., Thompson, B.E. and Albert, S.K., 2018. Avian demographic responses to drought and fire: a community-level perspective. *Ecological applications*, *28*(7), pp.1773-1781.

Sauchyn, D.J. and Skinner, W.R., 2001. A proxy record of drought severity for the southwestern Canadian Plains. *Canadian Water Resources Journal*, *26*(2), pp.253-272.

Sauer, P.E., Eglinton, T.I., Hayes, J.M., Schimmelmann, A. and Sessions, A.L., 2001. Compound-specific D/H ratios of lipid biomarkers from sediments as a proxy for environmental and climatic conditions. Geochimica et Cosmochimica Acta, 65(2), pp.213-222.

Seki, O., Meyers, P.A., Kawamura, K., Zheng, Y. and Zhou, W., 2009. Hydrogen isotopic ratios of plant wax n-alkanes in a peat bog deposited in northeast China during the last 16 kyr. *Organic Geochemistry*, *40*(6), pp.671-677.

Sessions, A.L., Sylva, S.P., Summons, R.E. and Hayes, J.M., 2004. Isotopic exchange of carbon-bound hydrogen over geologic timescales. Geochimica et Cosmochimica Acta, 68(7), pp.1545-1559.

Shabbar, A., Bonsal, B. and Khandekar, M., 1997. Canadian precipitation patterns associated with the Southern Oscillation. *Journal of Climate*, *10*(12), pp.3016-3027.

Shabbar, A., Higuchi, K., Skinner, W. and Knox, J.L., 1997. The association between the BWA index and winter surface temperature variability over eastern Canada and west Greenland. *International Journal of Climatology: A Journal of the Royal Meteorological Society*, *17*(11), pp.1195-1210.

Shanahan, T.M., Hughen, K.A., Ampel, L., Sauer, P.E. and Fornace, K., 2013. Environmental controls on the 2H/1H values of terrestrial leaf waxes in the eastern Canadian Arctic. *Geochimica et Cosmochimica Acta*, *119*, pp.286-301.

Shanley, C.S., Pyare, S., Goldstein, M.I., Alaback, P.B., Albert, D.M., Beier, C.M., Brinkman, T.J., Edwards, R.T., Hood, E., MacKinnon, A. and McPhee, M.V., 2015. Climate change implications in the northern coastal temperate rainforest of North America. *Climatic Change*, *130*(2), pp.155-170.

Shorthouse, J.D., 2010. Ecoregions of Canada's prairie grasslands. *Arthropods of Canadian grasslands*, *1*, pp.53-81.

Smith, F.A. and Freeman, K.H., 2006. Influence of physiology and climate on δD of leaf wax n-alkanes from C3 and C4 grasses. *Geochimica et Cosmochimica Acta*, *70*(5), pp.1172-1187.

Smith, L.M., Haukos, D.A., McMurry, S.T., LaGrange, T. and Willis, D., 2011. Ecosystem services provided by playas in the High Plains: potential influences of USDA conservation programs. *Ecological Applications*, *21*(sp1), pp.S82-S92.

Stagge, J.H., Tallaksen, L.M., Gudmundsson, L., Van Loon, A.F. and Stahl, K., 2015. Candidate distributions for climatological drought indices (SPI and SPEI). *International Journal of Climatology*, *35*(13), pp.4027-4040.

Su, M., Stolte, W.J. and Van der Kamp, G., 2000. Modelling Canadian prairie wetland hydrology using a semi-distributed streamflow model. *Hydrological Processes*, *14*(14), pp.2405-2422.

Szymczak, S., Joachimski, M.M., Bräuning, A., Hetzer, T. and Kuhlemann, J., 2011. Comparison of whole wood and cellulose carbon and oxygen isotope series from Pinus nigra ssp. laricio (Corsica/France). *Dendrochronologia*, *29*(4), pp.219-226.

Taylor, S.H., Hulme, S.P., Rees, M., Ripley, B.S., Ian Woodward, F. and Osborne, C.P., 2010. Ecophysiological traits in C3 and C4 grasses: a phylogenetically controlled screening experiment. *New Phytologist*, *185*(3), pp.780-791.

Terzer, S., Wassenaar, L.I., Araguás-Araguás, L.J. and Aggarwal, P.K., 2013. Global isoscapes for δ 18 O and δ 2 H in precipitation: improved prediction using regionalized climatic regression models. *Hydrology and Earth System Sciences*, *17*(11), pp.4713-4728.

Thomas, E.K., McGrane, S., Briner, J.P. and Huang, Y., 2012. Leaf wax δ 2 H and varve-thickness climate proxies from proglacial lake sediments, Baffin Island, Arctic Canada. *Journal of paleolimnology*, *48*(1), pp.193-207.

Thornthwaite, C.W., 1948. An approach toward a rational classification of climate. *Geographical review*, *38*(1), pp.55-94.

Tierney, J.E., Russell, J.M., Damsté, J.S.S., Huang, Y. and Verschuren, D., 2011. Late Quaternary behavior of the East African monsoon and the importance of the Congo Air Boundary. *Quaternary Science Reviews*, *30*(7-8), pp.798-807.

Toney, J., 2011. *Brown Digital Repository | Theses And Dissertations*. [online] Repository.library.brown.edu. Available at: <https://repository.library.brown.edu/studio/collections/dissertation/?q=Toney&selected_facets=mods_dateAll_year_ssim%3A2011&selected_facets=keyword%3ABiochemical+markers&selected_facets=ir_collection_name%3AEarth%2C+Environmental+and+Planetary+Sciences&search_field=> [Accessed 30 September 2020].

Van der Kamp, G. and Hayashi, M., 1998. The groundwater recharge function of small wetlands in the semi-arid northern prairies. *Great Plains Research*, pp.39-56.

Van der Kamp, G., Hayashi, M. and Gallen, D., 2003. Comparing the hydrology of grassed and cultivated catchments in the semi-arid Canadian prairies. *Hydrological Processes*, *17*(3), pp.559-575.

Van der Kamp, G. and Hayashi, M., 2009. Groundwater-wetland ecosystem interaction in the semiarid glaciated plains of North America. *Hydrogeology Journal*, *17*(1), pp.203-214.

Van Stempvoort, D.R., Edwards, T.W.D., Evans, M.S. and Last, W.M., 1993. Paleohydrology and paleoclimate records in a saline prairie lake core: mineral, isotope and organic indicators. Journal of Paleolimnology, 8(2), pp.135-147.

Vicente-Serrano, S.M., Beguería, S., López-Moreno, J.I., Angulo, M. and El Kenawy, A., 2010. A new global 0.5 gridded dataset (1901–2006) of a multiscalar drought index: comparison with current drought index datasets

based on the Palmer Drought Severity Index. *Journal of Hydrometeorology*, *11*(4), pp.1033-1043.

Vogts, A., Badewien, T., Rullkötter, J. and Schefuß, E., 2016. Near-constant apparent hydrogen isotope fractionation between leaf wax n-alkanes and precipitation in tropical regions: Evidence from a marine sediment transect off SW Africa. *Organic geochemistry*, *96*, pp.18-27.

Wang, T., Hamann, A., Spittlehouse, D.L. and Murdock, T.Q., 2012. ClimateWNA—high-resolution spatial climate data for western North America. *Journal of Applied Meteorology and Climatology*, *51*(1), pp.16-29.

Wara, M.W., Ravelo, A.C. and Delaney, M.L., 2005. Permanent El Niño-like conditions during the Pliocene warm period. Science, 309(5735), pp.758-761.

Wayne, C.P., 1965. Meteorological drought. *Res. Pap*, *45*, p.58.

Wells, N., Goddard, S. and Hayes, M.J., 2004. A self-calibrating Palmer drought severity index. *Journal of Climate*, *17*(12), pp.2335-2351.

Wiken, E., Gauthier, D., Marshall, I., Lawton, K. and Hirvonen, H., 1996. A perspective on Canada's ecosystems: an overview of the terrestrial and marine ecozones. occasional paper 14. *Canadian Council on ecological Areas, ottawa, ontario, Canada*.

Wolfe, S.A., Ollerhead, J., Huntley, D.J. and Lian, O.B., 2006. Holocene dune activity and environmental change in the prairie parki and and boreal forest, central Saskatchewan, Canada. The Holocene, 16(1), pp.17-29.

Xia, X. and Gao, Y., 2019. Kinetic clumped isotope fractionation during the thermal generation and hydrogen exchange of methane. Geochimica et Cosmochimica Acta, 248, pp.252-273.

Xia, Z.H., Xu, B.Q., Mügler, I., Wu, G.J., Gleixner, G., Sachse, D. and Zhu, L.P., 2008. Hydrogen isotope ratios of terrigenous n-alkanes in lacustrine

surface sediment of the Tibetan Plateau record the precipitation signal. *Geochemical Journal*, *42*(4), pp.331-338.

Xu, C., Sano, M. and Nakatsuka, T., 2011. Tree ring cellulose δ18O of Fokienia hodginsii in northern Laos: A promising proxy to reconstruct ENSO?. *Journal of Geophysical Research: Atmospheres*, *116*(D24).

Xu, G., Liu, X., Sun, W., Chen, T., Zhang, X., Zeng, X., Wu, G., Wang, W. and Qin, D., 2018. Application and verification of simultaneous determination of cellulose δ 13 C and δ 18 O in Picea shrenkiana tree rings from northwestern China using the high-temperature pyrolysis method. *Journal of Arid Land*, *10*(6), pp.864-876.

Xu, G., Liu, X., Qin, D., Chen, T., Sun, W., An, W., Wang, W., Wu, G., Zeng, X. and Ren, J., 2014. Drought history inferred from tree ring δ 13 C and δ 18 O in the central Tianshan Mountains of China and linkage with the North Atlantic Oscillation. *Theoretical and Applied Climatology*, *116*(3-4), pp.385-401.

Yang, H. and Huang, Y., 2003. Preservation of lipid hydrogen isotope ratios in Miocene lacustrine sediments and plant fossils at Clarkia, northern Idaho, USA. *Organic Geochemistry*, *34*(3), pp.413-423.

Zargar, A., Sadiq, R. and Khan, F.I., 2014. Uncertainty-driven characterization of climate change effects on drought frequency using enhanced SPI. *Water resources management*, *28*(1), pp.15-40.